EFFECTS OF GRAPE SEED EXTRACT AND CALORIE RESTRICTION ON AGING PROCESS

CHEN JIE

(Master of Medicine)

A THESIS SUBMITTED

FOR THE DEGREE OF DOCTOR OF PHILOSOPHY

DEPARTMENT OF OTOLARYNGOLOGY

YONG LOO LIN SCHOOL OF MEDICINE，NATIONAL UNIVERSITY OF SINGAPORE

2007

ACKNOWLEDGEMENTS

This work was performed through a joint program between the National University of Singapore (NUS) and Institute of Bioengineering and Nanotechnology (IBN), the Agency for Science, Technology and Research (A*STAR) from January 2004 to December 2007.
I take this opportunity as a pleasure to express my gratitude to everyone who supported me during these years. Firstly, the thesis is dedicated to my family for their precious support during the course of completion.

I am very grateful for the responsible direction given to me by my supervisor, Dr Lynne Lim, Associate Professor, who supervises my final year study when the help is really needed.

I express my sincere gratitude to Dr. Ruan Runsheng, Assistant Professor, my previous supervisor, for his responsible supervision and guidance in my project, as well as his kind support during the course of my Ph. D. program.

I deeply thank Dr. Chidambaram Natesa Velalar, Senior Research Scientist, IBN, for his advice in my project, revising the manuscripts and thesis and the directions provided.

I would like to thank Prof. Jackie Y. Ying, Executive Director, and Ms. Noreena AbuBakar, Director, of IBN and Dr Thomas Loh**,** Head of the Department of

Otolaryngology, Yong Loo Lin School of Medicine, NUS, for their permission to perform my graduation studies through their institutions.

I appreciate the help of Dr. Liesbeth Kilsdonk, Dr. Yang Zheng, May Way and Dr. Zhao Tianxia for proofreading this thesis.

I thank all the past and current members of our laboratory: Meng Qingying, Dr. David A. Rider, Lee Fan, Myranda Lee, Tan Tiong Gee Brian, Ye Chaopeng, Yee Ting Wong, Dr. Kurisawa Motoichi, Dr. Muthukumarasamy Shanmugam, Dr. Gopalan Began, Karishma Sachaphibulkij, and Kokheng Foong as well as other colleagues in IBN and NUS for their help when we were working together.

I thank all my friends: Bao zhang, Dr. Chen zhiqiang, Li chunwei, Dr. Zhu Xiaoming, Dr. Long Meixiao, Dr. Li da, and TeongBeng Soo for their help in research and life.

Last but not the least; I would like to thank NUS for offering me research scholarship and good research environment. I also thank IBN, A* STAR, and the Biomedical Research Council for financial support for this project.

PUBLICATIONS

Chen J, Ruan R. Identifying stable reference genes for evaluation of antioxidative enzyme gene expression in auditory cortex and cochlea of young and old Fischer 344 rats . *Acta Otolaryngol*. 2008 Aug 8:1-9. [Epub ahead of print]

Chen J, Velalar CN, Ruan R. Identifying the changes in gene profiles regulating the amelioration of age-related oxidative damages in kidney tissue of rats by the intervention of adult-onset calorie restriction . *Rejuvenation Res.* 2008; 11:757-63.

Chen J, Rider DA, Ruan R. Identification of Valid Housekeeping Genes and Antioxidant Enzyme Gene Expression Change in the Aging Rat Liver. *J Gerontol A Biol Sci Med Sci*. 2006; 61:20-27.

Meng Q, Wong YT, **Chen J**, Ruan R. Age-related Changes in Mitochondrial Function and Antioxidative Enzyme Activity in Fischer 344 Rats. *Mech Age Dev*. 2007; 128:286-292.

Chen J, Ruan R. Effects of calorie restriction initiated at middle age on antioxidative enzyme gene expression in kidney ageing of F344 rat. 36th Annual Meeting of the American Aging Association. Texas, USA, 2007, Abstract, Page 41-42.

TABLE OF CONTENTS

SUMMARY

Based on the free radical theory of aging, the imbalance between free radicals and antioxidant defense system causes oxidative damage of major biomolecules, the accumulation of which is attributed to the aging process. We hypothesized that grape seed extract (GSE) and calorie restriction (CR) attenuated age related oxidative damage in middle-aged rats. To choose the most suitable tissue for the evaluation of anti-aging intervention of GSE and CR we started by quantifying the gene expression of the major antioxidant enzymes in rat liver, kidney, auditory cortex and cochlea during the aging process since these enzymes form the major antioxidant defense. For accurate gene expression quantification, real time RT-PCR with valid housekeeping gene (HKG) protocol was established, and the necessity of the validation of HKG was investigated. The second part was aimed at evaluating the effect of GSE and CR in middle-aged rats by detecting age-related oxidative damage in rat kidney tissue, which was suggested as the most suitable tissue for the evaluation of anti-aging intervention based on the first part results. The molecular mechanism was further explored using microarray and real time RT-PCR at the gene expression level. The extent of protective effects of GSE and CR were evaluated by pathological grading of the kidney.

Firstly, real time RT-PCR with valid HKG protocol was established. We found for the first time that a wide variation in HKG expression existed during the aging process in liver, kidney, cochlear and auditory cortex of rats. Our data also showed that invalid

HKGs could result in the misinterpretation of gene expression levels, and that choosing appropriate HKGs was vital for accurate gene quantification and analysis in aging research. Furthermore, we found the significantly decreased catalase expression in both rat liver and kidney during aging while Cu/Zn-superoxide dismutase (SOD) expression was decreased in kidney aging. No significant antioxidative gene changes were found in auditory cortex and cochlea. Our data suggested that the decreased catalase gene expression might be involved in the decline of the antioxidant defense system in the rat liver aging process, and the decreased Cu/Zn-SOD and catalase gene expression might be involved in the decline of the antioxidant defense system in the rat kidney aging process.

Secondly, the effect of GSE and CR in middle-aged rats was investigated. 12 months old rats were fed a NIH31 diet for 6 months with either a low GSE dose (0.2% w/w), high GSE (1% w/w), or controls without GSE. The CR group was fed a NIH31/NIA Fortified diet, which was enriched in vitamins to ensure the same level of vitamins consumption with control group to avoid confounding. We found the low and high dose GSE and CR significantly decreased urinary 8-isoprostane, a reliable marker of lipid peroxidation ($P<0.05$) and the high dose GSE and CR have significantly decreased protein carbonyl, a marker of protein oxidation, in kidney ($P<0.05$). Furthermore, microarray and real time RT-PCR data showed that the mRNA expression of 15 lipoxygenase (15-LO) and S100 calcium binding protein A8 (S100A8) was significantly down regulated by high dose GSE in kidney ($P<0.05$). In addition, CR decreased age related renal pathological changes. The mRNA expression of catalase, Mn-SOD and kallikrein was significantly increased and the mRNA expression of complement 3 (C3) and chemokine C-C motif-

ligand 5 (CCL-5) was significantly decreased by CR. Our data indicated that GSE could prevent age related oxidative damages, even those initiated in middle age, which might be regulated through the decreased 15-LO and S100A8 genes expression. Furthermore, 6 months CR retarded age related oxidative damages and renal pathological changes, which might be regulated through the increased catalase, Mn-SOD and kallikrein and the reduced expression of C3 and CCL-5 gene expression.

.

LIST OF TABLES

LIST OF FIGURES

Abbreviations

15-LO	15-Lipoxygenase
C3	complement 3
CCl_4	carbon tetrachloride
CCL-5	chemokine C-C motif-ligand 5
CCRCC	clear cell renal cell carcinoma
Cdc25B	cell division cycle 25B
CR	calorie restriction
CYPa	cyclophilin A
EF	eukaryotic translation elongation factor
FRET	fluorescent resonance energy transfer
GAPDH	glyceraldehyde-3-phosphate dehydrogenase
GC	gas chromatography
GPX	glutathione peroxidase
GSE	grape seed extract
HKG	Housekeeping gene
HPRT	hypoxanthine phosphoribosyl-transferase
LC	liquid chromatography
LMNB1	lamin B1
MS	mass spectrometry
NF	normalization factor

RNS	reactive nitrogen species
ROS	reactive oxygen species
RT-PCR	reverse transcription polymerase chain reaction
S100A8	S100 calcium binding protein A8
SOD	superoxide dismutase
TP53	tumor suppressor gene P53
UBC	ubiquitin C
YWHAZ	tyrosine 3-monooxygenase/tryptophan 5-monooxygenase activation protein zeta polypeptide

Chapter I: Introduction

1.1 Free radical theory of aging

The exact mechanism of aging has not been established until now. Among the several theories that were proposed to explain the aging process, the free radical theory of aging (Harman, 1956) has become increasingly popular as numerous investigations support this theory (Bokov et al., 2004). The discovery of the enzyme Cu/Zn-superoxide dismutase (Cu/Zn-SOD) provided support for this theory because the sole function of the intracellular enzyme, Cu/Zn-SOD, is to scavenge superoxide, which indicates that free radicals must be continuously produced in cells (McCord and Fridovich, 1969). Later, Harman modified the free radical theory of aging and proposed the mitochondrial theory of aging in 1972, emphasizing the central role of mitochondria because mitochondria are the major sources of reactive oxygen species (ROS) (Harman, 1972). With new findings, the theory is continuously refined. Many ROS and reactive nitrogen species (RNS), which are not free radicals, had an important role in the formation of oxidative damage. Thus, this theory was finally refined as the oxidative stress theory of aging (Sohal et al., 1996). The theory can be illustrated in Figure 1.1. In brief, the imbalance of free radicals and antioxidant defense causes oxidative damage to major biomolecules, the accumulation of which contributes to the aging process.

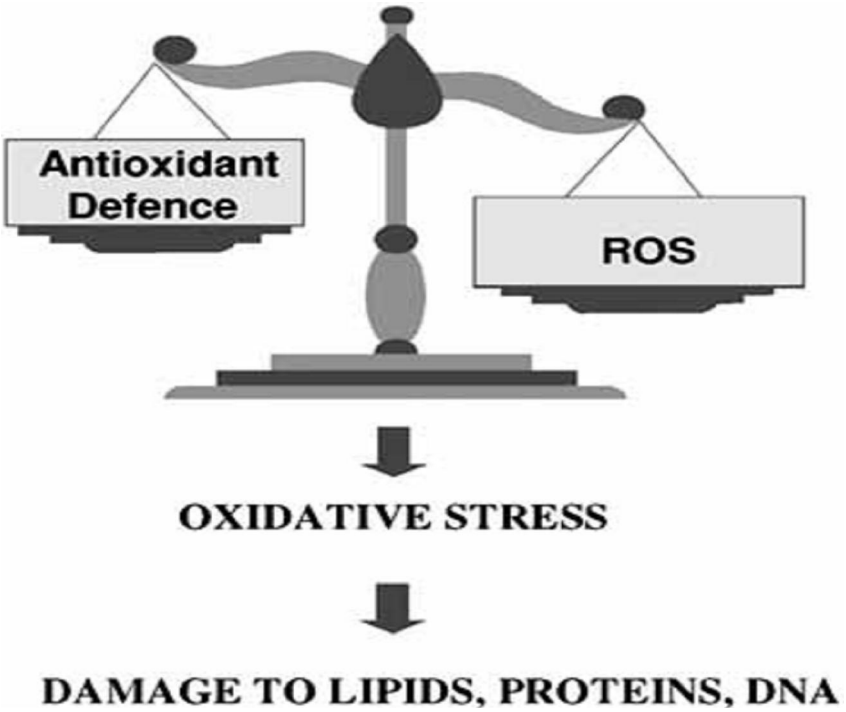

Figure 1.1 A summary of the free radical theory of aging (Reproduced with permission from Hermans et al., 2007)

Free radicals are any molecules or ions which have one or more unpaired electrons (Halliwell & Gutteridge, 1999). Free radicals are generally more reactive than their parent species because the unpaired electrons are unstable. ROS comprise of free radicals such as superoxide, hydroxyl and hydroperoxyl, and certain nonradicals that are also oxidizing agents such as hydrogen peroxide (Halliwell et al., 2004). RNS include free radicals such as nitric oxide, and nonradicals, such as peroxynitrite anion (Halliwell et al., 2004). ROS and RNS are produced in multiple ways. The major source of ROS generation is mitochondrial electron transport, which couples oxidative phosphorylation and cellular respiration (Cadenas & Sies, 1998). In addition, lipid metabolism in the

peroxisomes (Valko et al., 2004), activated phagocytes in imflammatory response (Chanock et al., 1994) and cytochrome P450 reactions are capable of generating ROS under normal and pathological conditions (Goeptar et al., 1995). Nitric oxide is generated by nitric oxide synthases (Ghafourifar et al., 2005). Peroxynitrite anion is generated from the reaction between nitric oxide and superoxide, which is a powerful oxidant (Carr et al., 2000).

ROS/RNS have multiple functions depending on different biological milieu. They have some beneficial functions such as the regulation of vascular tone, antimicrobial agents and intra- and inter-cellular signaling mechanisms. For example, free radicals produced by activated phagocytes can kill foreign invaders. Resting phagocytes consume little oxygen, whereas activated phagocytes have a large increase in oxygen uptake at the onset of phagocytosis. Activated phagocytes produce superoxide and hydrogen peroxide, which are toxic to bacteria (Segal, 2005). In addition, nitrogen oxide is an important signaling molecule to regulate vascular tone. Nitrogen oxide produced by the vascular endothelial cells activates guanylate cyclases of vascular smooth muscle cells that cause more cyclic guanosine monophosphate (GMP) generation. Cyclic GMP can further decrease intracellular free calcium concentration, which causes the dilation of vessel and lowers the blood pressure (Bredt, 1999). Nitrogen oxide also has other important physiological roles, such as the inhibition of platelet aggregation and bladder control (Bredt, 1999).

However, the overproduction of ROS and RNS causes harmful effect on related targets such as protein oxidation, lipid peroxidation and DNA damage. For example, hydroxyl

attacks polyunsaturated fatty acids of membrane phospholipids, which causes lipid peroxidation chain reaction and affects the function of membrane proteins and oxidizing cholesterol (Utteridge et al., 1990). With the accumulation of lipid peroxidation, cell membrane is destabilized, causing ion leakage. These potential harmful effects of ROS/RNS are controlled by the antioxidant defense system. This system includes antioxidant enzymes, low-molecular-mass antioxidants and sequestration of transition metal ions. Antioxidant enzymes consist of Cu/Zn-superoxide dismutase (SOD), Mn-SOD, catalase and glutathione peroxidase (GPX). Cu/Zn-SOD can convert superoxide into hydrogen peroxide, which is further catalyzed into water molecules by catalase or GPX. In addition, a variety of low-molecular-mass antioxidants such as vitamin C and E, also participate in scavenging free radicals. Finally, several kinds of proteins can sequester transition metal ions to avoid being the catalyst, which causes the conversion of fairly inactive ROS into highly active ROS. For example, ferritin and transferrin can sequester iron. If transition metal ions are available, lipid peroxidation will be more serious.

Even though there are several antioxidant defenses in the biological systems, oxidative damage occurs frequently because of the imbalance between ROS/RNS and antioxidant defenses. According to free radical theory of aging, ROS/RNS can attack many important biological molecules such as DNA, protein and lipids, resulting in oxidative damage, which impairs the normal physiological function of cells and organs and prompts the occurrence of the aging process and aging-related diseases. Numerous investigations have been reported to support this theory. The major evidence is as follows: (1) there was

an increase in age-related oxidative biomolecular damage in organisms from invertebrates to humans (Warner, 1994; Bohr and Anson, 1995). (2) Calorie restriction, which prevented the aging process and aging-related diseases, decreased the aging-related accumulation of oxidative damage in rodents (Yu, 1996). (3) $P66^{shc}$ knockout mice had an increased resistance to oxidative stress, resulting in a significantly longer life span of mice (Migliaccio et al., 1999). (4) Cu/Zn-SOD knockout mice had an elevated oxidative damage in plenty of the tissues, and suffered from the accelerated age-related pathologies and a decrease of life span (Elchuri et al., 2005). Moreover, overexpression of catalase in mitochondria of mice extended the life span of mice and decreased age-related oxidative damage changes (Schriner et al., 2005). However, some studies indicated that oxidative stress was not the only key factor in the aging process, because mice with growth hormone receptor/binding protein knockout had increaseded life span, while the mice had the decreased resistance to oxidative stress (Hauck et al., 2002). Thus, the current free radical theory of aging still needs further modification.

1.2 Anti-aging Intervention

With increasing understanding of the aging process, how to retard the aging process and age related diseases has become the most intriguing research area. Currently, there are three major anti-aging interventions such as calorie restriction, dietary supplementation and genetic manipulation.

1.2.1 Calorie restriction

1.2.1.1 Calorie restriction: history and mechanisms

Calorie restriction (CR), also known as dietary and food restriction, refers to the consumption of less diet while essential nutrients are provided to avoid malnutrition (Yu, 1996). The effect of CR on aging process was for the first time explored by McCay in 1935 (McCay et al., 1935). They found that CR, initiated from weaning, markedly increased the life span of rats. Since then, CR has been proven to effectively extend life span of diverse animals such as nematodes, fish, dogs and hamsters, and also prevent age related diseases, such as tumors, diabetes and heart diseases (Weindruch, 1996). An ongoing investigation of the effect of CR on nonhuman primate models also shows that CR may have an anti-aging effect, even though a final conclusion will not be available for 20 years because the maximum life span of rhesus monkey is above 40 years (Anderson and Weindruch, 2006). Therefore, CR has been regarded as the only most accepted intervention to extend the life span of mammalian animal models (Warner et al., 2000) and has also been used as a powerful tool for exploring the aging process and age related diseases. The exact mechanism of the effect of CR on the aging process is still unknown. Several hypotheses have been proposed, such as oxidative damage attenuation hypothesis, growth retardation hypothesis, the attenuation of insulin-like signaling hypothesis and the hormesis hypothesis (Masoro, 2005). Among them, the oxidative damage attenuation hypothesis is the most accepted hypothesis at present (Sohal and Weindruch 1996). Thus, this hypothesis will be discussed in detail.

According to the oxidative damage attenuation hypothesis, CR extends life span and slows aging by decreasing age related oxidative damage accumulation. There are many reports that support this hypothesis. (1) CR could effectively prevent age related increase in lipid peroxidation (Ward et al., 2005); protein oxidative damage (Youngman et al., 1992; Sohal et al., 1994) and DNA oxidative damage (Hamilton et al., 2001). (2) The formation of ROS was reduced by CR in rat liver mitochondria (Lambert et al., 2004). (3) DNA oxidative damage could be effectively repaired in CR rats (Guo et al., 1998).

The mechanisms mediating the prevention of oxidative damage by CR remain unclear. One possible mechanism is that CR reduces the generation of free radicals during the aging process. Sohal et al reported that CR could decrease the formation of superoxide and hydrogen peroxide in kidney and heart in mice during aging (Sohal et al., 1994). Another possible mechanism is that CR improves the antioxidant defense system. CR was reported to increase the antioxidant enzyme activity by increasing their gene expression in rat liver (Rao G et al., 1990). However, it was noticed that different tissues had different antioxidant gene expression changes under CR (Mote et al., 1997). Thus, it is interesting to further examine whether CR can affect antioxidant defense systems to slow the aging process.

1.2.1.2 Adult-onset CR

The age of animals for CR implementation had an important effect on the results of CR. The majority of CR studies that initiated after weaning or early in life showed the consistent effect of extending life span in different animals (Weindruch, 1996). In contrast, adult-onset CR studies were very limited and the findings were contradictory, especially the effect of CR on life span (Masoro, 2006). However, adult onset CR had more practical implications for application and important significance for the exploration of the fundamental mechanisms in CR. CR initiated in C57 BL/6J mice at 12 months of age could extend life span and decrease cancer incidence (Weindruch, 1982). CR, initiated at 6 months of age in F344 rats, could also extend life span and reduce age related disease such as heart diseases and renal diseases (Maeda et al., 1985). However, when CR was initiated in C57 BL/6L mice at 10 months of age, there were no life span changes (Goodrick et al., 1990). These differences among studies might be attributed to different experimental methodologies and rat strains.

Although the effects of adult-onset CR on life span were inconsistent, some investigations showed that adult-onset CR might have beneficial effects on age related diseases and the aging process. The incidence of liver tumors could be decreased by 8 weeks of CR initiated at 19 months of age of rats (Spindler, 2005). Age related renal pathological changes were also reduced by adult-onset CR initiated at 18 months of age

in male Fischer 344 x Brown Norway hybrid rats (McKiernan et al., 2007). Adult-onset CR was reported to reduce protein carbonylation of rat skeletal muscles (Radak et al., 2002). Thus, these findings indicated that adult-onset CR might be helpful to improve quality of life by reducing the risk of age related disease.It is worth further investigating the effect and mechanism of adult-onset CR.

1.2.1.3 Challenges for the applications of CR

One of the major ultimate purposes of CR research is to improve the health of human beings. Even though positive effects of CR on non-human primates are reported, there are several considerations to be evaluated for the possible applications of CR in human beings. The first question is the compliance of the methods for human beings. The advantages of CR have continuously been proven in animal models (Weindruch, 1996; Yu, 1996). CR refers to consume fewer calories while essential nutrients were provided to avoid malnutrition (Yu, 1996). If people follow CR, they have to eat a restricted diet for several years. For most of people, it is not practical. In addition, the beneficial effect of adult-onset CR needs further investigation to confirm. Finally, even though the effectiveness of the life long CR was confirmed in many animal models, it is not likely that one would apply CR in the childhood or adolescence of human beings. Moreover, the side effects of CR should also be noticed. For example, CR might increase the incidence of osteoporosis and sarcopenia in elderly people (Dirk et al., 2006).

1.2.2 Dietary supplements intervention

1.2.2.1 Dietary supplements intervention

According to the free radical theory of aging, oxidative damage plays an important role in the aging process. Dietary supplements, which have antioxidant effects, are likely to slow the aging process by correcting the imbalance between free radicals and antioxidant defense and decreasing oxidative damage. Many kinds of dietary supplements such as vitamin E (Miquel et al., 1982), vitamin C (Davies et al., 1977), butylated hydroxytoluene (Clapp et al., 1979) and thiazolidine carboxylic acid (Economos et al., 1982) have been evaluated in different animal models since the 1970s. But, these investigations could not provide the definitive conclusion of whether the life span of animals was effectively extended. Some possible explanations are as follows: (1) some antioxidants such as vitamin E and C (Yu et al., 1998), had pro-oxidant effects under certain physiological conditions. (2) Free radicals are involved in the normal signaling process. The dosages of dietary supplements are required to be optimized so that they could remove the harmful effects of free radicals and keep the beneficial effects of free radicals (Finkel et al., 2000; Kitani et al., 2006).

Recently, several dietary supplement interventions appear to be promising: lifespan was extended in nematode C. elegans by using SOD/catalase mimetics (EUK-8 and EUK-

134) (Melov et al., 2000). Oxidative stress-related diseases such as age-related learning deficits were effectively reversed and brain oxidative stress in mice were also reversed by using SOD/catalase mimetics (EUK-189 and EUK-207) (Liu et al., 2003). Deprenyl supplement has been reported to extend life span of four animal species: mice (Archer et al., 1996), rats (Kitani, et al., 2005), hamsters (Stoll et al., 1997) and dogs (Ruehl et al., 1997), when an optimized dose was used. The possible mechanism of deprenyl protection was attributed to the up-regulation of antioxidant enzyme gene expression and enzyme activity in many organs, such as heart, kidney, brain and spleen (Carrillo et al., 2000; Kitani et al., 2006).

Resveratrol has also been reported to increase lifespan in several different organisms such as worm (Wood et al.,2004) and a short-lived fish, Nothobranchius furzeri (Valenzano et al.,2006). The survival of mice on a high-calorie diet can also be improved by resveratrol (Baur et al., 2006). These mice that were supplemented with resveratrol had a 27.5% lower risk of death than other mice on the high-calorie diet. Based on microarray assay, the supplement of resveratrol reversed the change of 144 out of 153 significantly altered gene pathways by high caloric intake. Further evidence came from the National Institute on Aging's Interventions Testing Program, in which the potential dietary supplements were evaluated using sufficient mice to detect 10% changes in lifespan at three investigation sites: the Jackson Laboratory, University of Michigan, and University of Texas. Observations from these sites found that nordihydroguiaretic acid (NDGA) significantly increased the life span of mice (Miller et al., 2007). The exact mechanisms of resveratrol and NDGA were still unknown. The common characteristic of resveratrol

and NDGA was their powerful antioxidant effect. The antioxidant effect of NDGA was more powerful than vitamin C of the same concentration (Abou-Gazar et al., 2004). NDGA could prevent oxidative stress and pathological changes in diabetic nephropathy of rats (Anjaneyulu et al., 2004). Resveratrol was reported to scavenge the superoxide anion and inhibit the production of free radicals by decreasing complex III activity of the mitochondrial respiratory chain and inhibition of human LDL oxidation (Zini et al., 1999; Frankel et al., 1993).

In summary, compared with CR, dietary supplements are more practical intervention for retarding the aging process and age related diseases. After more than thirty years investigation, dietary supplements begin to appear promising. But, the knowledge of the overall regulation of the internal antioxidant defense and the interaction between dietary supplements and internal antioxidant defense remains unclear, bringing the challenges to the investigation of the anti-aging effects of dietary supplements.

1.2.2.2 Grape seed extract

The main active component of grape seed extract (GSE) is proanthocyanidins, which became noticed because of the “French Paradox”. The “French Paradox” stems from the people in southern France, who eat a high-fat diet, but they have a relatively low incidence of coronary heart disease. Proanthocyanidins have been proposed as a candidate to elucidate this Paradox (Rasmussen et al., 2005; Corder et al., 2006).

1.2.2.2.1 Chemistry and food sources of proanthocyanidins

Proanthocyanidin is a specific group of polyphenolic compounds. Proanthocyanidins comprise different flavan-3-ols subunits, the monomers of proanthocyanidin. The most common types of flavan-3-ols subunits are catechin, epicatechin, epiafzelechin, afzelechin and gallocatechin, which form the major subclass of proanthocyanidins, such as procyanidin, propelargonidin and prodelphinidin (Figure 1.2).

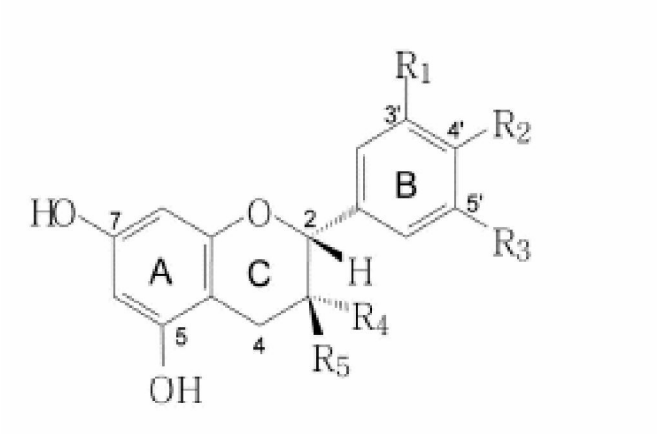

flavan-3-ols subunits	Subclass of proanthocyanidins	R1	R2	R3	R4	R5
afzelechin	propelargonidins	H	OH	H	H	OH
epiafzelechin	Propelargonidins	H	OH	H	OH	H
catechin	Procyanidin	H	OH	OH	H	OH
epicatechin	Procyanidin	H	OH	OH	OH	H
Gallocatechin	Prodelphinidin	OH	OH	OH	H	OH

Figure 1.2 Chemical structures of proanthocyanidins.

Proanthocyanidins are oligomers or polymers of flavan-3-ols subunits, which are linked mainly through C4 → C8 bond, and can also be linked through C4 → C6 bond, or ether bond between C2 and C7.

Proanthocyanidins are mainly found in fruits and berries, but also in nuts and beans, which are summarized in Table 1 (Rasmussen et al., 2005). This table clearly shows that grape seeds have plenty of proanthocyanidins. In addition, since the method to purify adequate proanthocyanidins is not well developed, proanthocyanidin-rich extracts such as grape seed extract and cocoa are used in most animal studies. The major proanthocyanidin monomers of GSE are catechin and epicatechin (Santos-buelga et al., 1995). Gas chromatography - mass spectrometry analyses showed that grape seed extract comprised 54 % proanthocyanidin dimer, 13 % proanthocyanidin trimer, 7 % proanthocyanidin tetramer, and small amounts (<5% each) of monomeric and high-molecular-weight oligomeric proanthocyanidins (Pataki, et al., 2002).

Table 1.1 Content of proanthocyanidins in common foods [a)]

Food	Monomers	Dimers	Trimers	4–6-mers	7–10-mers	>10-mers	Total	Type[b)]
	(mg/100 g fresh weight foods or mg/L beverages)							
Blueberries	4.0 ± 1.5	7.2 ± 1.8	5.4 ± 1.2	19.6 ± 3.4	14.5 ± 2.0	129.0 ± 47.3	179.8 ± 50.8	PC
Black-currants	0.9 ± 0.2	2.9 ± 0.4	3.0 ± 0.3	10.6 ± 1.7	9.9 ± 1.4	122.4 ± 28.0	147.8 ± 33.0	PC, PD
Cranberries	7.3 ± 1.5	25.9 ± 6.1	18.9 ± 3.4	70.3 ± 13.1	62.9 ± 14.7	233.5 ± 49.1	418.8 ± 75.3	A, PC
Strawberries	4.2 ± 0.7	6.5 ± 1.3	6.5 ± 1.2	28.1 ± 6.5	23.9 ± 3.5	75.8 ± 13.4	145.0 ± 24.9	PP, PC
Apples[c)]	9.6 ± 0.9	13.8 ± 0.6	9.3 ± 0.4	30.2 ± 1.2	25.4 ± 1.2	37.6 ± 2.6	125.8 ± 6.8	PC
Apple juice	1 ± 0	2 ± 0	1 ± 0	4 ± 0	1 ± 0	ND	9 ± 0	PC
Pears	2.7 ± 1.5	2.8 ± 1.3	2.3 ± 0.9	6.5 ± 1.9	4.6 ± 1.0	13.1 ± 11.3	31.9 ± 7.8	PC
Plums	11.4 ± 3.4	31.5 ± 7.4	23.9 ± 5.1	58.0 ± 12.5	33.8 ± 11.9	57.3 ± 24.4	215.9 ± 50.7	A, PC
Peaches	4.7 ± 1.4	7.0 ± 2.2	5.0 ± 1.4	17.7 ± 5.5	10.9 ± 3.7	22.0 ± 7.7	67.3 ± 20.9	PC
Avocados	1.0 ± 0.8	1.5 ± 0.8	1.4 ± 0.4	3.2 ± 0.8	0.4 ± 0.7	ND	7.4 ± 4.3	A, PC
Sorghum, sumac bran	27.8 ± 1.2	78.2 ± 3.4	99.2 ± 7.7	585.5 ± 50.0	734.3 ± 69.3	2440.4 ± 271.0	3965.4 ± 402.5	PC
Barley	11.0 ± 0.3	21.4 ± 1.1	14.6 ± 1.0	27.2 ± 0.6	ND	ND	74.2 ± 3.0	PC
Pinto beans, raw	14.8 ± 0.9	32.0 ± 2.6	28.3 ± 2.1	125.9 ± 9.2	135.6 ± 10.4	459.6 ± 34.2	796.3 ± 58.7	PP, PC
Red kidney beans	21.9 ± 0.2	26.4 ± 0.7	29.1 ± 0.7	117.7 ± 2.8	105.3 ± 2.2	263.4 ± 4.1	563.8 ± 10.4	PP, PC
Hazelnuts	9.8 ± 1.6	12.5 ± 3.8	13.6 ± 3.9	67.7 ± 20.3	74.6 ± 21.9	322.4 ± 102.5	500.7 ± 152.0	PC, PD
Pistachios	10.9 ± 4.3	13.3 ± 1.8	10.5 ± 1.2	42.2 ± 5.2	37.9 ± 4.9	122.5 ± 37.1	237.3 ± 52.0	PC, PD
Almonds	7.8 ± 0.9	9.5 ± 1.6	8.8 ± 1.7	40.0 ± 8.5	37.7 ± 8.4	80.3 ± 28.1	184.0 ± 48.2	PP, PC
Walnuts	6.9 ± 3.4	5.6 ± 0.9	7.2 ± 1.2	22.1 ± 3.3	5.4 ± 0.8	20.0 ± 9.3	67.3 ± 14.7	PC
Peanuts	5.1 ± 1.0	4.1 ± 0.7	3.7 ± 0.5	2.8 ± 0.2	ND	ND	15.6 ± 2.3	A, PC
Peanut butter	2.0 ± 0.9	3.0 ± 0.7	8.1 ± 3.5	ND	ND	ND	13.2 ± 5.2	A, PC
Black chocolate	31.4 ± 0.2	31.2 ± 0.9	21.1 ± 0.8	55.5 ± 3.5	38.5 ± 3.0	68.2 ± 8.8	246.0 ± 0.3	PC
Milk chocolate	26.9 ± 3.0	26.2 ± 2.5	19.3 ± 2.6	51.4 ± 9.8	35.3 ± 7.2	32.8 ± 9.2	192.0 ± 28.8	PC
Beer	4 ± 0	11 ± 1	3 ± 0	4 ± 0	ND	ND	23 ± 2	PC, PD
White wine[d)]	15.1	ND	ND	–	–	–	15.1[d)]	–
Rosé wine[d)]	17.1	ND	ND	–	–	–	17.1[d)]	–
Red wine[d)]	190.0	274.3	93.4	–	–	–	557.7[d)]	–
Red wine	20 ± 1	40 ± 1	27 ± 1	67 ± 2	50 ± 1	110 ± 2	313 ± 5	PC, PD
Grape juice	18 ± 0	34 ± 0	19 ± 0	80 ± 0	69 ± 0	303 ± 2	524 ± 2	PC, PD
Grape seed (dry)	660.3 ± 8.3	417.3 ± 4.8	290.2 ± 4.5	664.0 ± 8.2	400.3 ± 31.3	1100.1 ± 86.3	3532.3 ± 105.8	PC

a) All data are obtained from (Gu et al., 2004) unless otherwise is stated in a footnote. Values are means ± SD, n = 4–8. See (Gu et al., 2004) for detailed data on food content of proanthocyanidins. ND = not detected

b) Type: PP, propelargonidins, PC, procyanidins, PD, prodelphinidins, A, A-type linkage (Gu et al., 2004)

c) Red delicious with peel

d) Data are obtained from (Auger et al., 2004). Mean of 95 different French wines, see original paper for ranges in the wines. Only monomers (catechin and Epicatechin) up to trimers were measured. The total given is the sum of monomers to trimers.

(Reproduced with permission from Rasmussen et al., 2005)

1.2.2.2.2. Absorption and bioavailability of proanthocyanidins

The absorption and bioavailability of proanthocyanidins are not well studied because purification of sufficient amounts of pure proanthocyanidins is very difficult. From available data, absorption and bioavailability of proanthocyanidins depends on their chemical structures. The low-molecular-weight monomers and dimmers of proanthocyanidins can be absorbed in the gastrointestinal tract. The monomers and dimers of proanthocyanidins were found to be permeable in the Caco-2 human intestinal cell line (Deprez et al., 2001). In addition, Spencer et al. reported that epicatechin was the primary bioavailable form of the procyanidin dimers B2 and B5 after crossing the small intestine (Spencer et al., 2000). In rats, procyanidin B2 was found to be absorbed and excreted in urine and a portion of procyanidin B2 was degraded as epicatechin (Baba et al., 2002). In humans, proanthocyanidins dimers have been detected in the plasma, after drinking a cocoa beverage (Holt et al., 2002). However, the high-molecular-weight oligomers were poorly absorbed and were proposed to have local effects in the digestive tract (Hagerman et al., 1998), where they were degraded into small phenolic acids by the colonic microflora (Manach et al., 2005). In summary, these preliminary studies showed that low-molecular-weight oligomers could be bioavailable. The detailed mechanisms of absorption and metabolism of proanthocyanidins still remain to be investigated.

1.2.2.2.3. Safety evaluation of proanthocyanidins

As a natural compound, proanthocyanidins have been reported to be very safe. Most of the safety data was available from studies using GSE. In an acute oral toxicity study, the LD50 of GSE administered by gavage in rat was more than 5000mg/kg, and no detrimental effects were observed at the necropsy (Ray et al., 2001). In a chronic toxicity study, no toxicological effects were found in B6C3F1 mice fed with 500mg GSE/kg/day for 6 months (Ray et al., 2001). Similarly, no toxicological effects were found in Fischer 344 rats fed with 2.0% GSE supplement for 90 days (Yamakoshi et al., 2001). Sprague-Dawley rats fed with 2.0% GSE supplement for 90 days, which was equal to 1586 mg GSE/kg/day, did not cause significant toxicological effects (Wren et al., 2002). The specific advantages of proanthocyanidins over the flavonols, such as quercetin, were their high stability and inability to transform into potential prooxidants (Bors et al., 2000).

1.2.2.2.4. The protection effects of proanthocyanidins

Proanthocyanidins have powerful antioxidant effects and multiple biological activities. The main benefit was attributed to its antioxidant properties against oxidative damage (Cos et al., 2003). Proanthocyanidins effectively scavenged free radicals, chelated transition metals, and inhibited prooxidative enzymes, (Cos et al., 2004). Major evidence is as follows: (1) Free radical scavenging. Proanthocyanidins from GSE effectively removed superoxide anion and also suppressed hydroxyl radical using a spin-trapping electron spin resonance method (Yamaguchi et al., 1999). (2) Chelation of transition

metals. Proanthocyanidins could sequester iron and copper and prevent the ions from acting as catalyst in the the formation of hydroxyl (Maffei et al., 1996). (3) Inhibition of prooxidative enzymes. Proanthocyanidins could prevent lipid peroxidation by inhibiting the enzyme activity of 15-Lipoxygenase (Schewe et al. 2001). (4) Proanthocyanidins, as a powerful antioxidant, showed the ability to prevent oxidative damage. GSE could suppress lipid peroxidation caused by oxidative stress in animal models such as: experimental ischemia in brain (Feng Y et al., 2005) and heart (Bagchi et al., 2003). GSE provided a higher protection than vitamin E, C and β-carotene against 12-O-tetradeca-noylphorbol-13-acetate (TPA) induced lipid peroxidation and DNA damage in liver and brain tissue of mice (Bagchi et al., 1998). Flavanol-rich cocoa drink, of which the main active component was proanthocyanidins, was reported to lower plasma F2- isoprostane concentrations in humans (Wiswedel et al., 2004).

In addition to the antioxidant activity, proanthocyanidins have other beneficial effect such as anticancer and cardioprotective effect. In anticancer effect, proanthocyanidins had been reported to have anti-proliferative effect in various tumor cell lines, including human breast cancer cells (Agarwal et al., 2000), human prostate carcinoma cells (Tyagi et al., 2003) and human colorectal carcinoma cells (Kaur et al., 2006). In animal experiments, proanthocyanidins exerted chemopreventive effect in rats bearing carcinogen-induced mammary cancer (Kim et al., 2004). Proanthocyanidins inhibited the formation of azoxymethane-induced colonic aberrant crypt foci in the colons of rats by 72–88 % (Singletary et al., 2001). Moreover, several studies suggested that proanthocyanidins had cardioprotective effect. (1) Platelet aggregation contributes to the

formation of atherosclerosis. The thrombin-induced platelet aggregation was inhibited by proanthocyanidins in rats (Xia et al., 1998), and similar effect was observed in dogs and monkeys (Osman et al., 1998). (2) The oxidation of low-density lipoprotein (LDL) is a key factor of the formation of atherosclerosis (Steinberg et al., 1989). The protective effect of proanthocyanidins on inhibiting LDL oxidation has been proposed in vitro and in vivo studies. In vitro, proanthocyanidins were reported to inhibit the copper-catalyzed oxidation of human LDL (Frankel et al., 1995; Aviram 2002). The number of oxidized LDL-positive macrophage-derived foam cells in atherosclerotic lesions in the aorta of rabbits was decreased by proanthocyanidins (Yamakoshi, et al., 1999). The decrease in oxidized LDL in the plasma of human was observed after taking proanthocyanidins for 12 weeks (Sano et al., 2007). (3) The protective effects of proanthocyanidins on heart diseases have also been investigated in animal models. In apolipoprotein E deficient mice, the atherosclerotic lesion areas were reduced by 41% after taking proanthocyanidins for 10 weeks (Fuhrman et al., 2005). After rats were fed proanthocyanidin-rich extract for 3 weeks, the recovery of the reperfusion-induced injury in rat hearts was improved (Pataki et al., 2002).

In aging research, the protective effect of GSE is only limitedly studied. It was reported that GSE could prevent age related oxidative protein damage in the central nervous system in aged rats (Balu et al., 2005). However, the protective effects of GSE on other organs during aging have not been explored. In addition, the complexity of the aging process and diverse effects of GSE make it difficult to explore the mechanism of GSE. The detailed mechanism of GSE has not been elucidated. However, microarray method

that can study the gene expression profiling of whole genome at short time makes it possible. In this study, microarray analysis was used to explore the molecular mechanism of GSE protective effects.

1.2.3 Genetic manipulation

Even though genetic manipulation can effectively extend the life span of several kinds of animals, this intervention is mainly used to identify aging determinant genes that control the life span in the present stage because the knowledge of the complex genome systems in eukaryotic organisms is limited and the feasibility of such manipulation is widely questionable (Yu, 1999). Thus, genetic manipulation will only be concisely discussed here. Although the practicability of genetic manipulation is problematic, genetic manipulation in aging research provide the powerful tools to understand the mechanism of aging. The drosophila with Cu/Zn-SOD-null phenotype had a shortened life span with only about 20% life span of normal drosophila, and was more sensitive to oxidative stress (Phillips et al., 1989). The inducible overexpression of CuZnSOD in drosophila could extend the life span and increase the resistance to oxidative stress (Parkes et al., 1994). Similar results were reported in Mn-SOD-null drosophila (Duttaroy et al., 2003; Sun, et al., 2002). In addition, the average life span of Cu/Zn-SOD knockout mice was decreased by about 30% (Sentman et al., 2006), and plasma F2-isoprostane was increased twofold compared to control mice (Muller et al., 2006). These investigations provided further support for the free radical theory of aging. However, Mn-SOD+/- mice, which had increased oxidative damage and higher tumor incidence, had similar survival curves with

control mice, even though the activity of Mn-SOD was decreased by 50% (Van Remmen et al., 2003). These investigations remind us that the free radical theory of aging still needs to be further refined.

1.3 Biomarkers of aging

The ideal biomarker of the aging process should predict remaining longevity and reflect some basic biological process of aging (Warner, 2004). Biomarkers of aging are highly desirable and will be very helpful for evaluating anti-aging interventions. Even though many traits vary with age, validated biomarkers of aging in animal models have not been found (Warner, 2004).

According to the free radical theory of aging, biomolecular oxidative damage plays an important role in the aging process, which is also related to the development of age related diseases. In general, the evaluation of oxidative damage of biomolecules is more important than the evaluation of the amount of free radical generated because free radicals might react with unimportant targets, rather than with important biological molecules such as DNA, protein and lipids. Pathological assessment can predict the later development of diseases, even though pathological assessment is not sensitive in evaluating the effect of the anti-aging intervention. Thus, biomarkers of oxidative damage and pathological assessment are recommended to evaluate anti-aging interventions (Warner, et al., 2000).

1.3.1 Biomarkers of oxidative damage

Oxidative damage is the damage of biomolecules caused by direct attack of ROS/RNS (Halliwell et al., 2004). An ideal biomarker of oxidative damage should fulfill the following requirements. First of all, the biomarker should predict the progression of diseases. Another critical criterion is that it should detect a certain percentage of total oxidative damage in vivo and have a relatively small variation between different individuals. Finally, the biomarker should be stable and not be interfered by diet during detection (Halliwell et al., 2004). Unfortunately, the ideal biomarker of oxidative damage has not been identified. However, some new biomarkers of oxidative damage meet several criteria and are better than previous biomarkers. To some extent, these new biomarkers of oxidative damage, such as 8-isoprostane and carbonyl protein, can accurately reflect the changes of oxidative damage (Morrow et al., 1990; Dalle-Donne et al., 2003). These new biomarkers will be reviewed in this thesis.

1.3.1.1 8-isoprostane

Isoprostanes are non-enzymatic free radical-catalysed peroxidation products of arachidonic acid, which are prostaglandin-like compounds (Morrow et al., 1990). They are also called F2- isoprostanes because they have F-type prostane rings. In structure, there are almost exclusive *cis* side chains to the cyclopentane ring in isoprostanes; while there are *trans* orientations in the prostaglandins. The formation of isoprostanes is

illustrated in Figure 1.3 (Morrow et al., 1990). In step 1, arachidonic acid abstracts a bis-allylic hydrogen atom. In step 2, an oxygen molecule is added to arachidonic acid, forming a peroxyl radical. In step 3, endocyclisation occurs. In step 4, prostaglandin-like compounds are formed by the addition of another molecule of oxygen. In step 5, these unstable prostaglandin-like compounds are transformed to be parent isoprostanes by the reduction of glutathione. Based on the carbon atom to which the side chain hydroxyl is attached, isoprostane regioisomers are denoted as 5-, 12-, 8-, or 15-series regioisomers (Taber, 1997). In theory, each isoprostane regioisomer has 16 stereoisomers. Thus, a total of 64 isoprostane isomers can be formed (Morrow et al., 1990). 5- and 15-series regioisomers were reported to be more abundantly present than 12-and 8-series regioisomers (Yin, 2004). Isoprostanes were formed in situ in esterified form to phospholipids in tissue, and could be released by phospholipases to form free isoprostanes (Morrow et al., 1992).

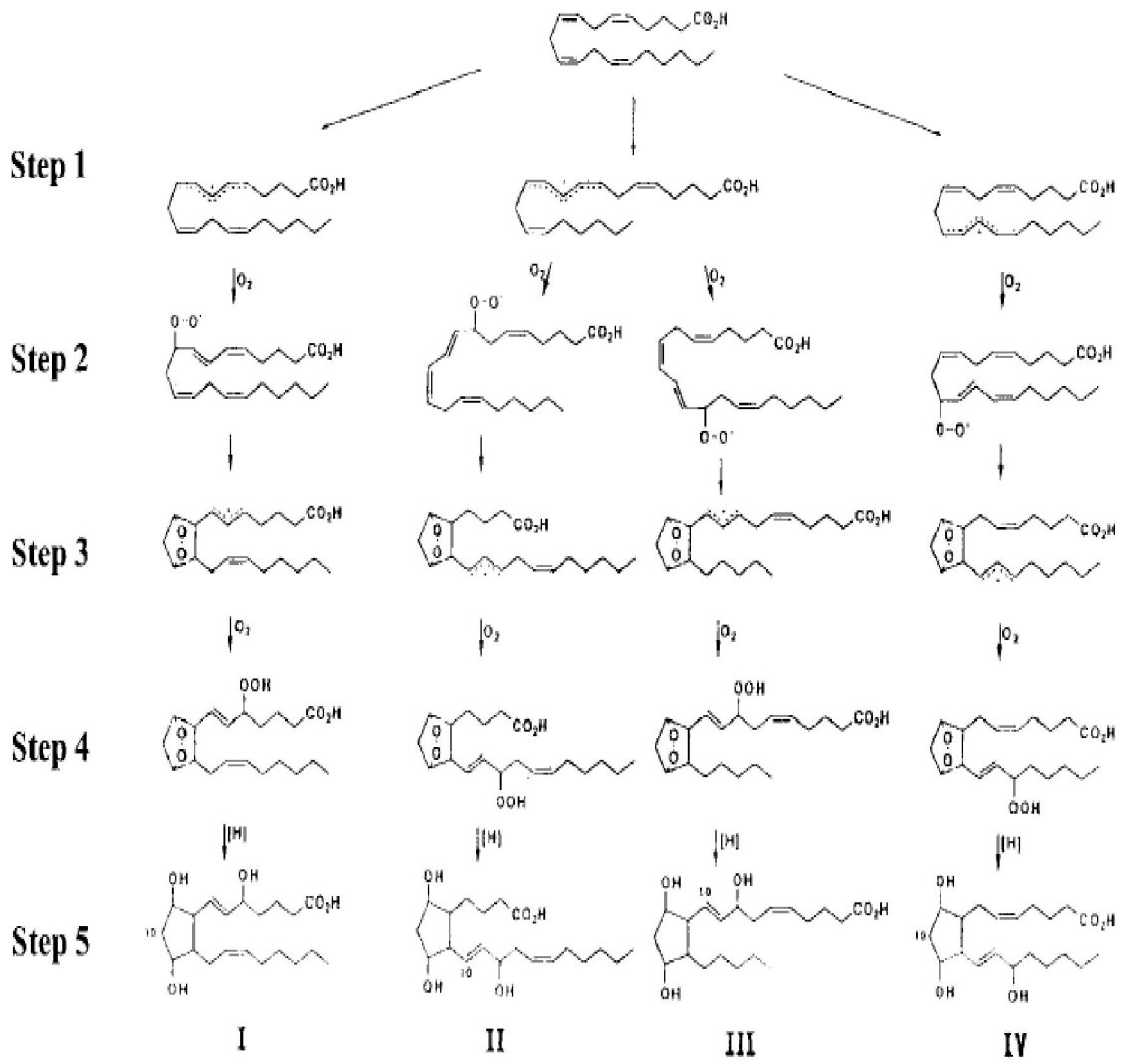

Figure 1.3 Mechanism of formation of isoprostanes (Reprinted with kind permission from Morrow et al., 1990)

8-isoprostane, a member of 15-series regioisomers, is the most extensively studied isoprostane and is considered to be a reliable biomarker of lipid peroxidation (Roberts LJ et al., 2000; Cracowski et al., 2002). 8-isoprostane is also called 8-iso-PGF2a, 8-epi-PGF2a and 15-F2t-isoprostane. 8-isoprostane is chemically stable and can be detected in many tissues or body fluids. More importantly, rats treated with carbon tetrachloride (CCl4), which is a classical model of oxidative stress, had a time- and dose-dependent increase of urinary and plasma 8-isoprostane (Kadiiska et al., 2005). 8-isoprostane was also reported to reflect oxidative stress in several kinds of diseases of animals and human beings, such as diabetes (Davi, et al., 1999; Murai et al., 2000) and atherosclerosis (Praticò et al., 1997), and could be modulated by dietary antioxidant supplementation (Roberts and Morrow, 2000). In addition, unlike malondialdehyde (MDA), 8-isoprostane is a specific free radical-catalysed lipid peroxidation product, which is not affected by diet (Richelle et al., 1999). 8-isoprostane can be measured by several methods, such as gas chromatography with mass spectrometry (GC-MS), liquid chromatography (LC)-MS, LC-MS-MS and enzyme immunoassays. MS based methods are regarded as the best methods because of its high sensitivity and specificity (Roberts and Morrow, 2000). However, MS based methods require expensive equipment and well-trained technical personnel, making these methods unavailable for general laboratories. Enzyme immunoassays have been widely used in this research area owing to the low cost and relative ease of use, even though they have less sensitivity and specificity than MS based methods. To avoid these problems, purification of samples is desirable before immunoassay. Urine and plasma samples after purification by immunoaffinity or solid phase extraction give good correlation to GS-MS method. A recent report also showed

that the detection of urinary 8-isoprostane was well consistent between GS-MS method and immunoassay method in CCl4 -induced oxidative stress in rats (Kadiiska et al., 2005). But, the accuracy of detecting 8-isoprostane in tissue samples is still problematic using immunoassay method because 8-isoprostane extracted from tissue samples may bring potential bias.

Compared with plasma samples, urine samples have several advantages in 8-isoprostane assay. The circulating half life of 8-isoprostane is only about 16 minutes so that plasma 8-isoprostane only reflect a single time point, while 24 hour urinary 8-isoprostane can overcome this problem (Proudfoot et al., 1999). In addition, plasma samples are lipid-containing samples, which are easy to generate artifactual 8-isoprostane, whereas urinary 8-isoprostane is relatively stable. Finally, urinary 8-isoprostane is a 'whole body' measurement because most of them come from the blood circulation (Meagher et al., 1999; Burke et al., 2000), even though one part of urinary 8-isoprostane originates from the kidneys. Thus, 24 hour urinary 8-isoprostane assay is used as a general marker of oxidative stress in our experiments.

1.3.1.2 Protein carbonyl

Protein carbonyl is the most commonly used and well characterized biomarker of protein oxidation (Levine, 2002; Dalle-Donne et al., 2003). There are several sources of the formation of protein carbonyl. (1) A main source of protein carbonyl in biological samples is from direct oxidation of lysine, arginine, proline and threonine amino acid

residues. Metal-catalysed oxidation of protein systems catalyze the conversion of arginine and proline to glutamic semialdehyde and the conversion of lysine to aminoadipic semialdehyde, which are the major carbonyl products of metal-catalysed oxidation of proteins (Requena, et al., 2001). (2) Proteins react with aldehydes (4-hydroxy-2-nonenal, malondialdehyde) derived from lipid peroxidation, causing carbonyl groups to be introduced into proteins (Esterbauer et al., 1991). (3) The reaction of reducing sugars or their oxidation products with lysine residues of proteins generates reactive carbonyl derivatives (ketoamines, ketoaldehydes, deoxyosones), which further react with proteins and then introduce carbonyl groups into proteins (Baynes, 1996). Thus, protein carbonyl has been widely used as a biomarker of protein oxidation.

The physiological importance of protein carbonyl has been identified. Glutamine synthetase was inactivated by introducing carbonyl groups to this enzyme (Levine, 1983). In addition, carbonylation affects the degradation of protein. For example, when sufficient iron caused the metal-catalysed oxidative modification of iron regulatory protein 2, carbonylated iron regulatory protein 2 was ubiquitinylated and then degraded by the proteasome (Iwai K et al., 1998). Most of the protein carbonyl is irreversible and repaired by protein turnover. Only a few protein carbonyls are reversible such as methione sulfoxide (Moskovitz et al., 1995).

Several methods have been developed to quantitate protein carbonyl. The most common and reliable method is based on the reaction between protein carbonyl with 2, 4-dinitrophenylhydrazine, forming a 2, 4-dinitrophenylhydrazone, which can be analyzed

spectrophotometrically (Levine, 2002). This method is used to determine protein carbonyl in most investigations. In addition, Western blot and ELISA techniques are also available because antibodies directed against the dinitrophenyl group are commercially available. The advantage of Western blot analysis is the ability of identifying specific oxidatively modified protein.

Protein carbonyl is a good biomarker of age related protein oxidation, as supported by the following facts. (1) An age-related increase in protein carbonyl has been found in different species, such as C. elegans (Adachi et al., 1998), rat liver (Starke-Reed, et al., 1989) and human brain (Smith et al., 1991). (2) Methionine sulfoxide reductase knockout mice had a reduced life span with increased protein carbonyl (Moskovitz et al., 2001). (3) Mice fed with a calorie restriction diet had an increased life span with decreased level of protein carbonyl (Youngman et al., 1992). (4) Strains of short life span houseflies had higher levels of protein carbonyl than their longer lived strains, when compared at the same chronological age (Sohal et al., 1993).

1.4 Animal models in aging research

The animal models in aging research include invertebrates and vertebrates. Invertebrates, such as caenorhabditis elegans and drosophila, have been used for identifying possible pathways and genes that influence longevity. For example, the increased expression of Sir-2 gene could extend the lifespan of caenorhabditis elegans by up to 50%, which suggested that Sir-2 was an important longevity controlling gene (Tissenbaum et al., 2001). In addition, the short lifespan of invertebrates makes them useful animal models

to screen the possible anti-aging compound. However, considerable differences in age-related pathologies between invertebrates and vertebrates limit invertebrates as animal models for evaluating the likely effect of anti-aging interventions on humans in future.

Rodents are the most widely used animal models in aging research. More than 70% of total animal models used in aging research were rat and mice (Masoro, 1998). There are some advantages of using rodents as animal models in aging research. (1) They are mammals and their life span is relatively short. (2) Rodents have been extensively used as animal models in many biomedical research fields for many years. Extensive information about their pathological and gerontologic characteristics is available, which is very useful for designing further gerontologic experiments (Masoro, 1998).

1.4.1 Fischer 344 rat

The Fischer 344 rat originated at Columbia University Institute for Cancer Research in 1920 (Boorman et al., 1990). National Institutes of Health (NIH) bred Fischer 344 rats in 1951(Hansen et al., 1982). National Institute on Aging (NIA) bred Fischer 344 rats using Harlan Sprague Dawley Inc.'s pedigreed stock that came from NIH stock in 1988. The Fischer 344 rats became a standard animal model to be used in the study of aging.

Fischer 344 rats are inbred rats. They were obtained by multiple sequential (brother x sister) mating applied for at least 20 generations so that their genetic background is homogeneous. The theoretical inbreeding coefficient is more than 0.99 (Falconer, 1981). Thus, the animals are genetically constant for a long time, even though new gene

mutations may cause some genetic changes over long periods. In order to avoid possible gene mutations, Fischer 344 rats from NIA are monitored regularly to detect genetic changes. In addition, inbred rats are phenotypic uniformity because they are genetically identical. This characteristic of Fischer 344 rats is of particularly importance for aging research because the aging process is under strong genetic control. For example, the overexpression of catalase or Klotho extended life span and slowed the aging process in mice (Schriner et al., 2005; Kurosu et al., 2005). The experimental variation of inbred rats will be less than that of outbred rats because inbred rats are phenotypic uniformity. Thus, the study requires fewer inbred animals than outbred animals, and the results from different laboratories were more comparable. Finally, two individuals of inbred rats will only differ from nongenetic factors such as dietary conditions, which is helpful to evaluate the effect of antiaging intervention. One disadvantage of inbred rats is that the decline of breeding performance may be caused by “inbreeding depression” in the early stage of producing a new inbred rat, and then some inbred rats die out. However, it is not a problem in Fischer 344 rats because Fischer 344 rats have been bred for more than eighty years. No further decline in breeding performance in Fischer 344 rats is reported. Thus, Fischer 344 rats were chosen as the animal model in this study.

The Fischer 344 rat is very well characterized because it is a popular animal model in cancer and toxicology research. About 400 toxicity/carcinogenicity studies of the National Cancer Institute/National Toxicology Program (NCI/NTP) used the Fischer 344 rat as their animal model, which included data on over 100,000 rats and more than eight million histological slides. Based on these studies, Boorman et al exhaustively described

the pathology of Fischer 344 rats in “Pathology of the Fischer rat”, which also included relevant information from the anatomy, physiology and gerontology (Boorman et al., 1990). This book provided an invaluable resource for further study using the Fischer 344 rat as an animal model.

In aging research, the Fischer 344 rat is also very widely used. More than 50% of papers that were published in the Journal of Gerontology, a leading journal in aging research, used Fischer 344 rats as animal models (Weindruch et al., 1991). Through these studies, the gerontologic characteristics were elaborately described. Sass et al reported a median lifespan of 31 months in male rats and a median lifespan of 29 months in female rats (Sass et al., 1975).

Aging process of different tissues differs (Grune et al, 2001). The tissues that are more likely to follow the free radical theory of aging were chosen for this study. Liver, kidney, cochlea and auditory cortex tissues were chosen as candidates in this study because these tissues have relatively high oxygen consumption (Rolfe et al., 1997; Susan et al., 2007; Mgbor et al., 2004) and a higher likelihood of having an imbalance in free radicals and antioxidant defenses, thus producing oxidative damage based on the free radical theory of aging (Rolfe et al., 1997). This inference has been supported by the fact that the increase of age related oxidative damage had been found in these tissues. Ward et al. reported that there were age related increases in lipid oxidation and DNA damage in kidney and liver tissues of Fischer 344 rats (Ward et al., 2005). Yee et al. also found similar results in kidney and liver tissues of Fischer 344 rats (Yee et al., 2006). Age-dependent increase in

lipid oxidation was also reported in brain tissues of Fischer 344 rats (Cai et al., 1996). Seidman et al. reported an age related increase in DNA damage in the cochlea of Fischer 344 rats (Seidman et al., 2000).

In kidney tissue of Fischer 344 rats, the age related renal pathological changes are well characterized because chronic nephropathy is a very common and age-related renal disease (Maeda et al, 1985). Yu et al. classified age related renal pathological changes into Grade 0 (no lesions), Grade 1-4 (damage at different levels) and Grade E (end-stage lesions), based on glomeruli and tubule lesions, inflammation, interstitial fibrosis and cast formation (Yu, et al, 1982).Six-month-old rats were found to have Grade 1 lesions. The severity of renal pathology changes progressed with age. From 12-month-old to 18-month-old Fischer 344 rats, there were obvious age related pathological changes in kidney tissue, but renal function did not change obviously so that the detection of biomarkers was not affected (Maeda et al, 1985). Twenty-seven-month-old rats were found to have Grade E lesions, and their renal function was significantly decreased (Maeda et al., 1985). In addition, the age related decrease in the activities of antioxidant enzymes in kidney tissues has been reported in several research groups (Rao et al., 1990; Tian et al., 1998), which was proposed to explain age related increase in oxidative damage. There were only limited studies on the gene expression of antioxidant enzymes in kidney during the aging process in Fischer 344 rats.

In liver tissue of Fischer 344 rats, the age related pathological change is not very distinct. The incidence of bilary hyperplasia and portal fibrosis increased with age, but the

hepatocytes did not have obvious changes (Yu, et al, 1982). The decline of liver function during the aging process was relatively small (Maeda et al, 1985).Several studies reported the age related decrease in the activities of antioxidant enzymes in liver tissues, which might be one reason of age related increase in lipid peroxidation (Rao et al., 1990; Tian et al., 1998; Grune et al, 2001). However, the effect of age on the gene expression of antioxidant enzymes in liver tissues was only limitedly studied and findings were contradictory (Rao et al, 1990; Thomas et al, 2002).

The cochlea in the Fischer 344 rat during the aging process has been extensively studied because it is a common animal model of age related hearing loss. Fischer 344 rats have a dramatic, progressive age related hearing loss, mainly at high frequencies in Fischer 344 rats older than 12 months (Popelar et al., 2006). The pattern of age related hearing threshold changes in Fischer rats is similar to age related hearing loss in human beings (Meisami et al., 2002), indicating that it is a suitable animal model for investigating age related hearing loss. From pathological data, the pronounced outer hair cell loss in the cochlea has been observed in old Fischer 344 rats. The number of outer hair cell loss was more than 50%, and the number of inner hair cell loss was relatively small and did not exceed 10% in old Fischer 344 rats (Popelar et al., 2006). Auditory cortex is the central neural system for hearing function and might participate in the formation of age related hearing loss (Jennings et al., 2001). The gene expression of antioxidant enzymes in the cochlea and auditory cortex in Fischer 344 rats has not been reported until now, which may be caused by the fact that gene expression is hard to detect in these small tissues.

The incidence of spontaneous diseases, especially cancer, started to increase after the middle age in Fischer 344 rats (Sass et al., 1975). The obvious age related renal pathological changes and hearing function changes from 12-month-old to 18- month-old Fischer 344 rats. Thus, the middle-aged Fischer 344 rats were chosen as animal model to evaluate whether the effects of GSE and CR could prevent age related change.

1.5. The methods of gene quantification

Because the major regulation of cellular function takes place through gene expression, accurate gene expression quantification is important to understand the mechanisms of aging and anti-aging interventions.

Investigating gene expression relies on techniques to detect mRNA, which includes several methods such as northern blot analysis, ribonuclease protection assay, conventional reverse transcription-polymerase chain reaction (RT-PCR) and real time RT-PCR. In the past, Northern bolt analysis was widely used because this technique was relatively easy. Different RNA species were separated based on size by denaturing gel electrophoresis and detected by isotopic or non-isotopic labeled probes. This method can assess the size of mRNA and compare the abundance between samples on a membrane. However, its sensitivity is limited and RNA quality obviously influences the reliability of this method (Reue et al., 1998). In addition, the requirement of large amounts of RNA makes it impossible to detect gene expression change from small samples, such as cochlea and auditory cortex. A more sensitive method is ribonuclease protection assay,

which could detect 5pg mRNA and provided at least 10-fold higher sensitivity than Northern blot (Dvořák et al., 2003). But, similar to Northern blot assay, densitometry is also used to quantify the mRNA, which limits further improvement on the sensitivity of ribonuclease protection assay.

The sensitivity of conventional RT-PCR has been largely improved, compared to the relatively low sensitivity in northern blot analysis and ribonuclease protection assay. However, the end point of PCR reaction analyses used in this approach influences the accuracy of the results. A PCR reaction can be divided into four phases: lag, exponential, linear and plateau phase (Freeman, 1999). Four phases are related to the change in PCR reaction efficiency, which is caused by the decrease of reagent concentration and enzyme instability during PCR. Conventional RT-PCR measures the total of accumulated PCR product at the end of the PCR cycle, which is from the non-exponential phase and are not accurate. Moreover, agarose gels are used to detect final product, which limits the sensitivity of this method and increases the possibility of contamination, causing false positive detection.

1.5.1. Real time RT-PCR

Real time RT-PCR is the most sensitive and popular technique of gene quantification (Bustin, 2002), which is about 10,000 and 1,000 times more sensitive than northern blot and ribonuclease protection assay, respectively (Dvořák et al., 2003). Real time RT-PCR has overcome the drawback conventional RT-PCR of by collecting all information from

the PCR product changes during PCR reaction, using fluorescent reporter dyes. The number of amplified product generated is directly proportional to the increase of fluorescent reporter dyes during the exponential phase of PCR. The data acquired in the exponential phase of amplification are analyzed because amplification only in this phase is extremely reproducible and precise. In the exponential phase, there is a doubling of PCR product every cycle since all of the PCR components are available. Thus, real time RT-PCR can quantify gene expression more reliably.

1.5.2. Two major formats of Real time PCR

Real time RT-PCR has two major formats, SYBR Green I dye and probe format. The principle of the SYBR Green I dye is that the SYBR Green I dye will bind all double-stranded DNA, and generate increasing fluorescence at the same time without inhibition of PCR. During the progress of PCR, more PCR product is generated. The increase in fluorescence signal is proportionate to the amount of PCR product during each PCR cycle through the SYBR Green I dye binding to double-stranded DNA. The advantages of the SYBR Green I dye are as follows. (1) Assay setup and running costs are more economical, compared with probe methods because no probe is required. (2) The assay design is relatively simple because only two primers are needed and probe design is not necessary. The disadvantages of the method include the relatively lower specificity because the SYBR Green I dye binds to any double-stranded DNA and it also bind to the possible nonspecific PCR products. The optimizations of PCR and melt curve analysis

are necessary to avoid this problem. In addition, the format cannot be used to detect several target genes in a single PCR reaction.

Probe format has several kinds of probes generated by different companies. The basic principle is similar, using fluorescent resonance energy transfer (FRET) or similar interactions between donor and quencher molecules. The most popular probe is Taqman probe, which is an oligonucleotide probe containing a reporter fluorescent dye on the 5´ end and a quencher dye on the 3´ end. When the probe is intact, the quencher dye greatly decreases the fluorescence emitted from the reporter dye by fluorescence resonance energy transfer (FRET). During the progress of PCR, Taqman probe anneals PCR products and is cleaved by the 5´ nuclease activity of Taq DNA polymerase, which causes the separation of the reporter dye and the quencher dye, thus increasing the reporter dye signal. The increase in fluorescence signal is directly proportionate to the amount of amplicons during each PCR cycle. The advantages of this method are the improved specificity from the specific probes binding to amplicons, and detecting several target genes in a single PCR tube by being labeled with distinguishable reporter dyes. The major disadvantage of the method is the expensive costs, particularly multiple genes to be quantified.

1.5.3 Challenges and strategies

Real time RT-PCR includes three steps: (1) RNA isolation and quantification. (2) cDNA was synthesized from RNA through reverse transcription (3) real time PCR amplification using cDNA as the template.

With the increasing use of real time RT-PCR in gene quantification, some problems that influence the accuracy of this method have been widely noticed. The quality of RNA is regarded as the most important determinant of the reliability of real time RT-PCR (Bustin and Nolan, 2004). The quality of RNA includes the RNA integrity and whether it is free of genomic DNA contamination. The degradation of RNA is the most noticeable problem because the ubiquitous RNase is ready to cause the degradation of RNA, which directly affects the accurate gene quantification using real time RT-PCR method. The best way is to evaluate RNA integrity, using formaldehyde gel electrophoresis or 2100 Bioanalyzer to inspect the 28S and 18S ribosomal RNA bands. For a limited amount of RNA, such as the total RNA extracted from cochlea, 2100 Bioanalyzer is the only choice. In addition, genomic DNA contamination is common during RNA isolation. Bustin showed that most of non-DNase treated RNA samples isolated from tissue samples had genomic DNA contamination (Bustin, 2002). Genomic DNA will obviously prevent accurate quantification, especially when studying genes with unknown intron/exon structure, or the existence of pseudogenes (Overbergh et al., 1999). Peters et al. exhaustively discussed the necessity of combining on-column and off-column DNase treatment in real time RT-PCR and its impact on efficiency of removing genomic DNA contamination (Peters et al., 2004).

1.5.3.1 The selection of housekeeping gene in real time RT-PCR

How to choose the appropriate housekeeping gene (HKG) is another major challenge of real time RT-PCR. HKG corrects variation in RNA integrity, reverse transcription efficiency and initial sample amount among different samples (Dheda et al., 2004). These widely used HKGs have been assumed to be stable in previous experiments. In fact, they vary so considerably that invalid HKGs can cause confusing, even misleading interpretation of gene expression data. For example, in a study of the effect of inhaled corticosteroids on human asthma, when interleukin-2 was normalized to β-actin, a significant difference was detected between the control group and the treatment group. In fact, the difference was not due to interleukin-2, but β-actin gene expression that changed during that study (Glare, et al., 2002). Glyceraldehyde-3-phosphate dehydrogenase (GAPDH), a common used HKG, has also been questioned because it varied in many experimental conditions (Ke et al., 2000, Suzuki et al., 2000). This might partly be attributed to the fact that GAPDH was not only implicated in the basal cell metabolism as an important glycolytic pathway enzyme, but also participated in other functions, such as DNA replication and repair, phosphotransferase activity, cytoskeletal organisation and exocytotic membrane fusion (Sirover 1999). In addition, 18S rRNA was regarded as unsuitable HKG because its high abundance, compared with most target mRNAs, might cause different amplification kinetics in real time PCR. In addition, the transcription of rRNA could be affected by biological factors and drugs (Spanakis, 1993). It has been recognised that a valid HKG is a prerequisite for accurate quantification, especially for in vivo samples, which vary more obviously than in vitro samples. However, unfortunately,

the expression of these assumed HKGs vary greatly in different tissues and different experimental conditions, making the selection of a 'universal' HKG for all experiments problematic. This has brought about the proposal that appropriate HKGs should be validated in each specific experiment (Vandesompele, 2002).

There are some software packages available that can be used for the process of HKG validation. The GeNorm software is regarded as the authoritative method for analysis and is consequently the most popular method used (Bustin, 2004). It chooses a valid HKG based on average expression stability values that represent the average pairwise variation of a HKG compared with all other HKGs. In iterative steps, the least stable HKG was excluded in each step, and finally the two most stable HKG were found. The two most stable HKGs could not be further ranked because gene ratios were used for gene stability measurement. Lower average expression stability values indicate more stable gene expression. The use of more than one HKG for normalization has been proposed because of the obvious HKG expression variations in some experiments. In those cases, the normalization factor calculated from several HKGs was believed as a robust method, bringing more accurate normalization (Huggett et al., 2005). The cost and limited amount of samples may restrict the application of the normalization factor using two or more HKGs.

However, co-regulation of HKGs will influence the efficiency of GeNorm method because of the pairwise comparison used in this method. Trying to predict the co-regulation of HKGs is difficult because in addition to their basic roles, some HKGs also

have other diverse functions (Singh et al, 1993; Ishitani et al, 1996). The alternative software Normfinder ranks gene stability by stability values which are derived from intra-group variation and inter-group variation (Andersen et al., 2004). According to their theory, this method may be more effective to control the influence of co-regulation of HKGs and can choose the stablest HKG, instead of the two most stable HKGs by GeNorm software. Compared to GeNorm software, it is less used in published paper partly because GeNorm software was available earlier and easier to use than Normfinder software. Thus, both methods were used in this study to select for the appropriate HKG in the detection of aging process in animal tissues.

.

1.5.3.2 The appropriate housekeeping gene chosen in aging research

In aging research, real time RT-PCR has been increasingly used to detect changes in gene expression (Masternak et al., 2004; Mohamed et al., 2004; Salles et al., 2005). However, as yet there has not been a study to identify valid HKGs to use in aging research. Under certain experimental conditions and disease states, the expression of some HKGs can vary greatly whilst other HKGs remain relatively stable (Thellin et al., 1999; Warrington et al., 2000). Because these candidate genes affect the final chosen HKG, we try to choose the possible stable HKGs for kidney, liver, cochlea and auditory cortex from available information, respectively. In the present study, we used real time RT-PCR to study the expression of commonly used HKGs: β-actin, GAPDH, ubiquitin C (UBC), HPRT, EF, cyclophilin A (CYPa) or tyrosine 3-monooxygenase/tryptophan 5-monooxygenase activation protein, zeta polypeptide (YWHAZ) in young and old Fischer

344 rats and chose a valid HKG using the HKG identification softwares, GeNorm and Normfinder. The chosen HKGs were selected as they all have different physiological functions - cytoskeleton (β-actin), carbohydrate metabolism (GAPDH), protein folding (CYPa), metabolic salvaging of nucleotides (HPRT), protein degradation (UBC), translation elongation factor activity (EF) and signal transduction (YWHAZ), thus minimizing the risk that the aging process would affect all these genes. Each of the genes studied here has been recommended as a suitable HKG in at least one biological condition (Choi et al., 1991; Foss et al., 1998; Warrington et al., 2000; Wall et al., 2002; Kim et al., 2003; Biederman et al., 2004; Peinnequin et al., 2004;). GAPDH, β -actin and 18s rRNA or 28s rRNA were the most commonly used HKGs for gene expression studies (Suzuki et al., 2000). But, 18s rRNA or 28s rRNA was continually argued as an inappropriate HKG because there was the differential gene expression pattern between mRNA and rRNA (Spanakis, 1993; Vandesompele et al., 2002). UBC and HPRT had relatively constant expressions in 13 different human tissues (Vandesompele et al., 2002). EF was also regarded as a stable HKG in many experimental conditions (Warrington et al., 2000; Hamalainen et al. 2001). Kim et al showed that UBC was recommended as the stable HKG in liver diseases (Kim et al., 2003), while YWHAZ was recommended as the stable HKG in kidney disease (Biederman et al., 2004). So, for liver aging studies in this thesis we chose the most stable HKG from the HKGs reported in literature (β-actin, GAPDH, HPRT, CYPa and UBC). Based on literature the suitable HKG for kidney aging was chosen from β-actin, GAPDH, HPRT, EF and YWHAZ, and for cochlea and auditory cortex aging from β-actin, GAPDH, UBC, HPRT, and EF.

Chapter II: Objectives and Significance

Objectives

We hypothesized that GSE and CR attenuated age related oxidative damage in middle-aged rats. Further, the molecular mechanisms mediating the prevention of oxidative damage by GSE and CR were explored by microarray, and confirmed by real time RT-PCR. The extent of protective effects of GSE and CR was evaluated by pathological grade.

This study consisted of two parts:

I) Intrinsic antioxidant defense changes in liver, kidney, cochlea and auditory cortex during the aging process.

For detecting gene expression changes in the intrinsic antioxidant defence system, real time RT-PCR with valid HKG protocol was established. The mRNA expression changes of major antioxidant enzymes with age were explored in rat liver, kidney, auditory cortex and cochlea by real time RT-PCR with validated HKG method. The most suitable tissue for the evaluation of anti-aging intervention of GSE and CR were chosen.

II) Evaluate effects of GSE and CR on age related oxidative damage and gene expression profile in middle-aged rats.

1) Effects of GSE and CR on age related oxidative damage and age related renal pathological changes, using 8 isoprostane and carbonyl protein as oxidative markers.

2) Explore the molecular mechanisms mediating the prevention of oxidative damage by GSE and CR using microarray and real time RT-PCR from gene expression level in rat kidney tissue.

In order to illustrate the experimental design of objective I and II, a flow chart is summarized in Figure 2.1 and Figure 2.2, respectively.

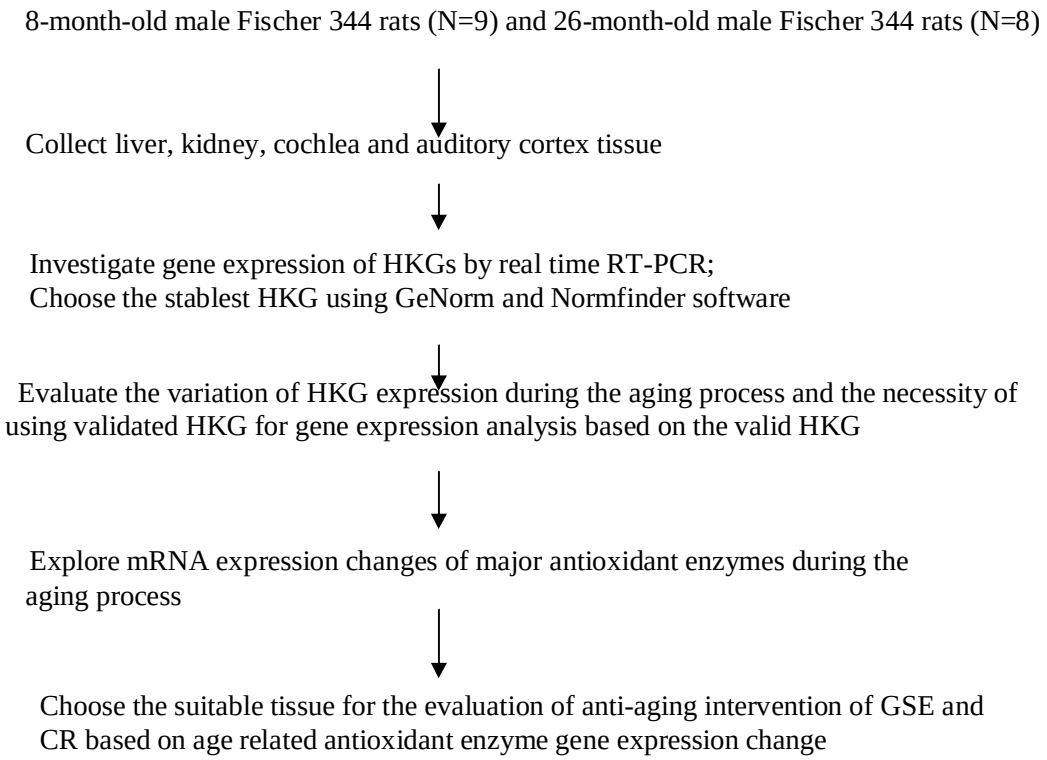

Figure 2.1 the flow chart of evaluating antioxidant enzyme gene expression change in the aging rat liver, kidney, auditory cortex and cochlea

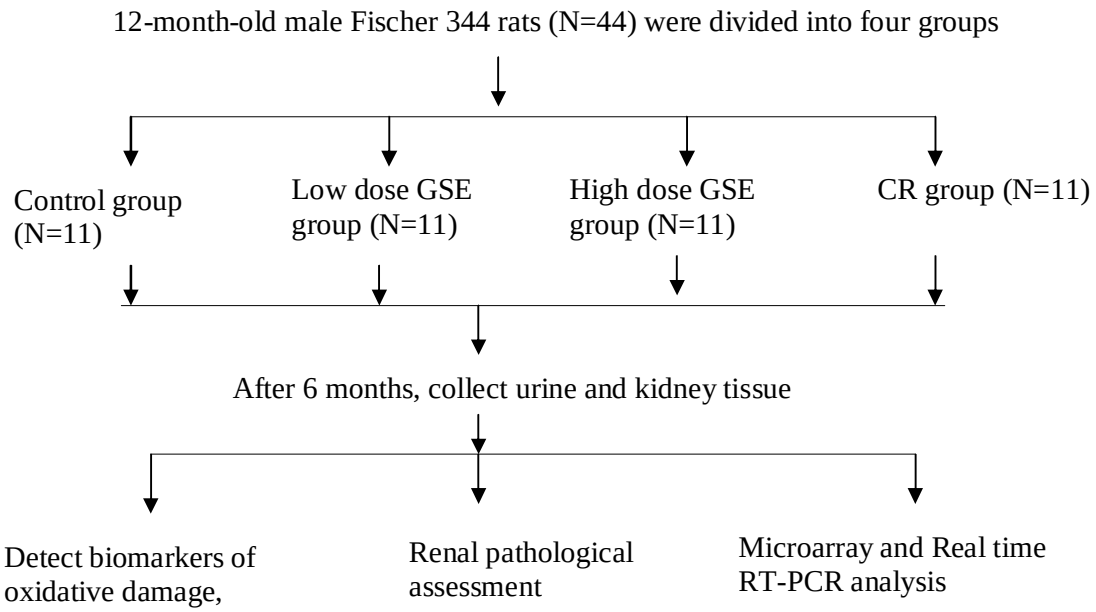

Figure 2.2 the flow chart of evaluating effects of GSE and CR on age related oxidative damage and gene expression profile in middle-aged rats

Significance

The free radical theory of aging relies heavily on two major components, the formation of free radicals and antioxidant protection. Antioxidant enzymes constitute the major part of the antioxidant protection system. More recently, investigations on age related antioxidant enzyme gene expression changes are becoming fundamental parts of aging research. Investigating age related antioxidant enzyme gene expression changes in four different rat tissues not only helped us choose the most suitable tissue to effectively evaluate the effect of GSE and CR on age related oxidative damage, but also answered the fundamental question in aging.

Real time RT-PCR with valid HKG protocol was established for accurately quantifying age related antioxidant enzyme gene expression changes. This is the first report discussing validation of HKGs in aging research, which will improve gene quantification not only by real time RT-PCR, but also by other methods that use HKGs for normalization, such as Northern blot analysis. For the first time a wide variation in HKG expression was found during the aging process in liver, kidney, cochlear and auditory cortex of rats. Our studies showed that choosing appropriate HKGs was vital for accurate gene quantification and analysis in aging research because invalid HKGs caused the misinterpretation of gene expression levels, even though aging was regarded as a physiological process. In addition, the real time RT-PCR with valid HKG protocol was

also very useful to validate the microarray data, which was used to explore the molecular mechanism of the effects of GSE and CR on age related oxidative damage.

This is the first report using real time RT-PCR with a validated HKG to accurately evaluate antioxidant enzyme gene expression changes in the rat liver, kidney, cochlea and auditory brain during the aging process, which provides us with a better understanding of the mechanisms of aging. We found that age related antioxidant enzyme gene expression changes in these four tissues were different, and the most obvious antioxidant enzyme gene expression changes occurred in kidney tissue. Thus, kidney tissue was chosen as the suitable tissue to evaluate the effects of GSE and CR on age related oxidative damage.

2.2 Evaluate effects of grape seed extract and calorie restriction on age related oxidative damage and gene expression profile in middle-aged rats

With increasing understanding of the aging process, aging research becomes a more and more intriguing research area. Currently, the only generally accepted intervention to retard aging across many species is CR that was initiated after weaning or early in life (Weindruch, 1996). More significantly, age related diseases are also prevented by CR (Weindruch, 1996). But, the practicability of CR limits the application of CR in human being because CR means eating less than 30-40% for a long time. Based on the free radical theory of aging, antioxidant intervention is regarded as a more reasonable and practical approach (Finkel et al, 2000). GSE has powerful antioxidant effects and multiple biological activities. The main active constituent of GSE is proanthocyanidins,

which was proposed to be related to increased longevity from epidemiological data (Corder et al., 2006). But, the relation between aging and proanthocyanidins was less known.

This is the first report to explore the effect of GSE supplementation on the gene expression profiling of whole genome in vivo. In addition, we showed that GSE could reduce age related lipid oxidative damage based on measuring 8 isoprostane, a reliable marker of lipid peroxidation. This paper will be helpful to other researchers to further investigate the potential therapeutic effects of GSE. Moreover, age related diseases are also closely related with oxidative damage. It can be suggested that GSE might have the potential therapeutic effects for age related diseases because GSE can effectively prevent age related oxidative damage.

In addition, this is also the first report to explore the effect of CR in middle-aged rats on the gene expression profiling of whole genome in kidney tissue. Our data showed that age related oxidative damage and age related renal pathological changes were effectively decreased by adult-onset CR, suggesting that CR initiated in middle-aged was a promising rejuvenation model in aging studies.

Chapter III: Materials and Methods

3.1 Antioxidant enzyme gene expression change in the aging rat liver, kidney, auditory cortex and cochlea

3.1.1 Animals and harvesting tissues

Young (8 months, n=9) and old (26 months, n=8) male specific pathogen free Fischer 344 rats were obtained from the National Institute of Aging (USA), and the livers and kidneys were removed following euthanasia. The Liver and kidney tissues were immersed in RNALater (Ambion, USA) overnight at 4 ℃ before storage at -20°C until analysis. Auditory cortexes, identified based on brain maps (Swanson, 1992), and cochleae were collected. Auditory cortexes were immersed in RNALater (Qiagen, Germany) overnight at 4 °C before storage at -20°C, and cochleae were frozen in liquid nitrogen and stored at -80°C. All animal procedures were approved by the Institutional Animal Care and Use Committee of National University of Singapore, Singapore.

3.1.2 RNA isolation using the RNeasy Mini kit and quantification

Total RNA was isolated from liver, kidney and auditory cortexes using the RNeasy Mini kit (Qiagen, Germany), based on the manufacturer's instructions. In brief, animal tissues were taken out for RNAlater and were weighed. After 600ul RLT buffer was added,

about 15mg tissue was homogenized by a power homogenizer. The tissue lysate was centrifuged for 3minutes at maximum speed, and then the supernatant was transferred to a new tube. After one volume of 70% ethanol was added and mixed, 700ul sample was loaded into RNeasy mini column and centrifuged for 15 s at 10,000 x g. It was followed by washing with 350ul Buffer RW1, and adding 80ul DNase I (RNase-free DNase set, Qiagen) incubation mix for 15 minutes at room temperature, and then washing with Buffer 350ul RW1. After RNeasy mini column was washed by 500ul Buffer RPE two times, the column was centrifuged at full speed for 1 minute in a new tube. Finally, RNA was eluted by 50 ul RNase-free water. To avoid contamination with genomic DNA, an off-column (Amplification Grade DNase I kit, Invitrogen, USA) was also performed, following the manufacturer's instructions. RNA sample, 1 ul10X DNase I Reaction Buffer, 1 ul DNase I, Amp Grade and DEPC-treated water were added into 0.5ml tube. After the incubation of 15 min at room temperature, 1 ul of 25 mM EDTA solution was added to the reaction mixture and heated for 10 min at 65°C to make the DNase I inactivated. The concentration of total RNA was quantified using a spectrophotometer at 260nm, with the OD260/OD280 ratio routinely between 2.00 and 2.12.

3.1.3 RNA isolation using the RNAqueous-Micro Kit and quantification

Before RNA isolation, cochleae were immerged in RNAlater-ICE (Ambion, TX). All external cochlear tissue was removed. Bone parts of the cochlea were removed using fine forceps. Total RNA was isolated from the membranous parts of the cochlea using RNAqueous-Micro Kit (Ambion, TX), including DNase I treatment (Ambion, TX) to

remove genomic DNA contamination. In brief, cochlea in 100 µl Lysis Solution was homogenized by a power homogenizer. After that, one-half volume of 100% ethanol was added. 150ul sample was put into a Micro Filter Cartridge Assembly, and then 180 µl wash Solution 1, and 2 x 180 µl wash Solution 2/3 s were added sequentially to wash the filter. The column was centrifuged at full speed for 1 minute in a new tube. Finally, RNA was eluted by 10 µl preheated elution solution. 1 µL TURBO DNase and 0.1 volume 10X TURBO DNase Buffer was added to the RNA, and then incubated at 37˚C for 30 minutes. 0.1 volume 10X TURBO DNase Buffer was added and incubated for 2 minutes at room temperature. After centrifuging, RNA was transferred to a fresh tube. To effectively control genomic DNA contamination, a second DNase digestion of total RNA from cochleae was carried out using Amplification Grade DNase I kit (Invitrogen, CA), according to the manufacturer's instructions. The quality of total RNA was evaluated by an Agilent 2100 Bioanalyzer (Agilent, CA) using RNA 6000 Nano kit, which also quantify total RNA from auditory cortexes (in triplicate). Only qualified samples were further investigated. Since the concentration of total RNA from cochleae was below the detectable limit by Bioanalyzer, it was quantified by Tecan Safire² (Switzerland) using Ribogreen RNA quantitation kit (Molecular Probes, CA) in triplicate.

3.1.4 RNA integrity analysis using formaldehyde agarose gel electrophoresis.

RNA integrity from kidney and liver tissue was evaluated by formaldehyde agarose gel electrophoresis, following the protocol in the manual of Qiagen RNeasy Mini kit. The high secondary structure of RNA could be denatured by formaldehyde. Mixed 2 gram

agarose, 10ml 10X formaldehyde agarose buffer (200mM MOPS, 50mM sodium acetate and 10mM EDTA) and 90 ml RNase free water. After the mixture being heated to melt agarose, 8ml 37% formaldehyde and 1ul of 10 mg/ml ethidium bromide were added into the cooled mixture. The mixed gel was immediately poured into a gel tank to assemble. After 30 minutes, 1X formaldehyde agarose buffer was added to cover the gel. About 1 ug RNA was incubated with 5X loading buffer for 5 minutes at 65˚C, chill on ice, and then loaded into the wells of the gel. Electrophoresis was carried out at 5V/ml for about 1 hour. The bands were visualized on a UV transilluminator.

3.1.5 RNA integrity analysis using Agilent 2100 Bioanalyzer

RNA integrity from cochlea and auditory cortexes tissue was evaluated by Agilent 2100 Bioanalyzer (Agilent, CA) using RNA 6000 Nano kit. Compared with formaldehyde agarose gel electrophoresis, Agilent 2100 Bioanalyzer only needed very small amount of RNA, which was suitable for cochlea and auditory cortexes because small amount of RNA from cochlea and auditory cortexes were available. In brief, 1 µl of RNA 6000 Nano dye was added into a 65 µl aliquot of filtered gel, and 9 ul of the gel-dye mix was loaded in appropriate wells in RNA 6000 Nano chip. After the chip was primed, 5 µl of RNA 6000 Nano marker and 1 µl of heat denatured RNA ladder or heat denatured sample were loaded in suitable wells, respectively. The chip was horizontally vortexed for 1 min at 2400 rpm, and then was put in the Agilent 2100 Bioanalyzer.

3.1.6 Reverse transcription

Based on accurate quantification of total RNA, the same amount of total RNA were loaded in reverse transcription. First-strand cDNA was synthesized using the SuperScript III First Strand Synthesis System (Invitrogen), according to the manufacturer's instructions with OligodT 20 and 600 ng RNA. Briefly, appropriate RNA sample, 1 ul 50 µM oligodT20, 1 ul 10 mM dNTP mix and DEPC-treated water were added to 10ul into 0.5ml tube. After the incubation of 5 min at 65°C, 10 µl of cDNA Synthesis Mix (2ul 10X RT buffer, 4ul 25 mM MgCl2, 2 µl 0.1 M DTT, 1ul RNaseOUT and 1ul SuperScript III RT) was added to the reaction mixture and incubated 50 min at 50°C. The reaction was terminated at 85°C for 5 min. 1 µl of RNase H was added and incubated for 20 min at 37°C. CDNA was stored at -20°C. One sample without reverse transcriptase (RT) was included as the negative control.

3.1.7 Optimization of Polymerase chain reaction and Real time PCR

Optimization was carried out using the QuantiTect SYBR Green PCR kit (Qiagen), using the gradient procedure of a DNA Engine Opticon 2 (MJ research, USA). The specificity of PCR products was confirmed by both melting curve analysis. Real time PCR was performed under optimal conditions using the following PCR amplification mixture (20µl total) – 2x QuantiTect SYBR Green PCR master mix, 0.3uM forward and reverse primers (Table 3.1), and 0.8ul of 1:10 dilution cDNA. The cycling conditions were: 15 minutes initial activation step at 95 °C; then 94°C for 15 s, annealed at optimal temperature for 30

s, and 72℃ for 30 s, repeated for 40cycles. Finally the melting curve analysis was performed, and samples were then cooled to 10 °C. Fluorescent data was acquired at high temperatures to avoid inference of non-specific fluorescence signals (Ball et al, 2003). Each assay included a no-template control and a RT negative control. For each gene tested, all samples were detected in triplicate in the same plate, avoiding inter-plate variation. A relative standard curve was produced from a three-fold dilution series across five data points to calculate amplification efficiencies and correlation coefficient (R^2). Amplification efficiencies were calculated using the equation: $E=10^{[-1/slope]}-1$.

Table 3.1 PCR primers for detecting housekeeping genes and antioxidant genes expression

Gene	5'-3' primer sequence		Reference
HPRT‡	For	CTCATGGACTGATTATGGACAGGAC	Peinnequin et al,2004
	Rev	GCAGGTCAGCAAAGAACTTATAGCC	
CYPA‡	For	TATCTGCACTGCCAAGACTGAGTG	Peinnequin et al,2004
	Rev	CTTCTTGCTGGTCTTGCCATTCC	
GAPDH	For	AGGGCTGCCTTCTCTTGTGAC	Zhang et al,2004
	Rev	TGGGTAGAATCATACTGGAACATGTAG	
UBC	For	TCGTACCTTTCTCACCACAGTATCTAG	Depreter et al,2002
	Rev	GAAAACTAAGACACCTCCCCATCA	
β-actin	For	ATCGCTGACAGGATGCAGAAG	Noda et al,2003
	Rev	AGAGCCACCAATCCACACAGA	
Cu/ZnSOD‡	For	CGAGCATGGGTTCCATGTC	Song et al,2001
	Rev	CTGGACCGCCATGTTTCTTAG	
Catalase‡	For	ACAACTCCCAGAAGCCTAAGAATG	Depreter et al,2002
	Rev	GCTTTTCCCTTGGCAGCTATG	
GPX	For	GGAGAATGGCAAGAATGAAGA	*
	Rev	CCGCAGGAAGGTAAAGAG	
EF	For	ATTGTTGCTGCTGGT GTTGG	#
	Rev	GTATGGTGGCTCGGTGGAA	
Mn-SOD	For	GCTGGCTTGGCTTCAATAAG	Pang et al,2002
	Rev	AATCCCCAGCAGTGGAATAA	

For - forward primer, Rev - reverse primer

‡ - Indicates primer sets that flanked intron sequences

* These primers were designed by Prime 3, and the accession number of GPX was X12367.

These primers were designed by Prime 3, and the accession number of EF was NM_175838.

3.1.8 HKG stability analysis

GeNorm 3.4 and Normfinder were used to evaluate HKG stability. GeNorm ranked gene stability by average expression stability values (M), which was the average pairwise variation of a HKG compared with all other HKGs. Normfinder ranked gene stability by stability values which were derived from intra-group variation and inter-group variation. More stable gene expressions indicated lower average expression stability values.

3.1.9 Normalization factor determination by GeNorm

The normalization factor (NF) was calculated from multiple HKG and was thought to be a more accurate method of normalization. In our experiment, a NF from HPRT-GAPDH-β actin was determined by GeNorm. The theory of choosing and calculating NF by GeNorm was described in Vandosempele et al (2002). From the stability analysis using GeNorm, it was known that the two most stable HKGs in our experiment were HPRT and GAPDH. The NF2 was based on the expression levels of these two genes and furthermore calculated using different combinations of genes by including the most stable remaining control gene (HPRT-GAPDH- β actin (NF3), HPRT-GAPDH- β actin-CYPa (NF4), and HPRT-GAPDH- β actin-CYPa-UBC (NF5)). For every series of NFn and NFn+1, pairwise variation was calculated, for example, NF2:NF3, then NF3:NF4 and finally NF4:NF5. A high pairwise variation value meant that the added gene had a significant effect on normalization and should be included in the NF. According to Vandosempele et al (2002), the ideal pairwise variation value is less than 0.15. Thus,

following the pair-wise variation analysis, it was decided that the NF would be derived from HPRT-GAPDH-β actin in our experiment.

3.1.10 Data analysis

Data analysis of HKG stability was carried out according to the manual of GeNorm 3.4 (http://medgen.ugent.be/%7Ejvdesomp/genorm/) (Vandesompele et al., 2002) and Normfinder (http://www.mdl.dk/publications_normfinder.htm) (Andersen et al. 2004), respectively. GeNorm software, an authoritative and popular method (Bustin and Nolan, 2004), chooses a valid HKG based on average expression stability values, which represent the average pair wise variation of a HKG compared with all other HKGs. But, average expression stability values are influenced by co-regulation of HKGs. In order to resolve this problem, the alternative software Normfinder was also used because it ranks genes according to their stability values, which are derived from intra- and inter- group variations and are more effective in controlling the influence of co-regulation of HKGs. Statistically significant differences were evaluated by the Mann Whitney U non parametric analysis. p values below 0.05 were considered significant differences. Data was presented as the mean ±SE (standard error).

3.2 Effect of grape seed extract and CR on gene expression

3.2.1 Animals and harvesting tissues

Specific pathogen free 12 months male Fischer 344 rats were obtained from (NIA, Bethesda, MD). The control group (n=11) was fed with NIH31 diet ad libitum. GSE (Interhealth Nutraceuticals Incorporated, Benicia, CA) was added to the NIH31 diet at the concentrations of 0.2% (w/w) as low dose group (n=11) and 1% (w/w) as high dose group (n=11). CR group(n=11) was fed with NIH31/NIA Fortified diet, which was enriched in vitamins to make sure the same level of vitamins consumption with control group to avoid the potential confounding in antioxidant supplement experiment. CR is gradually initiated from12 months of age, at first week at 10% restriction, increased to 25% restriction at second week and to 40% restriction at third week and was maintained throughout the experiment, according to the CR protocol of National Institute of Aging. Food consumption was measured every week. Animals were weighed every week in the first 3 months, and every two weeks in the last three months since the animal weight was relatively stable during this period.

After six months, 24h urine was collected by metabolic cages and stored at -80°C in the presence of 0.005% BHT, to avoid oxidative formation. These animals were sacrificed via anesthesia using a mixture of ketamine (40mg/kg) and xylazine (10mg/kg) by intraperitoneal injection. Before samples collection, a perfusion was performed using PBS solution. A portion of the renal cortex was collected and stored at -80°C for further

use, and the other portion was immersed in RNALater (Ambion, TX) overnight at 4 °C before storage at -20°C. In addition, a part of kidney tissue was placed in 4% paraformaldehyde to fix. These tissue were processed in the Tissue-Tek® VIP™ 5 Vacuum Infiltration Processor (Sakura finetek, USA), and paraffin-embedded for histological evaluation. All animal studies in this paper were approved by the Biological Resource Centre Institutional Animal Care and Use Committee.

3.2.2 RNA isolation, quantification and integrity analysis

RNA isolation and integrity analysis were carried out as previously described in 3.1.2 and 3.1.5, respectively. Briefly, total RNA was isolated using the RNeasy Mini kit (Qiagen, Germany) with on-column DNase digestion step using RNase-free DNase set (Qiagen, Germany). To effectively control genomic DNA contamination, a second DNase digestion of total RNA was carried out using Amplification Grade DNase I kit (Invitrogen, CA). The quality of total RNA was evaluated by an Agilent 2100 Bioanalyzer (Agilent, CA) using RNA 6000 Nano kit (Agilent). RNA was quantified by Nanodrop ND-1000 spectrophotometer. 1 ul of distilled water was used to blank the system. After that, 1.5 ul of RNA was placed onto the pedestal. OD_{260} and OD_{280} were measured at the same time. OD_{260}/OD_{280} ratio was between 2.00 and 2.18.

3.2.3 Microarray and data analysis

The GeneChip® Rat Genome 230 2.0 Array (Affymetrix, Santa Clara, CA, USA) was

used according to the instruction manual. In this study, total RNA from the kidney of 10 samples of control groups, 7 samples of high dose GSE group and 7 samples of CR group was used. In brief, 3 microgram of total RNA sample was converted into double-stranded cDNA using The One-Cycle cDNA Synthesis Kit (Affymetrix). After cleanup, the Biotin-labeled cRNA was synthesized by The IVT Labeling Kit (Affymetrix). After purification and fragmentation, the biotin-labeled cRNA fragment was hybridized to Rat Genome 230 2.0 Array for 16 hours. After incubation, the chips were washed and stained using the GeneChip® Hybridization, Wash, and Stain Kit (Affymetrix). These chips were scanned by a GeneChip Scanner 3,000 and converted into GeneChip Cell files (CEL) with the GeneChip Operating Software package.

Rat Genome 230 2.0 Array have the ability of measuring 30,000 transcripts and variants from over 28,000 well-substantiated rat genes. These CEL files were analyzed using the Genespring GX 7.3 software (Agilent Technologies). Normalization was performed using the GC RMA method. Expression filter was used to remove low unreliable measurements.

Volcano plot was used to identify the genes, which had 1.5 fold change and P value less than 0.05. For the comparison between control group and CR group, a Bejamini and Hochberg false discovery rate was used to control false positive. For the comparison between control group and high dose GSE group, false discovery rate filter was not used because the gene expression change by high dose GSE was so small that no gene passed

the false discovery rate filter. The related heatmaps were plotted by Genespring GX7.3 software.

3.2.4 Real time RT-PCR using Applied Biosystems 7300 Real Time PCR System

Real time RT-PCR was carried out to confirm microarray data. First-strand cDNA was synthesized using the SuperScript III First Strand Synthesis System with Oligo (dT) 20 (Invitrogen, CA), as described in 3.1.6. Real time RT-PCR was performed using Taqman universal PCR master mix kit in Applied Biosystems 7300 Real Time PCR System, and primer sets were used as described (table 3.2). The cycling conditions were: initial activation step at 50 °C for 2 min and 95 °C for 15 min; 40cycles at 94°C for 15 s, annealing and extension at 60°C for 60 s. According to Bustin's suggestion (Bustin and Nolan, 2004), for low expression genes whose Ct values were above 37, the reaction ran for 45 cycles. Since low copy genes have large variation, they were detected in quadruplicate. The replicate farthest away from the mean was regarded as the outlier according to Stankovic's method (Stankovic and Corfas, 2003). For other genes tested, all samples were performed in duplicate. Both a no-template control and a RT negative control were included in each assay.

Table 3.2 PCR primers from Applied Biosystems

Genes	Assay ID	Genes	Assay ID
β actin	Rn00667869_m1	Catalase	Rn00560930_m1
GAPDH	Rn99999816_s1	GPX	Rn00577994_g1
HPRT	Rn01527840_m1	Mn-SOD	Rn00566942_g1
EF	Rn01639851_g1	15-LO	Rn00696151_m1
YWHAZ	Rn00755072_m1	S100a8	Rn00587579_g1
Cu/Zn-SOD	Rn00566938_m1	Cdc25B	Rn00592081_m1
kallikrein	Rn01458139_g1	C 3	Rn00566466_m1
CCL5	Rn00579590_m1		

Based on our previous finding, there was a wide variation in housekeeping gene expression during aging and invalid housekeeping genes caused misleading results (Chen et al., 2006). GeNorm software was used to choose the reliable housekeeping genes. Data analysis of housekeeping gene stability was carried out according to the manual of GeNorm 3.4 (http://medgen.ugent.be/%7Ejvdesomp/genorm/) (Vandesompele et al., 2002). The GeNorm software, an authoritative and popular method (Bustin and Nolan, 2004), selects valid housekeeping gene based on average expression stability values, which represent the average pair wise variation of a housekeeping gene compared with all other housekeeping genes. To provide more accurate normalization, the normalization factor was calculated from multiple housekeeping genes in this experiment. The method has been described in 3.1.9 in detail.

3.2.5 Oxidative damage marker measurement

3.2.5.1 8-isoprostane: the marker of lipid peroxidation

Urinary 8-isoprostane was measured by 8-isoprostane enzyme immunoassay (EIA) kit (Cayman Chemical, Ann Arbor, MI, USA.) with purification by 8-isoprostane affinity column (Cayman Chemical), according to the manufacturer's instructions. Briefly, after centrifugation, 0.5ml of urine was added into 8-isoprostane affinity column. After that, the column was washed with 2ml column buffer and ultrapure water, sequentially. 8-isoprostane was eluted by 2ml elution solution. The final eluted fraction was evaporated with nitrogen gas, and then was resuspended in EIA buffer. Following the manual of 8-isprostane EIA kit, sample, standard, tracer and antiserum was added into the appropriate wells. The plate was incubated for 18 hours at room temperature, and then developed by Ellman's reagent. The plate was read at a wavelength of 412nm. EIADouble Excel workbook from Cayman Chemical was used to calculate the concentration of 8-isoprostane. To avoid the influence of muscle mass and dehydration among the different rats, the creatinine level of urine was measured by creatinine assay kit (Cayman Chemical, Ann Arbor, MI, USA.). In brief, following the manual of creatinine assay kit, sample and standard was added into the appropriate wells. 150 ul of alkaline picrate solution was added to all wells and incubated for 10minutes at room temperature, and then was read at a wavelength of 495nm as initial absorbance reading. 5 ul of acid

solution was added to the wells being used, and incubated for 20minutes at room temperature, and then was read at a wavelength of 495nm as final absorbance reading. Initial and final absorbance readings were used to calculate the concentration of creatinine following the manual of this kit.

3.2.5.2 Protein carbonyl: the marker of protein oxidation

The Protein oxidation in kidney tissue was measured by protein carbonyl, which was assayed by using the protein carbonyl assay kit (Cayman Chemical, Ann Arbor, MI, USA). Protein concentration was quantified by spectrophotometric method, according to the protein carbonyl assay kit's instructions. In brief, 100mg kidney tissue was homogenized by a power homogenizer in cold PBS buffer (containing 1mM EDTA). The tissue lysate was centrifuged for 15minutes at 10,000g at 4 ˚C, and then the supernatant was transferred to a new tube .To remove nucleic acids, samples were incubated with streptomycin sulfate at a final concentration of 1% for 15minutes at room temperature, and then centrifuged for 10minutes at 6,000g at 4 ˚C. The supernatant was kept for carbonyl assay. 200ul of supernatant was transferred to two plastic tubes, in which one was used as sample tube and another one was used as control tube. 800ul of DNPH was added into sample tube, while 800 ul of 2.5M HCl was added into control tube. After 1 hour incubation in the dark, 1ml of 20% TCA was added and vortexed. After centrifugation for 10minutes at 10,000g at 4 ˚C, the supernatant was discarded and the pellet was resuspended in 1ml of 10% TCA. After centrifugation for 10minutes at 10,000g at 4 ˚C, the supernatant was discarded and the pellet was resuspended in 1ml of

(1:1) ethanol/ethyl acetate mixture for three times. Finally, the pellet was resuspended in 0.5ml of guanidine hydrochloride. After centrifugation for 10minutes at 10,000g at 4 ˚C, 220 ul of the supernatant was transferred to a 96 well plate, and then measured at a wavelength of 370 nm using a plate reader. The formula from protein carbonyl assay kit was used to calculate the concentration of protein carbonyl.

3.2.6 Pathology evaluation

4 μm sections from the paraffin-embedded kidney were stained with hematoxylin and eosin staining for histological evaluation. According to Yu's method (Yu, et al, 1982), kidney pathological changes were classified. In brief, Grade 0, no lesions; Grade 1, all lesions were minimal and local in glomeruli and tubule, such as little changes in glomeruli and swollen tubular cells; Grade 2, lesions were mild severity in glomeruli and tubule, involving thickening of mesangial matrix and tubular atrophy; Grade 3, lesions were moderate severity in glomeruli and tubule involving the same structure of grade 2 but more widely, and thickening of Bowman's capsule and mild interstitial fibrosis; Grade 4, lesions were very severity and diffuse in glomeruli and tubule involving diffuse sclerosis in glomeruli; Grade E, end-stages lesions, involving a wide glomerulosclerosis and lack of normal morphological evidence of renal tissue. In addition, glomerulosclerosis and tubular atrophy were evaluated according to Melk's method (Melk et al., 2005). The pathological grading was carried out by a pathologist, in a blinded way.

.

3.2.7 Urinary protein quantification

The urinary protein was quantified according to Bio-Rad Protein Assay Kit II manual (Bio-Rad, CA).Briefly, dye reagent was prepared by diluting 1 part Dye Reagent Concentrate with 4 parts ultrapure water. Five dilutions of a protein standard (bovine serum albumin) were prepared. Each urine sample was diluted at a 1:20 dilution using ultrapure water. 10 µl of each standard or sample solution was pipette into a 96-well microtiter plate in triplicate. 200 µl of diluted dye reagent was added to each well. The plate was incubated for 15 minutes at room temperature. After incubation, the plate was read at a wavelength of 595 nm.

3.2.8 Data analysis

Data was presented as the mean ± SE (standard error). For data that are normality and homogeneity of variance, statistically significant differences were evaluated by one way ANNOVA; for all other data, the Mann-Whitney U non parametric analysis was used. P values below 0.05 were considered significant differences.

Chapter IV: Antioxidant enzyme gene expression change in the aging rat liver, kidney, auditory cortex and cochlea

4.1 Results

4.1.1 Real time RT-PCR specificity, efficiency and linearity

Following real time RT-PCR the resulting PCR products were analyzed to confirm the specificity of the reaction. The PCR products from each gene of interest were analyzed by melting curve analysis as shown in Figure 4.1.1A (Cu/Zn SOD) & 4.1.1B (HPRT). Only one single PCR product was evident in melting curve analysis, confirming the specificity of the PCR reaction. A relative standard curve method was used to calculate amplification efficiencies and correlation coefficients (R2). For all these tested genes, PCR efficiencies were above 96% and correlation coefficients were more than 0.99.This proved that the data obtained from the real time RT-PCR experiments were reliable and could be used for further analysis.

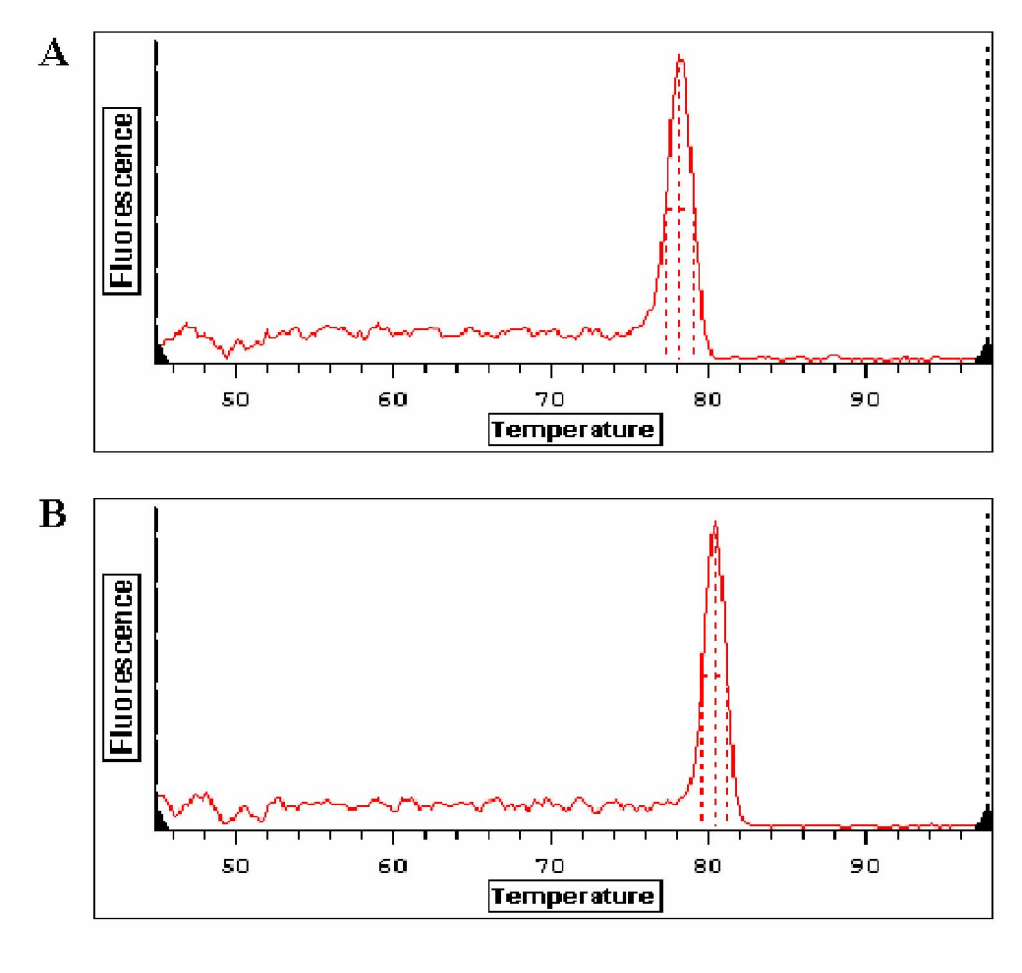

Figure 4.1.1 The real time RT-PCR was specific

In real-time RT-PCR, a melting curve analysis was performed to demonstrate the specificity of the reactions. The plots showed melting curves of (A) Cu/Zn-SOD and (B) HPRT. Only a single peak was evident in the melting curve demonstrating the high specificity of the reaction.

4.1.2 The stability sequence of HKGs in liver, kidney, auditory cortex and cochlea

To identify the HKG with the most stable expression in the liver during the aging process, the HKG selection software packages GeNorm and Normfinder were used. In liver tissue, HPRT was identified as the most stable HKG by both analysis packages. GeNorm identified GAPDH and HPRT as the most stable HKG (Figure 4.1.2) with stability values of 0.42 for both genes. When the analysis from Normfinder was also taken into account (Table 4.1.1), we were able to select HPRT over GAPDH as our HKG. This was based on the very small intra-group variation for HPRT compared to GAPDH (0.010 compared to 0.064 for young rats and 0.018 compared to 0.089 for old rats). The inter-group variations were comparable (0.040 for HPRT, 0.038 for GAPDH).

In kidney tissue, HPRT was also identified as the most stable HKG by both analysis packages. GeNorm identified HPRT and YWHAZ as the most stable HKG (Figure 4.1.3). The stability value of HPRT and YWHAZ was 0.379. Furthermore, Normfinder was used to evaluate gene stability by considering intergroup variation and intragroup variation (Table 4.1.2). The stability value of HPRT was 0.117, which was better than that of YWHAZ (0.148). The stability of HPRT was obviously better in intragroup variation of young and old rats (0.017 compared to 0.086 for young rats and 0.030 compared to 0.044 for old rats), and both genes had similar inter-group variations. Thus, HPRT was identified as the most stable housekeeping gene in rat kidney aging.

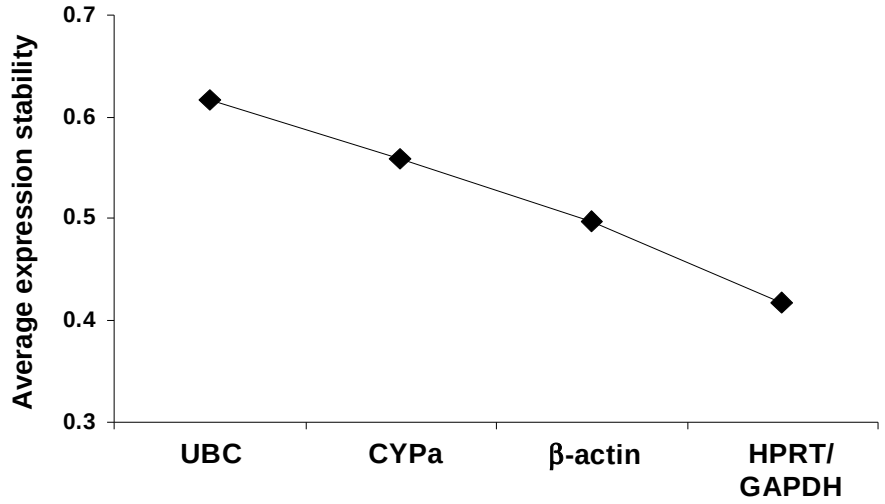

Figure 4.1.2 HPRT and GAPDH were the most stable housekeeping genes by GeNorm in liver

The GeNorm software was used to identify the most stable HKG using a pairwise variation analysis. The plot showed the average expression stability values for the HKGs, with a low value representing stable HKG expression.

Table 4.1.1 Expression stability of housekeeping genes evaluated by Normfinder in liver

Gene	Rank	Stability Value*	Intragroup Variation (Y)	Intragroup Variation (O)	Intergroup Variation
β-actin	3	0.182	0.021	0.155	0.065
CYPa	4	0.339	0.106	0.015	0.261
GAPDH	2	0.162	0.064	0.089	0.038
HPRT	1	0.096	0.010	0.018	0.040
UBC	5	0.343	0.033	0.142	0.248

* Stability values were derived from both intragroup and intergroup variation. The lower the value; the more stable the gene expression. (Y) = young rats; (O) = old rats

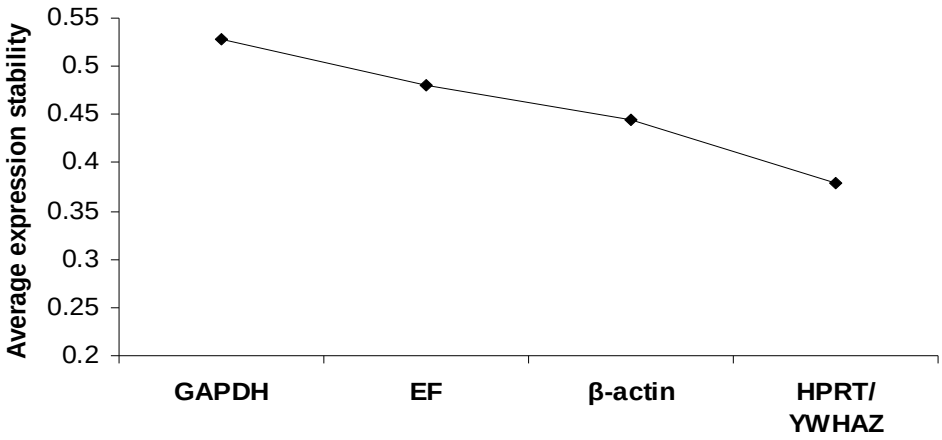

Figure 4.1.3 HPRT and YWHAZ were the most stable housekeeping genes by GeNorm in kidney
The GeNorm software was used to identify the most stable HKG using a pairwise variation analysis. The plot shows the average expression stability values for the HKGs, with a low value representing stable HKG expression.

Table 4.1.2 Expression stability of housekeeping genes evaluated by Normfinder in kidney

Gene	Rank	Stability Value*	Intragroup Variation (Y)	Intragroup Variation (O)	Intergroup Variation
β-actin	4	0.188	0.054	0.117	0.063
EF	3	0.171	0.130	0.003	0.179
GAPDH	5	0.231	0.071	0.016	0.120
HPRT	1	0.117	0.017	0.030	0.051
YWHAZ	2	0.148	0.086	0.044	0.049

* Stability values were derived from both intragroup and intergroup variation. The lower the value; the more stable the gene expression. (Y) = young rats; (O) = old rats

As shown in Figure 4.14, the stability of HKGs in the auditory cortex of rat was ranked using GeNorm software. EF and UBC were chosen as the two most stable HKGs with stability values of 0.208. However, GeNorm software could not determine any further ranking between EF and UBC since gene ratios were used for gene stability analysis in this software. As a result, Normfinder software was used to evaluate the stability of HKGs, and the values are summarized in Table 4.1.3. The stability of EF was better than the stability of UBC (0.058 for EF, 0.070 for UBC). This was based on the intergroup variation that was obviously smaller for EF as compared to UBC (0.011for EF, 0.033 for UBC), and the intragroup variations were relatively comparable between EF and UBC (0.003 compared to 0.004 in young rats and 0.022 compared to 0.012 in old rats). Thus, these results indicated that EF was the most stable HKG in rat auditory cortex.

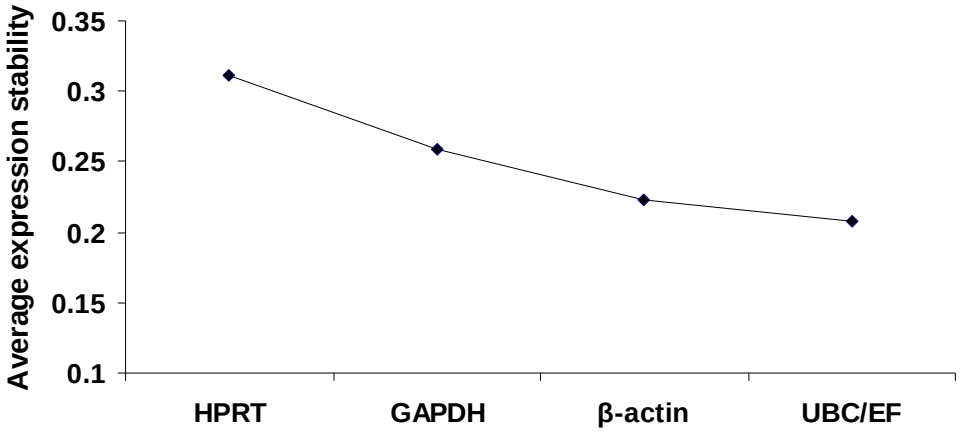

Figure 4.1.4 Housekeeping genes ranked by GeNorm software in rat auditory cortex
The picture shows the average expression stability values of the HKGs, with a low value representing stable HKG expression.

Table 4.1.3 Expression stability of Housekeeping genes was evaluated by Normfinder software in auditory cortex of rats.

Gene	Rank	Stability Value∗	Intra-group Variation(Y)	Intra-group Variation(O)	Intergroup Variation
β-actin	4	0.116	0.016	0.010	0.072
EF	1	0.058	0.003	0.022	0.011
GAPDH	3	0.107	0.049	0.014	0.040
HPRT	5	0.180	0.032	0.028	0.134
UBC	2	0.070	0.004	0.012	0.033

(Y) = young rats; (O) = old rats ∗ Stability values were derived from both intragroup and intergroup variation. The lower the value; the more stable the gene expression.

In rat cochlea, GAPDH was ranked as the most stable HKG by both software packages. GAPDH and HPRT were identified as the most stable HKG with stability values of 0.323 by GeNorm software (Fig.4.1.5), whereas the stability values of β-actin and EF were 0.461 and 0.425, respectively. Furthermore, Normfinder was used to evaluate gene stability by considering inter- and intra- group variations (Table 4.1.4). The stability value of GAPDH was 0.063, which was better than that of HPRT (0.081). The stability value of GAPDH was obviously better in intragroup variation of old rats than the stability value of HPRT (0.009 for GAPDH, 0.044 for HPRT). Thus, GAPDH is the most stable HKG in rat cochlea.

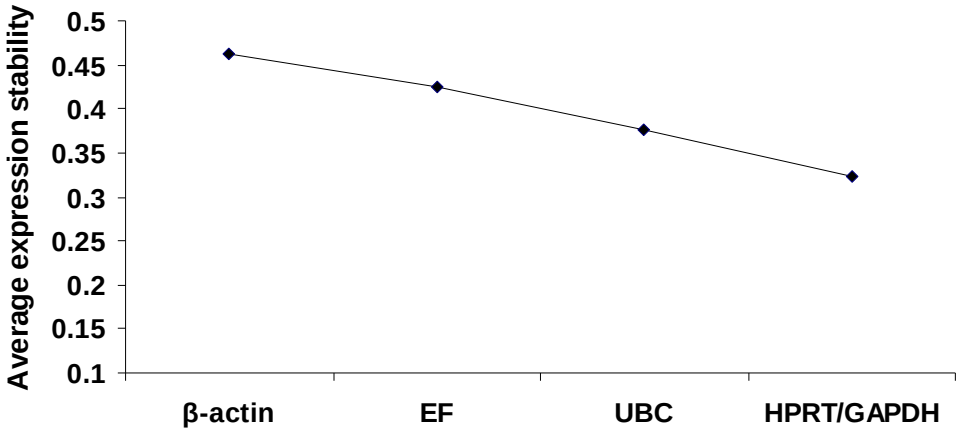

Figure 4.1.5 Housekeeping genes ranked by GeNorm software in rat cochlea
The picture shows the average expression stability values of the HKGs, with a low value representing stable HKG expression.

Table 4.1.4 Expression stability of Housekeeping genes was evaluated by Normfinder software in the cochlea of rats

Gene	Rank	Stability Value*	Intragroup Variation(Y)	Intragroup Variation(O)	Intergroup Variation
β-actin	5	0.123	0.084	0.124	0.009
EF	2	0.072	0.013	0.063	0.009
GAPDH	1	0.063	0.062	0.009	0.056
HPRT	3	0.081	0.047	0.044	0.017
UBC	4	0.097	0.035	0.099	0.056

(Y) = young rats; (O) = old rats. * Stability values were derived from both intragroup and intergroup variation. The lower the value; the more stable the gene expression.

4.1.3 The housekeeping genes expression variation between young and old rats in liver, kidney, auditory cortex and cochlea

Base on valid HKGs, the HKGs expression variation was further evaluated between young and old rats in liver, kidney, auditory cortex and cochlea, respectively. In liver tissue, after normalization to the confirmed HKG, HPRT, compared to young rats, mRNA expression of UBC was significantly decreased in old rats ($p<0.01$), while mRNA expression of CYPa was significantly increased in old rats ($p<0.01$) (Figure 4.1.6). There were no significant differences in GAPDH and β-actin between the two groups, even though β-actin mRNA in old rats increased by 29.6% compared to young rats ($p=0.07$).

In kidney tissue, as shown in Figure 4.1.7, mRNA expression of β-actin was significantly increased in old rats ($p<0.05$). There was no significant difference in GAPDH, EF and YWHAZ between young and old rats in kidney aging.

The variations of HKGs in auditory cortex and cochlea of rats are illustrated in Figure 4.1.8 and 4.1.9. In rat auditory cortex, mRNA expression of HPRT and β-actin significantly decreased ($p<0.05$) and increased ($p<0.05$) respectively in old rats as compared to young rats while no significant differences in GAPDH and UBC were found between the two groups of rats. In rat cochlea, the expression of UBC mRNA increased significantly in old rats ($p<0.05$). Therefore, these data suggested variations in HKGs in rat liver, kidney, auditory cortex and cochlea tissue during the aging process, and thus the importance of selecting a suitable HKG when analysing aging in specific tissue.

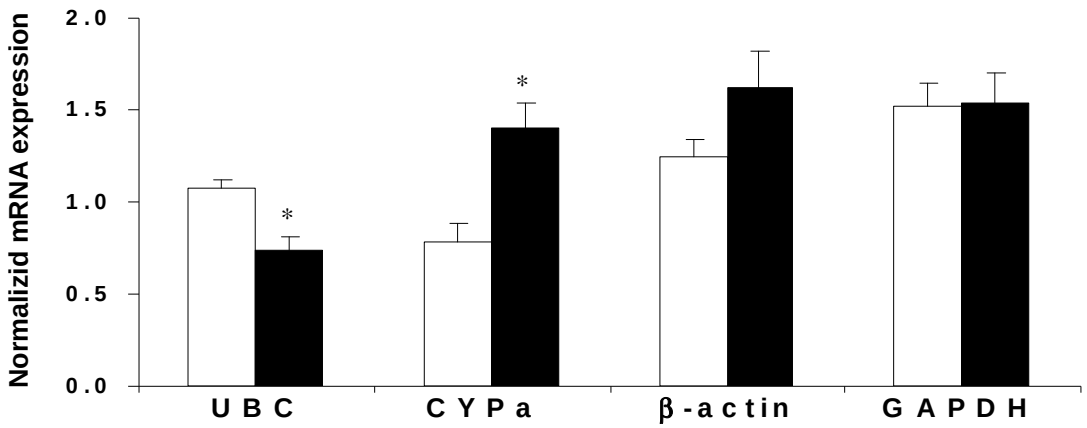

Figure 4.1.6 Housekeeping genes expression variation between young and old rats in liver

To compare the HKGs expression variation between young and old rats, each HKGs expression was normalized to the confirmed HKG, HPRT. The graph represents the average HKG gene expression in the liver of young (white bar, n=9) and old (black bar, n=8) rats ± SE (standard error). ∗ Represents $p<0.01$

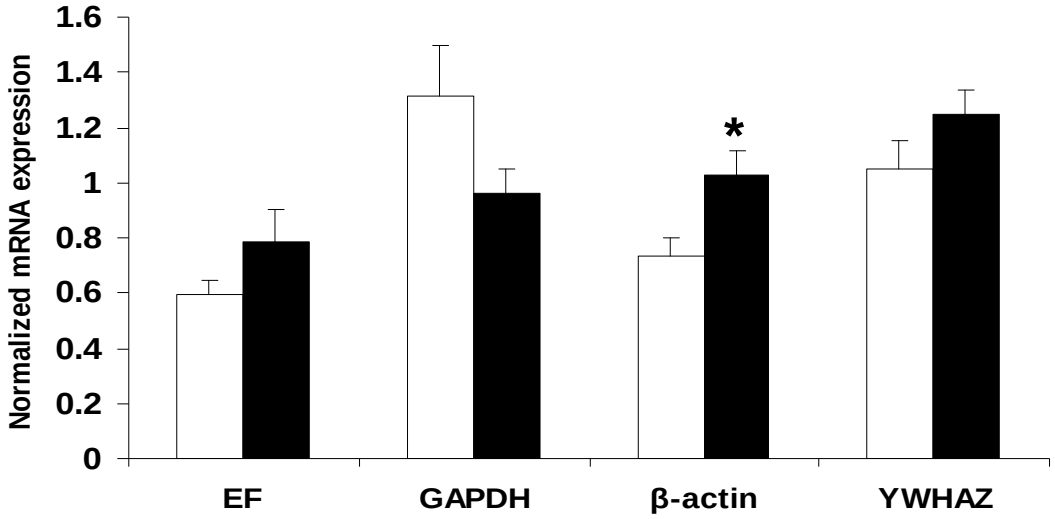

Figure 4.1.7 Housekeeping genes expression variation between young and old rats in kidney

To compare the HKGs expression variation between young and old rats, each HKGs expression was normalized to the confirmed HKG, HPRT. The graph represents the

average HKG gene expression in the liver of young (white bar, n=9) and old (black bar, n=8) rats ± SE (standard error). ∗ Represents $p<0.05$

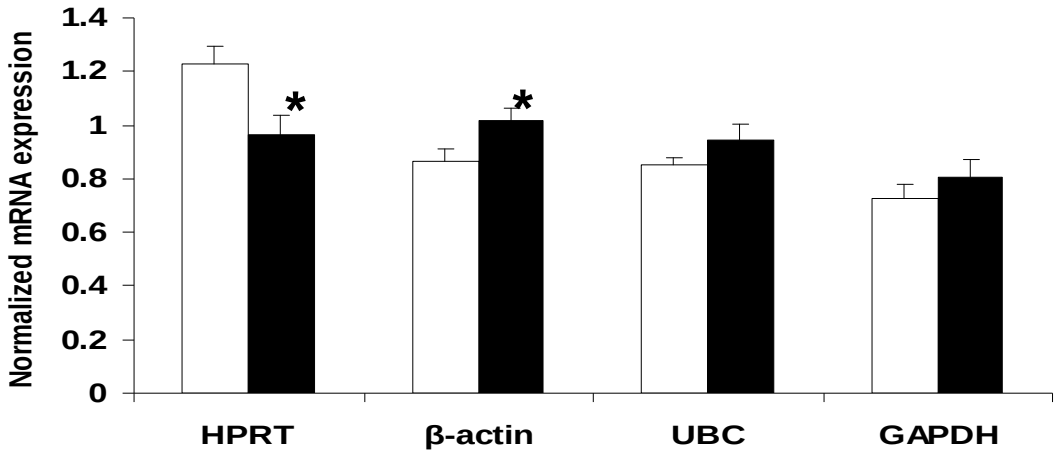

Figure 4.1.8 Housekeeping genes expression variation in auditory cortex
The level of different HKGs was normalized to the validated HKG, EF. Data were expressed as mean ± SE. Young rats (white bar, n=9) and old rats (black bar, n=8).
∗ represents $p<0.05$.

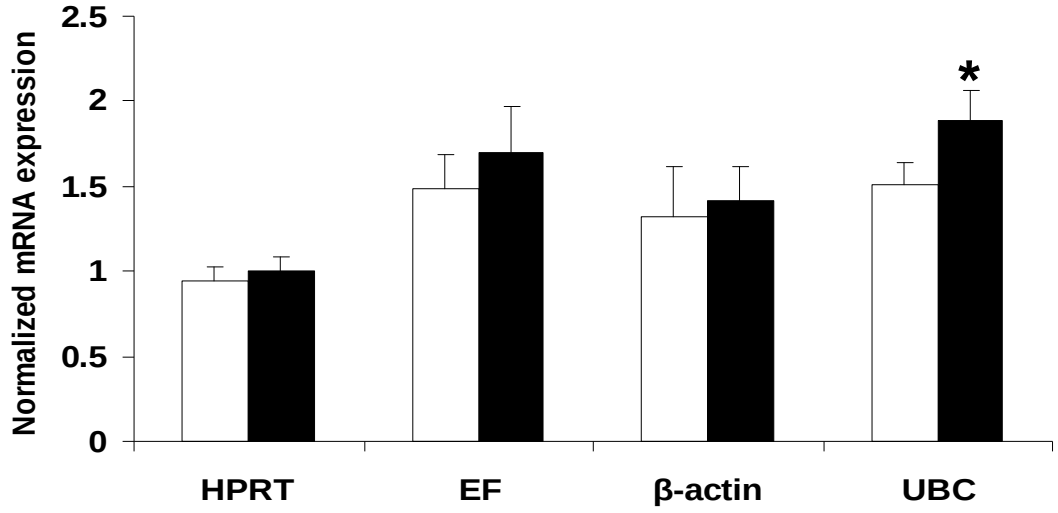

Figure 4.1.9 Housekeeping genes expression variation in cochlea
The level of different HKGs was normalized to the validated HKG, GAPDH. Data were expressed as mean ± SE. Young rats (white bar, n=8) and old rats (black bar, n=6).
∗ represents $p<0.05$.

4.1.4 Analysis of Cu/Zn-SOD and catalase gene expression normalized by different housekeeping genes

To demonstrate the importance of selecting the correct HKG when using gene expression analysis techniques, we used different HKGs to compare the gene expression of Cu/Zn-SOD and catalase in liver tissues from young and old rats. As shown in Figure 4.1.10, when expression levels were normalized using UBC, an invalid HKG, Cu/Zn-SOD expression had a significant difference in expression levels in liver tissues between young and old rats. On the contrary, after normalization to HPRT, the validated HKG, there was no statistically significant difference in Cu/Zn-SOD expression. An alternative method to quantify gene expression used the normalization factor (NF), which is based on the expression level of multiple HKGs. The GeNorm analysis software was used to calculate the NF in our samples, and then a NF value derived from HPRT-GAPDH-β actin expression was selected. When Cu/Zn-SOD expression was normalized using the NF, no statistically significant difference was seen (Figure 4.1.10). In addition, there was a statistically significant decease in catalase gene expression in liver during the aging process when it was normalized to HPRT ($p<0.001$) and UBC ($p<0.05$), yet it should be noted that compared to young rats, the level of catalase mRNA decreased by only 31.20% in old rats when normalized using UBC, which was about half value when normalized using HPRT (57.73%). This data demonstrated that selection of a validated HKG was essential for the correct interpretation of gene expression analysis data in aging research.

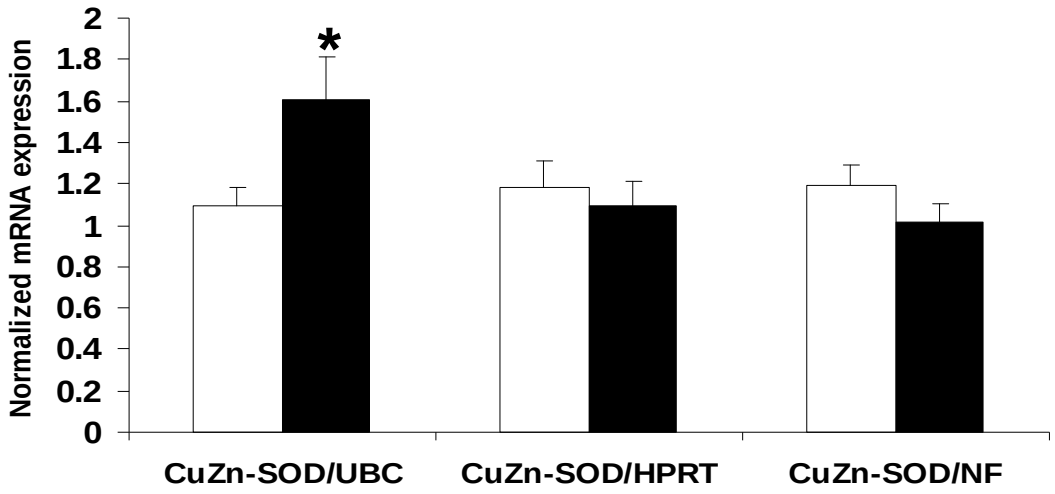

Figure 4.1.10 Influence of different housekeeping genes on interpretation of Cu/Zn-SOD mRNA expression in the rat liver aging process.

The level of Cu/Zn-SOD mRNA was normalized to UBC (first two bars), HPRT (middle two bars) and NF (last two bars), respectively. NF= normalization factor. Data were expressed as mean ± SE. Young rats (white bar, n=9) and old rats (black bar, n=8).
∗ represents $p<0.05$

Similarly, Figure 4.1.11 showed how different HKGs influenced the interpretation of Cu/Zn-SOD and catalase mRNA expressions in the aging process of rat auditory cortex. When Cu/Zn-SOD gene expression was normalized by EF, the validated HKG, no significant difference was found in auditory cortex between young and old rats. In contrast, when Cu/Zn-SOD gene expression was normalized by β-actin, the invalid HKG, there was a statistically significant ($p<0.05$) difference between young and old rats. This is due to the significant increase of β-actin expression in the auditory cortexes of old rats rather than the variations in Cu/Zn-SOD gene levels. A similar situation was observed in the interpretation of catalase gene expression. In the cochlea, no statistically significant difference in Cu/Zn-SOD gene expression was found when it was normalized to GAPDH ($p>0.05$) and UBC ($p>0.05$). However, it was worth noting that the level of Cu/Zn-SOD mRNA decreased in old rat cochlea by only 1.0% when normalized using GAPDH, the validated HKG, whereas it decreased by 18.4% when normalized using UBC, the invalid HKG. Thus, these results suggest that the validated HKG is a prerequisite for analyzing gene quantification.

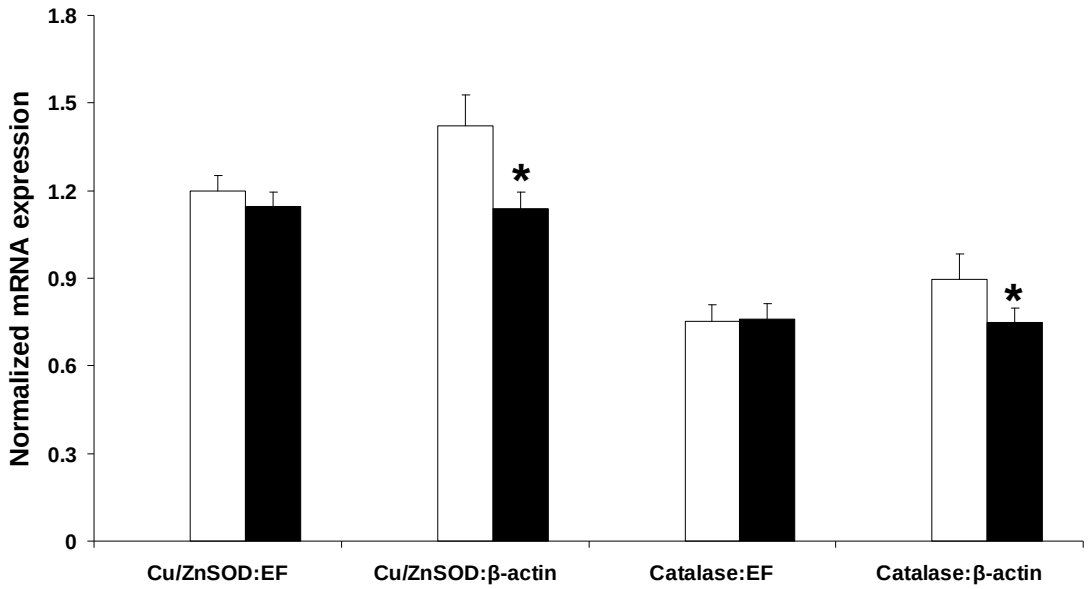

Figure 4.1.11 Interpretation of Cu/Zn-SOD and catalase gene expression by different housekeeping genes in rat auditory cortex.
The level of Cu/Zn-SOD mRNA and catalase mRNA was normalized to EF and β-actin respectively. Data were expressed as mean ± SE. Young rats (white bar, n=9) and old rats (black bar, n=8).

4.1.5 Antioxidant enzyme gene expression changes in the liver, kidney, auditory cortex and cochlea of aged rat

As shown in Table 4.1.5, mRNA expression of catalase decreased significantly in liver tissues between young and old rats with expression levels in the old rats' only 42.27% of that seen in the young rats. Similar to the results for Cu/Zn-SOD, there was no significant difference in GPX expression, however there did appear to be a trend for increased expression of GPX in the elderly rats, although it did not reach significance ($p=0.06$).

In kidneys, the mRNA of Cu/Zn-SOD and catalase was significantly lower in old rats than in young rats. The expression level of Cu/Zn-SOD mRNA decreased by 52.7%, while the level of catalase decreased by 46.2% between 8 and 26 months of age. There was no significant difference in the expression of Mn-SOD and GPX expression in kidney tissues between young and old rats (Table 4.1.5).

Antioxidant enzymes variations in rat cochlea and auditory cortex during the aging process were shown in Table 4.1.5. In rat cochlea and auditory cortex, there was no significant difference in Cu/Zn-SOD, Mn-SOD, catalase and GPX mRNA expressions between young and old rats. However, Mn-SOD mRNA expression decreased by 29.7% in the cochlea of old rats, compared with the young rats, even though there was no statistical difference.

Table 4.1.5 Antioxidant enzymes expression variation between young and old rats in liver, kidney, auditory cortex and cochlea

	Cu/Zn-SOD	Mn-SOD	Catalase	GPX
Young liver	1.18±0.13	1.61±0.23	1.45±0.11	0.69±0.05
Old liver	1.09±0.12	1.75±0.13	0.61±0.05*	1.23±0.24
Young kidney	1.31±0.13	0.71±0.06	1.17±0.06	1.31±0.13
Old kidney	0.62±0.08*	0.82±0.11	0.63±0.09*	1.21±0.16
Young Cochlea	2.24±0.36	1.48±0.29	1.50±0.15	1.61±0.29
Old Cochlea	2.22±0.26	1.04±0.08	1.72±0.04	1.96±0.30
Young auditory cortex	1.20±0.05	1.05±0.06	0.75±0.06	1.03±0.04
Old auditory cortex	1.14±0.05	1.03±0.06	0.76±0.05	1.00±0.05

To compare antioxidant enzymes expression variation between young and old rats, each antioxidant enzyme expression was normalized to the appropriate HKG. In liver and kidney, the confirmed HKG was HPRT. In cochlea and auditory cortex, the confirmed HKGs were GAPDH and EF, respectively. Data were expressed as mean ± standard error (SE). ∗ represents $p<0.05$.

4.2 Discussion

In this chapter, the most suitable tissue for the evaluation of anti-aging intervention of GSE and CR were chosen according to the mRNA expression changes of major antioxidant enzymes during the aging process. In previous studies using Northern blot analysis, an age-dependent decline in gene expression of antioxidant enzymes was found, and the extent of expressional change of these enzymes was less than 3 fold (Rao et al., 1990a, and b). The limited sensitivity of the Northern blot analysis might not be suitable for identifying small change in expression, so these results need to be investigated further. In addition, it was reported that more than 90% of age related gene changes were less than 3 fold in magnitude (Pahlavani et al., 1994; Van Remmen et al., 1995). Real time RT-PCR is believed to be able to determine changes as small as twofold using statistical methods (Walker, 2002). Therefore, the use of real time RT-PCR with valid HKGs will be a reasonable and practical tool for detecting age-related gene expression change.

In this study, real time RT-PCR was employed to detect the mRNA expression of the commonly used HKGs such as β-actin, GAPDH, UBC, EF, HPRT, YWHAZ or CYPa in the liver, kidney, auditory cortex and cochlea of young and old male Fischer 344 rats. HKGs selection software such as GeNorm and Normfinder were used to identify the most stable HKGs. Based on valid HKGs, we evaluated the variation of HKGs in the aging process in four different tissues. In addition, in order to illustrate the significance of choosing appropriate HKGs, normalization of Cu/Zn-SOD and catalase gene expression

to the different HKGs was performed in different tissues. After identification of the valid HKGs, mRNA expression of Cu/Zn-SOD, Mn-SOD, catalase and glutathione peroxidase (GPX) were evaluated based on the validated HKGs in liver, kidney, cochlea and auditory cortex of young and old rats.

4.2.1 Establishment of reliable real time RT-PCR

Obtaining reliable real time RT-PCR data is a prerequisite for selecting appropriate HKGs. Real time RT-PCR consists of multiple steps, and even small errors can significantly affect the reliability and reproducibility of final results. Thus, quality control must be performed in all stages. A number of measures were taken to achieve the desired specificity of PCR product in this study. Firstly, genomic DNA contamination was sufficiently controlled by DNase treatment both on-column and off-column, because traces of genomic DNA will obviously prevent accurate quantification, especially when studying genes with unknown intron/exon structure, or the existence of pseudogenes. Peters et al. (2004) exhaustively discussed the necessity of combining on-column and off-column DNase treatment in real time RT-PCR and its impact on efficiency. Secondly, primers that flanked introns were used to ascertain the absence of genomic DNA since genomic DNA would have the intron sequence amplified. Absence of genomic DNA was confirmed by the negative control of real time RT-PCR. Finally, the specificity of the PCR products was verified by melting curve analysis. In addition, during the real time RT-PCR, fluorescent data was acquired at a higher temperature, avoiding the inference of non-specific fluorescence signals (Zhang et al., 2004). During data analysis, PCR

efficiency corrected quantification was performed because small PCR efficiency differences between target genes and the HKG will have an effect on the calculation of gene expression

4.2.2 The selection of suitable HKG in rat liver, kidney, auditory cortex and cochlea during aging

We have identified HPRT as the most stable HKG to use for studying rat liver aging using the software GeNorm and Normfinder. Analysis using GeNorm identified HPRT and GAPDH as the two most stable HKGs in liver tissue, but could not differentiate further between them because the use of gene ratios was needed for gene stability measurements. When using Normfinder, HPRT had more stable intra-group variation and had similar inter-group variation when compared to GAPDH. Thus, HPRT was chosen as the most stable HKG in liver aging. Recently, HPRT had also been recommended as the best HKG to use in human cancer research (de Kok et al., 2005). UBC has previously been identified as the best HKG in human liver diseases (Kim et al., 2003) and human bone marrow by GeNorm method (Vandosempele et al., 2002). In contrast to those studies, UBC was ranked as the most unstable HKG by both methods in this present study of rat liver aging. This discrepancy might be attributed to different species and different experimental conditions. As shown in Table 4.2.1, one HKG was suitable HKG at one experimental condition, whereas it was unstable HKG at other experimental condition. These data suggested that a 'universal' HKG for all cell types or tissues did not exist (Vandosempele et al., 2002). In this study, HPRT, EF and GAPDH were identified

by GeNorm and Normfinder software as appropriate HKGs in rat kidney, auditory cortex and cochlea, respectively. These data supported the proposal that HKG had to be validated for a particular experimental condition on an individual basis (Vandosempele et al., 2002; Dheda et al., 2004).

Table 4.2.1 Housekeeping genes in different experimental conditions

House keeping genes	Pro	Con
β-actin	Rat mesocorticolimbic brain [a]	Human bone marrow
GAPDH	Human neuroblastoma	Rat pancreas [b]
UBC	Human bone marrow, Human liver diseases [c]	Human fibroblast
HPRT	Human fibroblast	Human leukocyte
EF	human T helper cell differentiation [d]	unknown
CYPa	Rat pro-inflammatory cytokine [e]	unknown
YWHAZ	Human leukocyte , rat kidney diseases [f]	Human neuroblastoma

a Data was referred to the paper(Koya et al., 2005); b Data was referred to the paper(Yamada, et al 1997); c Data was referred to the paper (Kim et al., 2003); d Data was referred to the paper (Hamalainen et al. 2001) ; e Data was referred to the paper(Peinnequin A et al.,2004); f Data was referred to the paper(Biederman et al., 2004). Other data was referred from the paper (Vandesompele et al., 2002.)

The appropriate HKGs might vary because of different rat strains or species. GAPDH was chosen as a valid HKG in Fischer 344 rat cochlea by GeNorm and Normfinder software. Laer *et al.* reported that HPRT and hydroxymethylbilane synthase were chosen as HKGs in the cochlea of mice by GeNorm software, but they did not specifically state the amount and type of HKGs to choose them (Van Laer et al., 2005). Similar situation

was found in auditory cortex. EF was the most stable HKG in auditory cortex of aging rats. However, the validation of HKGs in the medial prefrontal cortex by GeNorm software suggested that HPRT, neuron-specific enolase, and β-actin were the most stable HKG of 10 putative HKGs between high and low grooming Wistar rats (Koya et al., 2005). Taken together, these results suggested that the appropriate HKG should be validated according to the specific tissues and specific strains or species, which was in agreement with the conclusion that HKGs should be validated for different experimental conditions (Vandesompele et al., 2002; Andersen et al., 2004).

4.2.3 The variation of HKG expression in rat liver, kidney, auditory cortex and cochlea during aging

Based on valid HKGs, **t**he variation of HKG expression in rat liver, kidney, auditory cortex and cochlea during aging was evaluated, respectively. Although aging is a physiological process, we found that there was a wide variation in HKG expression during the aging process. Previous studies have identified obvious HKG variations which have been attributed to pathological changes (Aerts et al., 2004; Dheda et al., 2004 and de Kok et al., 2005) or cell differentiation (Hamalainen et al., 2001; Bas et al., 2004). UBC and CYPa had significantly different expression levels in liver tissue between young and old rats. In addition, β-actin mRNA level in the liver of old rats increased by 29.6 % although this finding did not reach statistical significance. Similarly, Moshier et al. (1993) found that β-actin expression was also different in rat gastric mucosa, where

there was a decrease in expression by 37% in old rats (24 months) compared to young rats (6 months) using Northern blot analysis. The difference in β-actin expression between our study and the study by Moshier and colleagues might be attributed to tissue specific HKG variation, as has been discussed above. However, the validation of the HKG could not be further improved at that time because of the lack of a powerful statistical method and the decreased sensitivity of Northern blot analysis compared with real time RT-PCR.

The obvious fluctuations in the expression levels of HKGs were also found in kidney, auditory cortex and cochlea of aging rats. β-actin increased significantly in kidney and auditory cortex of old rats when compared to young rats. β-actin was also repoted as a invalid HKG in asthmas and food deprivation (Glare et al., 2002; Yamada et al., 1997). Furthermore, Compared to young rats, mRNA expression of HPRT significantly decreased ($p<0.05$) in auditory cortex of old rats. HKG variation in cochlea was also present. The expression level of UBC in cochlea was significantly higher in old rats than young rats. These results suggested that the variation of HKGs expression was a common phenomenon during the aging process and was tissue specific.

4.2.4 Interpretation of Cu/Zn-SOD and catalase gene expression normalized by different HKGs

HKG variation could cause confusing, even misleading interpretation of gene expression data. Normalization to the confirmed HKG, HPRT, did not identify any significant

difference in Cu/Zn-SOD expression during rat liver aging process; while normalization to the invalid HKG, UBC, demonstrated significant differences in the same experiment. Normalization of Cu/Zn-SOD expression to the normalization factor (the normalization factor calculated from several HKGs) produced similar result to using HPRT alone and not that of UBC alone. Thus the variation in Cu/Zn-SOD expression normalized against UBC was attributed to the fluctuation in expression of the inappropriate HKG, UBC, instead of the fluctuation in Cu/Zn-SOD expression in the aging process. Even though normalization to different HKGs did not influence the findings for catalase expression, the quantification of catalase expression was distorted. When normalized to HPRT expression in the aged rats decreased by 57.73% compared to 31.20% when normalized to the invalid UBC gene.

Invalid HKG also misinterpreted the evaluation of target genes expression in rat auditory cortex during the aging process. When β-actin, the invalid HKG, was chosen as HKG, there was a significant decrease in the mRNA of Cu/Zn-SOD and catalase in rat auditory cortex; whereas, no significant difference in the expression of Cu/Zn-SOD and catalase was found when they were normalized with EF, the valid HKG. The variation of β-actin gene expression caused the misleading interpretation of Cu/Zn-SOD and catalase gene expression. From current data, most of the age-related gene expression changes occurred in the 0.3 to 3 fold range (Pahlavani et al., 1994; Van Remmen et al., 1995). Therefore, validation of HKGs in aging research is absolutely vital for accurate gene expression quantification.

Poor selection of HKGs can also invalidate the normalization process and lead to the generation of misleading information in cancer research. For example, in a study of human clear cell renal cell carcinoma (CCRCC), when the target gene, tumor suppressor gene P53 (TP53), was normalized to the selected HKG, lamin B1 (LMNB1), a significant difference was detected between normal and CCRCC groups. However, it was not TP53, but LMNB1 gene expression that changed during that study (Haller et al., 2004). Similar cases have been reported in human asthma (Glare et al., 2002).

The use of more than one HKG for normalization has been proposed because of the obvious HKG expression variations in some experiments (Vandesompele et al., 2002). In those cases, the NF calculated from several HKGs may bring more accurate normalization. In the present study, a NF calculated from HPRT-GAPDH-β-actin was recommended for gene expression analysis in rat liver aging process by GeNorm software. However, the feasibility of using NF has been argued (de Kok et al., 2005), especially in studies in which RNA is limited. Normalization of Cu/Zn-SOD expression to the NF or to HPRT alone produced similar results in this study. Our study showed that real time RT-PCR with valid HKGs was a reliable tool for the detection of alteration in age-related gene expression.

4.2.5 Antioxidant enzymes gene expression changes in rat liver, kidney, auditory cortex and cochlea

In our study, the expression of catalase was significantly decreased in old rats whereas Cu/Zn-SOD, Mn-SOD and GPX expression did not show a significant change in liver tissue between young and old male Fischer 344 rats. In liver tissue, studies using Northern blot analysis showed decreasing expression of Cu/Zn-SOD and catalase and no change in GPX expression with age in male Fischer 344 rats (Rao et al., 1990a); while a study using common RT-PCR showed no change in Cu/Zn-SOD with age in male Fischer 344 rats (Thomas et al., 2002). Thus, the investigations of age-related catalase and GPX gene expression were relatively consistent, and the discrepancy in Cu/Zn-SOD gene expression might be partly from different experimental methodologies. Interestingly, it has been reported that changes in antioxidant enzyme activities during aging may be dependent on the rat strains (Rikans et al., 1991; Jang et al., 2001), yet age related antioxidant enzyme gene expression changes presented here from male Fischer 344 rats were similar to those reported from male Wistar rats (Martin et al., 2002). A study using Northern blot analysis in Wistar rats showed increasing expression of Cu/Zn-SOD, catalase and GPX expression from 6 to 30 months of age (Sanz et al., 1997). Real time RT-PCR was also used in that study but without the use of a validated HKG, thus the differences in antioxidant enzyme gene expression in the two rat strains would still needed further validation. In addition, because Cu/Zn-SOD, catalase and GPX are major antioxidant enzymes in eukaryotes and the decrease of antioxidant defense had been widely demonstrated during rat liver aging (Rao et al. 1990a; Tian et al., 1998; Grune et al., 2001), the decrease in catalase gene expression might contribute to the diminution of the intricate antioxidant defense system in liver. GPX mRNA expression seemed to increase, even though it did not reach significance ($p=0.06$). The trend for increased

expression of GPX may compensate for the decreased expression of catalase because catalase and GPX cooperate to remove hydrogen peroxide. This inference needs further investigation. Thus, our data showed that catalase mRNA expression decreased during the rat liver aging process, which might be involved in the decline of the intricate antioxidant defense system.

In kidney tissue, Cu/Zn-SOD and catalase expression showed a significantly decreased expression in old rats, compared to young male Fischer 344 rats. These results were in agreement with previous studies in which age related decrease in Cu/Zn-SOD and catalase expression and no change in GPX expression with age were reported in kidney tissue using Northern blot method in male Fischer 344 rats, even though pooled RNA samples were used in that study because large amounts of RNA are needed for Northern blotting (Rao et al., 1990). However, a study using real time RT-PCR without validated HKG showed that the expression of Cu/Zn-SOD and GPX was significantly higher in old male Wistar rats than in young rats. The discrepancy might be partly due to the use of different rat strains (Rikans et al., 1991), and the use of invalid HKG might be another possible explanation. The age related decrease in enzyme activity of Cu/Zn-SOD and catalase in kidney tissue was consistently reported in these two rat strains (Cand at al, 1989; Semsei et al., 1989; Rao et al., 1990). Since Cu/Zn-SOD and catalase are major antioxidant enzymes, the decrease in Cu/Zn-SOD and catalase gene expression might be involved in the decline of the antioxidant defense system in the rat kidney aging process.

Based on validation of HKGs, antioxidant gene expression changes with age in rat cochlea and auditory cortex were evaluated between young and old Fischer 344 rats. Cu/Zn-SOD, Mn-SOD, catalase and GPX expression remained constant between 8 and 26 months of age male Fischer 344 rats. It was reported that Fischer 344 rats older than 12 months had a significant age-related hearing loss (Popelar et al., 2006). Similar results of Cu/Zn-SOD and catalase expression in temporal cortex of male Wistar rats were demonstrated by Tsay, *et al.* using ribonuclease protection assay method (Tsay et al., 2000). In contrast, previous studies showed a significant increase of Cu/Zn-SOD expression at 9 months of age in C57B16/J mouse cochlea by real time RT-PCR, compared with young mice, but with a large variance in their gene expression values (Staecker et al., 2001). For C57BL/6 mouse, hearing loss started from 6 months of age and then completely lost hearing at 12 months of age (Spongr et al., 1997). This discrepancy may be due to different animal models. In addition, the relatively small number of animals used in this study might not detect the very small statistical difference of antioxidant enzyme gene expression change with age, even though Fischer 344 rats are inbred rats and have a smaller experimental variation than outbred animals. Complete elimination of Cu/Zn-SOD in knockout mice prompted the formation of age related hearing loss (McFadden et al., 1999), but the total loss of Cu/Zn-SOD rarely occurred in the normal aging process. Recently, an investigation reported that the loss of 50% Cu/Zn-SOD activity did not bring about the increasing risk of age related hearing loss (Keithley et al. 2005). Further, some investigations showed that the over-expression of Cu/Zn-SOD could not effectively prevent age related hearing loss (Coling et al., 2003; Keithley et al. 2005). Taken together, these data indicated that the role of antioxidant enzyme during rat

cochlea and auditory cortex aging process was limited and complex as reported (Coling et al., 2003).

In summary, antioxidant enzyme gene expression changes in rat liver, kidney, auditory cortex and cochlea during the aging process were different. It was consistent with the report that antioxidant enzyme activity changes during the aging process were tissue-specific (Rao, et al., 1990). Antioxidant enzyme activity in rat liver and kidney decreased with age (Rao, et al., 1990; Tian et al., 1998), while antioxidant enzyme activity in rat diaphragm was unchanged during the aging process (Powers, et al., 1992). It reflected the complexity of the aging process.

4.3 Conclusion

Real time RT-PCR with valid HKG protocol was established. Based on this method, we found that there was a wide variation in HKG expression in liver, kidney, auditory cortex and cochlea during aging. We have identified HPRT as an appropriate HKG for accurate normalization during gene expression analysis of the effects of aging on the rat liver and kidney, and EF and GAPDH were appropriate HKGs in rat auditory cortex and cochlea during aging, respectively. These data suggested that different HKGs should be used for different experimental conditions. In addition, our results showed that invalid HKG caused the misinterpretation of targeted genes expression levels. To our knowledge, this is the first report discussing validation of HKGs in aging research where choosing appropriate HKGs is vital for accurate gene quantification and analysis. Further

investigation showed that antioxidant enzyme gene expression changes in liver, kidney, auditory cortex and cochlea during the aging process were different. Among them, kidney had the most obvious antioxidant enzyme gene expression changes during the aging process in the Fischer 344 rat. In addition, age related pathological changes in rat kidney had been well characterized (Yu, et al, 1982; Maeda et al, 1985).Thus, kidney tissue was chosen to explore the molecular mechanisms of the effects of GSE and CR.

Chapter V Effects of grape seed extract and calorie restriction on age related oxidative damage and gene expression profile in middle-aged rats

5.1 Results

12 month old male Fischer 344 rats were fed a NIH31diet with a low dose (0.2%) , high dose of GSE(1%) ,or without GSE as control group for 6 months.The rats CR groups were fed with NIH31/NIA fortified diets, which was enriched with vitamins to maintain similar consumption of vitamins as the rats in control group. Because GSE was added to the diet, the GSE intake paralleled the diet intake. The calculated average GSE consumption was 82.37 mg/kg per day in the low dose group, while it was 413.56 mg/kg per day in the high dose group.

5.1.1 Animal weight

There were no significant differences in animal weight between low dose GSE, high dose GSE and control group in this study. The body weight of low dose GSE group and high dose GSE group was 461.16 ± 7.80 gram and 477.25 ± 12.40 gram, respectively, compared to that of the control group (477.98 ± 10.78 gram). This indicated that GSE did not affect animal weight. Under CR condition, weight lost was observed. The body weight of CR group gradually declined to 282.25 ± 2.14 gram after 6 months , which was significantly lower than that of control group (477.98 ± 10.78 gram, $p<0.001$) .

5.1.2 Effect of GSE and CR on lipid and protein oxidative damage in urine and kidney

To determine the protective effect of GSE and CR on oxidative damage, urinary 8-isoprostane was measured as an indicator of lipid peroxidatio nafter feeding the rats in the different diet for 6 months. Figure 5.1 showed that both the low and high dose GSE significantly reduced urinary 8-isoprostane by 56.3% and 57.7%, respectively, compared to the control group(150.21 ±15.24 ng/mmol creatinine) ($p < 0.05$). Urinary 8-isoprostane was also significantly decreased in the CR group (87.3±23.2 ng/mmol creatinine) ($p < 0.05$).

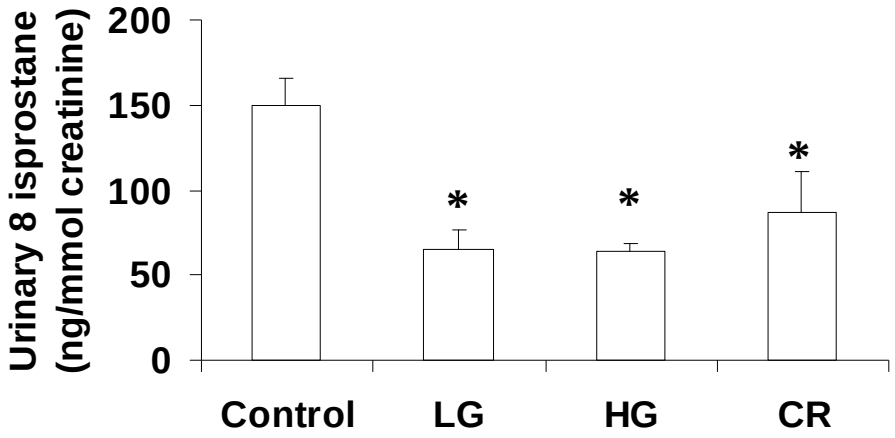

Figure 5.1 Effect of GSE and CR on urinary 8-isoprostane
Control represented control group rats (n=11), LG represented low dose GSE group rats (n=11), HG represented high dose group rats (n=11). CR represented calorie restriction group rats (n=11). Data was expressed as mean ± SE (standard error) (ng/mmol creatinine).
∗ represented $p<0.05$.

We further assessed whether GSE and CR could attenuate protein oxidative damage. Carbonyl protein, a biomarker of protein oxidative damage, was measured in kidney tissue. Compared to the control group (1.33 ± 0.22 nmol/mg protein), carbonyl protein in kidney tissue was significantly decreased in the high dose GSE group (0.81 ± 0.10 nmol/mg protein, $p<0.05$) and CR group (0.63 ± 0.12 nmol/mg protein, $p<0.05$) (Figure 5.2). No significant change in carbonyl protein content was detected in the low dose GSE group (1.29 ± 0.16 nmol/mg protein). Together, these findings indicated that GSE and CR could attenuate age related oxidative damage.

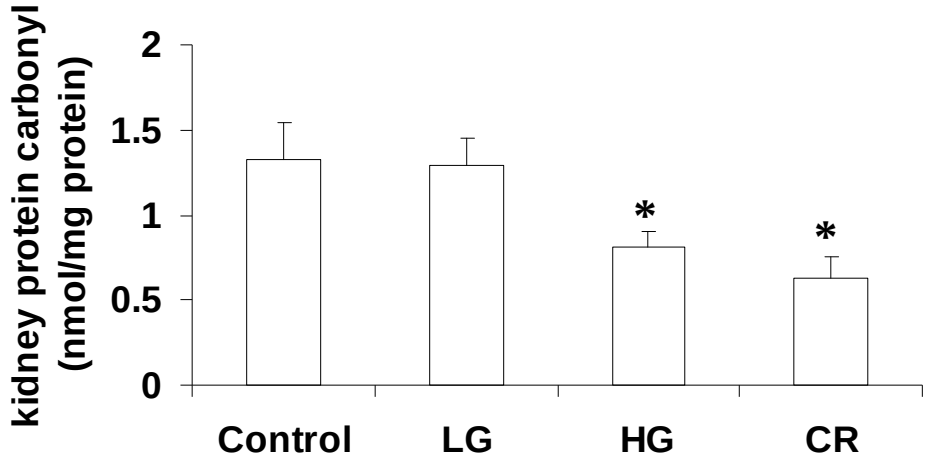

Figure 5.2 Effect of GSE and CR on protein carbonyl in kidney tissue
Control represented control group rats (n=11), LG represented low dose GSE group rats (n=11), HG represented high dose group rats (n=11). CR represented calorie restriction group rats (n=11).Data was expressed as mean ± SE (nmol /mg protein). ∗ represented $p<0.05$.

5.1.3 Renal pathological analyses and urinary protein quantification

Pathological scoring of renal sections was performed according to Yu's grading system (Yu et al., 1982). Scores in our tissue samples ranged from 1 to 4. None of the tissue samples had a grade of 0 (no lesions) or a grade of E (end stage) because middle-aged rats were used in this study. The photomicrographs of samples exhibiting representative lesions of each grading score used in this analysis were shown in the appendices (Figure 6.1). In the kidney tissues with the higher grading score, thickening of mesangial matrix became severer, which caused the wider of the individual lobules of glomerui. As the disease advanced, the incidence of tubular atrophy increased. The age-related pathological degenerative damage in kidney tissue was reduced significantly ($p<0.05$) in rats from CR group when compared with rats in the control group. Further, glomerulosclerosis and tubular atrophy were evaluated, and tubular atrophy was significantly less in the rats from CR compared to the control group. But, there was no significant difference between low dose GSE, high dose GSE and control group in the age-related pathological degenerative damage in kidney tissue (Table 5.1). However, there did appear to be a trend for decreased tubular atrophy in low and high dose GSE group, although it did not reach statistical significance. In addition, 24 hours of urinary protein quantification showed that urinary protein was significantly reduced to 15.29 ±1.52 mg/24 hours in rats from CR group when compared to control group (64.33±3.51

mg/24 hours). 24 hours of urinary protein quantification remained unchanged in low and high dose GSE group (69.65±13.69 mg/24 hours and 73.67± 6.07 mg/24 hours, respectively).

Table 5.1 Renal pathological grading

Group	Rat number with lesions of grade				Glomerulos clerosis	Tubular atrophy
	1	2	3	4		
Control	0	4	6	1	0.70±0.70%	4.43±1.65%
LG	0	5	3	3	1.31±0.61%	3.60±0.54%
HG	2	4	3	2	0.75±0.51%	2.74±0.89%
CR*	6	5	0	0	0.00±0.00%	1.54±0.35%*

Control represented control group rats (n=11), LG represented low dose GSE group rats (n=11), HG represented high dose group rats (n=11). CR represented calorie restriction group rats (n=11). There was a significant pathological difference in kidney tissue between CR and Control group. In addition, tubular atrophy was significantly lower in CR than in Control group. ∗ represented $p<0.05$.

5.1.4 Microarray analysis and real time RT-PCR validation

In view of the finding that high dose GSE and CR could attenuate oxidative damage in kidney tissue, the changes in gene profiles regulating the amelioration of age-related oxidative damage in kidney tissue of rats by high dose GSE and CR were outlined using microarray analysis. Because low dose GSE could not attenuate oxidative damage in kidney tissue, this group was not further analyzed with microarray. Genes that were significantly changed by high dose GSE and CR were listed in table 5.2 and table 5.3(in appendices), respectively. In microarray analysis, the expressions of the oxidative stress

related genes (15-lipoxygenase, 15-LO and S100 calcium binding protein A8, S100A8) and the DNA damage checkpoint related gene (cell division cycle 25B**,** Cdc25B) were significantly decreased by high dose GSE. The expression of oxidative stress related gene (kallikrein) was significantly increased and the expression of oxidative stress related genes (complement 3, C3 and chemokine C-C motif-ligand 5, CCL-5) was significantly decreased in CR group, whereas four major antioxidant genes: Cu/Zn-SOD, Mn-SOD, catalase and GPX remained unchanged among the three groups.

Table 5.2 Gene expression significantly changed by high dose grape seed extract

Probe	Fold Change	Gene name
1371245_a_at	8.693	Rat hemoglobin beta-chain mRNA
1371102_x_at	6.527	hemoglobin beta chain complex
1367985_at	6.145	aminolevulinic acid synthase 2
1367553_x_at	4.637	hemoglobin beta chain complex
1388608_x_at	4.592	hemoglobin, alpha 1
1370239_at	3.716	Similar to hemoglobin alpha chain (LOC367986), mRNA
1370240_x_at	3.468	Similar to hemoglobin alpha chain (LOC367986), mRNA
1375519_at	3.164	Similar to alpha globin (LOC287167), mRNA
1370034_at	2.632	cell division cycle 25 homolog B (S. pombe)
1387154_at	2.453	neuropeptide Y
1368494_at	1.996	S100 calcium binding protein A8 (calgranulin A)
1387796_at	1.965	arachidonate 15-lipoxygenase
1379794_at	1.786	granzyme B
1368289_at	1.743	group specific component
1370628_at	1.734	granzyme B
1370096_at	1.621	perforin 1 (pore forming protein)
1379368_at	1.613	Transcribed sequence with moderate similarity to protein sp:P00722 (E. coli) BGAL_ECOLI Beta-galactosidase
1383143_at	1.601	Transcribed sequence with weak similarity to protein ref:NP_115642.1 (H.sapiens) hypothetical protein DKFZp434G118 [Homo sapiens]
1379293_at	1.598	granzyme A
1368300_at	1.577	adenosine A2a receptor
1380142_at	1.559	homeo box B8
1368377_at	1.545	granzyme C
1397251_at	0.66	Transcribed sequences
1387149_at	0.648	type 1 tumor necrosis factor receptor shedding aminopeptidase regulator
1390671_at	0.644	Transcribed sequences
1380041_at	0.566	Transcribed sequences
1391533_at	0.559	Similar to MGC52019 protein (LOC362188), mRNA
1379768_at	0.559	Transcribed sequences
1394112_at	0.488	EST200622 Normalized rat liver, Bento Soares Rattus sp. cDNA clone RLIAG78 3' end, mRNA sequence.
1375475_at	0.433	UI-R-BJ1-ava-c-02-0-UI.s1 UI-R-BJ1 Rattus norvegicus cDNA clone UI-R-BJ1-ava-c-02-0-UI 3', mRNA sequence.

Fold change >1 indicated that the gene was down regulated in high dose grape seed extract, compared to control group, and vice-versa.

To validate the results of microarray and further identify the potential genes involved in the protective role of GSE and CR, four major antioxidant genes (Cu/Zn-SOD, Mn-SOD, catalase and GPX) in the kidney were quantified by real time RT-PCR in the high GSE, CR and control group. 15-LO, S100A8 and Cdc25B were quantified by real time RT-PCR in the high dose GSE and control group. Kallikrein, C3 and CCL-5 between CR and control group were also quantified by real time RT-PCR. The GeNorm software was used to choose suitable housekeeping genes to normalize the data of real tine RT-PCR. HPRT and β-actin were selected as the most stable housekeeping genes (Figure 5.3). Based on HPRT and β-actin, the normalization factor was calculated for real time RT-PCR analysis. As shown in Figure 5.4, the mRNA expressions of 15-LO, S100A8 and Cdc25B significantly decreased in rat kidney tissue in the high dose GSE group, compared to the control groups ($p<0.05$) by real time RT-PCR analysis, which were consistent with the results of microarray. In addition, there were no significant differences in Cu/Zn-SOD expression, Mn-SOD, catalase and GPX mRNA expression between the control group and the high dose GSE group ($p>0.05$) (Figure 5.4A), which were similar to the results of microarray. Real time RT-PCR analysis also showed that the expression of kallikrein was significantly increased and the expression of C3 and CCL-5 was significantly decreased in CR group, similar to the results of microarray (Figure 5.4B). However, the significant increase of Mn-SOD and catalase was found in CR group ($p<0.05$), even though these changes were not indicated by microarray analysis (Figure 5.4A). This might be attributed to a Bejamini and Hochberg false discovery rate

that was used to decrease the false positive rate in CR group microarray data analysis, which brought higher false negative rate at the same time.

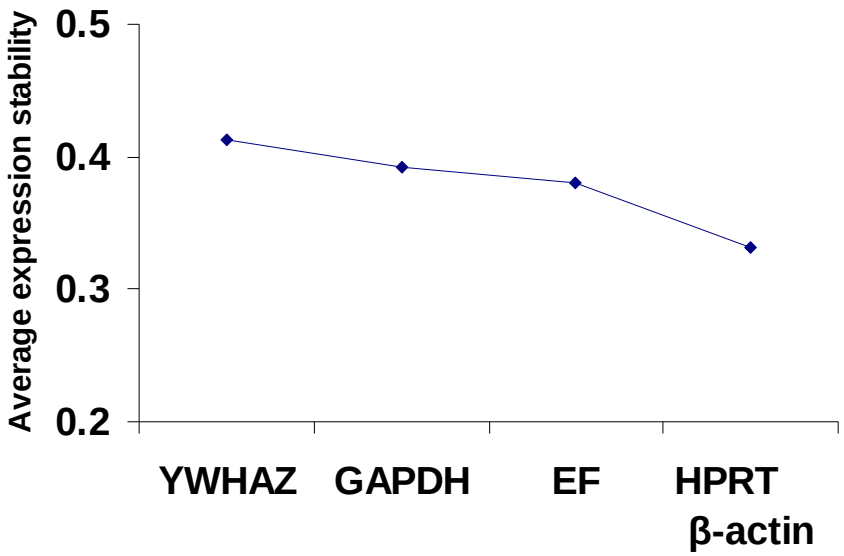

Figure 5.3 Housekeeping genes ranked by GeNorm software in rat kidney cortex.
The picture showed the average expression stability values of the housekeeping genes, with a low value representing stable housekeeping genes expression.

A

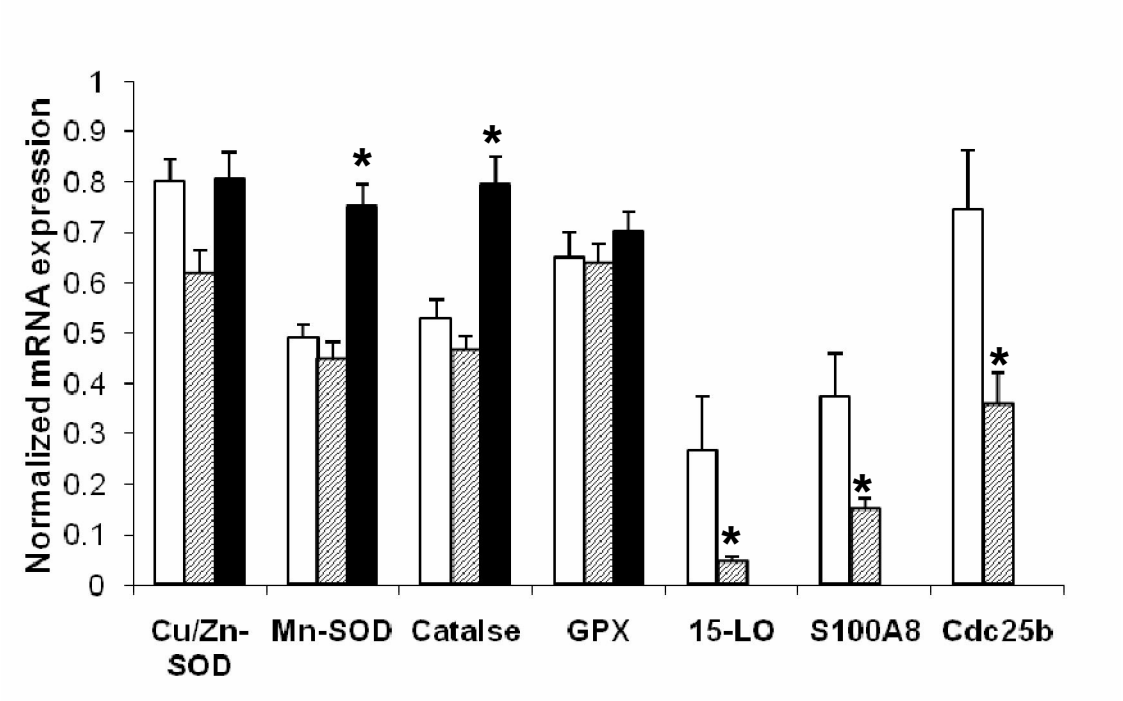

B

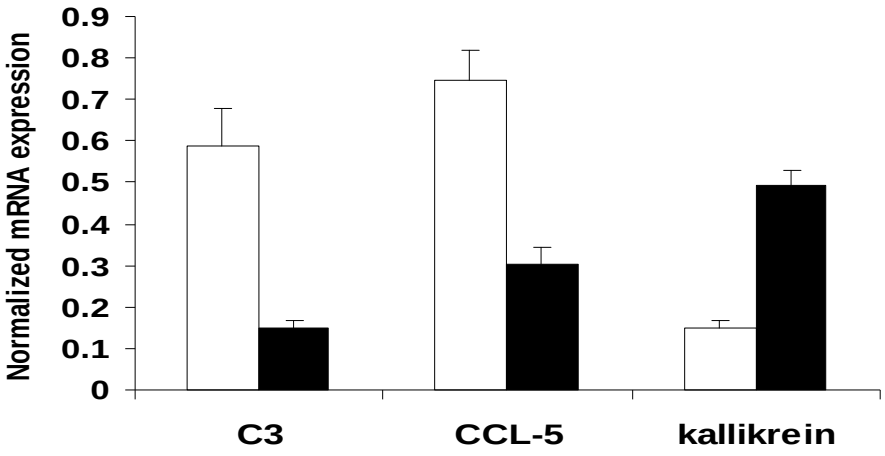

Figure 5.4 Effect of high dose GSE and CR on gene expression in kidney validated by real time RT-PCR method.
Control group (white bar, n=11), high dose group (slanted rule bar, n=11) and calorie restriction group rats (black bar, n=11). (A)Gene expression was normalized to the normalization factor respectively. (B) The gene expression of C3, CCL5 and Kallikrein was normalized to the normalization factor respectively. ∗ represents $p<0.05$.

5.2 Discussion

5.2.1 Effects of grape seed extract and calorie restriction on age related oxidative damage

We found that GSE supplementation and CR significantly attenuated urinary 8-isoprostane. 8-isoprostane was non-enzymatic free radical catalysed-peroxidation of arachidonic acid, which was regarded as a reliable marker of lipid peroxidation (Roberts and Morrow, 2000). The level of 8-isoprostane specifically reflected oxidative stress of animal models, and could be modulated by antioxidants (Roberts and Morrow, 2000). 8-isoprostane and other markers of lipid peroxidation have been reported to increase during the aging process (Ward et al., 2005) and age related pathological conditions, such as cancer and degenerative diseases. Until now, the majority of studies of GSE protection measured lipid peroxidation, based on malondialdehyde (MDA) (Bagchi et al., 2001). However, MDA had been widely questioned because it was an unstable compound, a nonspecific marker of lipid peroxidation and confounded by diet (Janero et al., 1990; Indart et al., 2002); whereas 8- isoprostane was a stable compound, a specific marker of lipid peroxidation and not confounded by diet (Halliwell et al.,2002). In our study, we showed that urinary 8-isoprostane was significantly reduced by GSE supplementation in middle-aged rats. To our knowledge, this was the first report to show that GSE could suppress age related lipid oxidative damage, based on 8-isoprostane.

For CR, it has been reported that CR, which was initiated in young-aged rats, effectively attenuated lipid peroxidation in kidney, liver and brain during aging based on the measurement of MDA (Cook and Yu, 1998). Recently, Ward et al. reported that CR initiated in young-aged rats significantly reduced plasma F2- isoprostane concentrations (Ward et al., 2005). In this study, our data for the first time showed that 6 months CR, which was initiated in middle-aged rats, reduced lipid peroxidation based on measurement of the reliable marker of lipid peroxidation, 8-isoprostane.

In addition, age related protein oxidative damage in rat kidney was also alleviated by high dose of GSE supplement and CR. But, low dose of GSE had no effect in kidney tissue. Ineffective of the lower dose of GSE might be attributed to the middle age onset supplementation, reducing the efficacy of the intervention. A similar situation was reported in the lifespan extension by daf-2 RNAi treatment. When daf-2 RNAi treatment was initiated in different ages of C elegans, the magnitude of the lifespan extension declined with age (Dillin et al., 2002). During the aging process, Goto et al. reported that carbonyl protein increased in aged kidney tissue (Goto et al., 1999). GSE has been reported to protect Adriamycin induced protein oxidative damage in hepatocytes (Valls-Belles et al., 2006) and protein oxidation in the brain of aged rats (Balu et al., 2005). In this study, high dose of GSE supplement effectively decreased the protein oxidative damage in kidney tissue, when initiated in middle age. These results showed that GSE protected protein oxidative damage. Although several studies showed that CR initiated in young age reduced age related increase of carbonyl protein in liver of rats (Youngman et al., 1992)and kidney, heart and brain of mice (Sohal et al., 1994), there was only limited

information on the effect of CR, initiated at middle-aged animal models, on protein oxidative damage. Radak reported that late onset CR could reverse age-related increase of carbonyl protein in rat tendon tissue, but no effect in rat skeletal muscle (Radak et al., 2002). In this study, 6 months CR, initiated in middle-aged rats, also attenuated carbonyl protein in kidney. Combined with the effect of GSE and CR on the urinary 8-isoprostane, these results showed that GSE and CR reduced lipid peroxidation and protein oxidation in middle-aged rats.

5.2.2 Effects of grape seed extract and calorie restriction on pathological changes

Even though 8-isprostante and carbonyl protein were regarded as good available biomarkers of oxidative damage and were suggested to be used as suitable biomarker for testing the effect of anti-aging intervention (Warner et al., 2000), the ideal biomarker of the aging process is still unavailable (Warner, 2004). Thus, pathological assessment was also suggested to evaluate anti-aging intervention because pathological assessment could provide the information of the later development of diseases, even though pathological changes were not so sensitive in reflecting the effect of the compound. To further evaluate the protection role of GSE and CR in middle-aged rats, age related pathological changes in kidney tissue were evaluated. The middle-aged Fischer 344 rats were chosen because there were obvious pathological changes in kidney tissue during this period. Moreover, there are very few other spontaneous diseases, such as cancers, during this period, avoiding the potential confusion (Sass et al., 1975).

We found that 6 months of adult-onset CR decreased the age-related renal pathological changes in Fischer-344 rats, and retarded renal tubular atrophy in middle-aged rats. The majority of renal pathological grading in control group is grade 3, whereas the majority of renal pathological grading in CR group is grade 1 and 2. In addition, there were many mitochondria in renal tubule, which might be more susceptible to oxidative damage because mitochondria were the major source of free radicals (McKiernan et al., 2007). Tubular atrophy is one of the early renal pathological changes during the aging process. Our results showed that age related tubular atrophy was prevented by CR. Proteinuria was correlated with the degree of severity of age-related renal pathological changes. It was generally accepted that the increased renal pathological lesions resulted in protein hyperfiltration (Hard et al., 2004). We also found that 24 hours of urinary protein quantification was significantly decreased by CR. Only limited studies had been reported on the effect of CR on renal pathological changes in middle-aged animal. Recently, it has been reported that the adult-onset CR reduced renal pathological changes in 18 months male Fischer-344 x Brown Norway hybrid rats, but its related mechanism was not fully studied (McKiernan et al., 2007). In this study, our data showed that age related oxidative damage in kidney tissue could be effectively suppressed by CR, suggesting that the protective effect of CR on age related renal pathological change might partly be caused by the reduction of oxidative damage in kidney tissue. Taken together, our data showed that 6 months adult onset CR could retard age related renal pathological changes, even if initiated in middle-aged rat. The detailed mechanism still needs to be further investigated. The possible molecular mechanisms of the protective effect of CR on age

related renal pathological change would be discussed in section 5.3.4, based on the data form microarray and real time RT-PCR.

Even though GSE could effectively prevent oxidative damage in rat kidney tissue, GSE had no significant effect on renal pathological changes and 24 hours of urinary protein quantification. This was consistent with the fewer genes affected by GSE supplement from microarray analysis. Another possible explanation was that renal pathological changes were not sensitive enough in evaluating the effect of the compound, compared to oxidative damage markers. In addition, though not statistically significant, low and high dose GSE were observed to prevent age related tubular atrophy dose dependently. It is worth further investigation to evaluate the protective effects of GSE in kidney.

5.2.3 The molecular mechanism mediating the prevention of oxidative damage by GSE in middle-aged rats

To explore the molecular mechanism of GSE protection, the effects of GSE on gene expression were further evaluated. In this study, we found that GSE decreased the expression of 15-LO and S100A8, two oxidative stress related genes, but the antioxidant genes(Cu/Zn-SOD, Mn-SOD, catalase and GPX) were not affected in kidney tissue. Previous reports showed that GSE inhibited the enzyme activity of 15-LO in vitro (Sadik CD, et al., 2003). Our data showed for the first time that GSE inhibited the mRNA expression of 15-LO in vivo. In addition, we found that protein oxidative damage was also diminished. This result was consistent with the following reports. The brain

isoprostane and protein carbonyl were significantly attenuated in brain tissue of 15-LO deficient mice (Chinnici et al., 2005). The urinary isoprostane level was also significantly decreased in 15-LO deficient mice (Cyrus et al., 2001). Kim et al. reported that oxidative stress was reduced in 15-LO knockout mice (Kim et al., 2003). These findings supported the hypothesis that activated 15-LO could promote the production of free radical, which caused the generation of oxidative damage products (Spiteller, 1996; Funk CD and Cyrus T, 2001), even though the exact mechanism between the 15-LO pathway and the non-enzymatic oxidative reaction is still poorly understood.

In this study, the interesting discovery was that S100A8 was also down regulated by GSE in rat kidney tissue. S100A8 was regarded as a pro-inflammatory mediator and biomarker for inflammation, which was involved in diverse pathological conditions, such as systemic lupus erythematosus and rheumatoid arthritis (Foell et al., 2004). In addition, S100A8 was proposed to import arachidonic acid (AA) into the cell through the formation of S100A8/A 9+AA complex at the inflammatory foci (Kannan, 2003; Nacken et al., 2003). Thus, the imported AA could serve as a substrate of 15-LO to worsen inflammation and oxidative stress at original inflammatory foci. The inhibition effect of GSE on the expression of S100A8 might reduce the availability of AA. Combined with the suppressive effect of GSE on 15-LO expression, the oxidative damage derived from the 15-LO pathway might be effectively suppressed by GSE. Thus, these results suggested that the decreased 15-LO and S100A8 gene expression might be involved in the protective effects of GSE on age related oxidative damage in kidney.

In addition, the mRNA expression of Cdc25B was also inhibited by GSE. Cdc25B primarily activates cyclinB-Cyclin-dependent kinase 1 (Cdk1), which is vital for G2 DNA damage checkpoint (Donzelli and Draetta, 2003). DNA damage checkpoint can cause cell cycle arrest and activate DNA damage repair. Notably, the overexpression of Cdc25B was found in many human cancers, which was regarded as a potential therapeutic target in anticancer therapy (Kristjansdottir and Rudolph, 2004). One merit of inhibiting Cdc25B was that Cdc25B deficiency did not obviously affect normal somatic mouse cells (Lincoln et al., 2002). GSE has been reported to have an anticarcinogenic effect in liver tumor (Ray et al., 2005) and to protect against smokeless tobacco extract-induced oxidative stress in human oral keratinocyte cells (Bagchi et al., 2001). These data indicated that the chemoprevention effect of GSE might be related to the modulation of Cdc25B gene expression by GSE. DNA damage was also regarded to be involved in the aging process (Dröge and Schipper, 2007). The beneficial effect of GSE on G2 DNA damage checkpoint might be helpful in preventing age related DNA damage through modulating Cdc25B expression.

The 15-LO was regarded as a potential therapeutic target in the kidney diseases and atherogenesis (Kasinath, 2003; Zhao and Funk, 2004). Our study showed that GSE effectively inhibited the expression of 15-LO, S100A8 and Cdc25B in kidney tissue, indicating that GSE might be a new promising therapeutic compound for kidney disease. Because we cannot find the protective effect of GSE on age related renal pathological change in this study, further investigations need to evaluate the potential application value of GSE. As nutritional antioxidant, excellent safety of GSE has been demonstrated

(Ray, et al. 2001; Wren, et al. 2002). In addition, GSE is a mixture of monomeric, dimeric, trimeric and other oligomeric proanthocyanidin. Further studies need to be performed to investigate a more effective composition of GSE.

In this study, we did not observe any effect of GSE on the expression of four major antioxidant enzyme genes: Cu/Zn-SOD, Mn-SOD, catalase and GPX, by both microarray and real time RT-PCR method. GSE was reported to increase GPX gene expression in human hepatocellular carcinoma cell line using real time RT-PCR without validated HKG (Puiggros et al., 2005). These differences among studies might be explained by different species and experimental methodologies. Two antioxidants, alpha-lipoic acid and coenzyme Q10 supplement, also did not have any effect on the four major antioxidant enzyme expression in the heart of aging mice (Lee et al., 2004).

In addition, the effects of antioxidants might be dependent on the tissue type, the dose and the time of antioxidants exposure (Skibola et al., 2000). Carrillo et al. reported that deprenyl, a kind of antioxidant, increased Mn-SOD and catalase enzyme activity in parietotemporal cortex and striatum of rats; whereas Mn-SOD and catalase enzyme activity in cerebellum remained unchanged (Carrillo et al., 1992). Moreover, the optimal dose of deprenyl to increase antioxidant enzyme activities varied widely based on different ages and sexes of rats (Kitani et al., 1996). The relation between antioxidants and antioxidant gene expression needs further detailed study.

5.2.4 The molecular mechanism mediating the prevention of oxidative damage and age related renal pathological changes by CR in middle-aged rats

The mechanisms of the anti-aging effects of CR were still unknown (Masoro, 2005). We found that 6 months of CR performed in middle-aged rats could attenuate the decline of antioxidant defenses during rat kidney aging. Compared with control rats, adult onset CR showed a significantly higher expression of catalase and Mn-SOD in rat kidney tissue using real time RT-PCR method. This study was the first report to show that 6 months adult onset CR could increase the expression of Mn-SOD and catalase in the kidneys of rats. Life long CR initiated at a young age could enhance the expression of Mn-SOD and Cu/Zn-SOD in the muscle of rats (Sreekumar et al., 2002). In the first part of this thesis, we found that mRNA expression of catalase and Cu/Zn-SOD decreased significantly in kidney tissue of old rats, which might be involved in the declination of antioxidant defense during aging. Mn-SOD and catalase are major antioxidant enzymes which defend against the attack of free radicals. Mn-SOD located in the mitochondria can convert superoxide into hydrogen peroxide, which is further catalyzed into a water molecule by catalase. In Mn-SOD$^{-/+}$ mice, the decreased Mn-SOD activity resulted in the increase in protein and DNA oxidative damage (Williams et al., 1998). Overexpression of Mn-SOD prevented the diabetes-induced DNA oxidative damage and the total antioxidant capacity in retina of mice (Kowluru, 2006). Overexpression of catalase had been reported to delay age related cardiac pathology and oxidative damage (Schriner et al., 2005). Overexpression of catalase was also reported to delay age related oxidative damage in skeletal muscle of mice and extended life span of mice (Schriner et al., 2005). These data

indicated that the effects of CR on reducing oxidative damage and age related renal pathological change might partly be caused by improving major antioxidant enzyme expression in kidney tissue.

In addition to the increased expression of Mn-SOD and catalase in CR, the increased expression of kallikrein was found in kidney tissue in this study. The effect of CR on kallikrein was not reported before. Kallikrein is a serine proteinase that cleaves high molecular weight kininogen to kinins, such as bradykinin and kallidin (Regoli et al., 1980). The kallikrein-kinin system (KKS) can be categorized into a circulating KKS, which is a member of the coagulation system, and a tissue KKS, which is involved in the local synthesis of kinins through a paracrine or autocrine fashion (Bhoola et al., 1992). Recently, Yao et al. reported that kallikrein could diminish NADH oxidase activity, superoxide formation and lipid oxidation in myocardial infarction of rats (Yao et al., 2007). Kinin, the product of Kallikrein, reduced renal fibrosis by inhibiting oxidative stress and oxidative damage (Chao et al., 2007). Overexpression of kallikrein in rats could inhibit isoproterenol-induced cardiac hypertrophy and fibrosis (Silva et al., 2000). In addition, adult onset CR significantly decreased the expression of C3 and CCL-5. C3-deficient mice showed decreased inflammatory cells infiltration and reduced oxidative damage (Mocco et al., 2006). CCL-5 is one of chemotactic factors and can cause leukocyte infiltration (Sorensen et al., 1999). Administration of anti-CCL5 decreased inflammatory cells infiltration accumulation and reduced inflammatory response (Glass et al., 2004). Although the effects of C3 and CCL5 on oxidative stress related pathological change was unavailable, these decreased inflammatory related genes

suggested that CR might suppress inflammation and the free radical generated from inflammation during aging because inflammatory response is the major resource of free radicals and causes the formation of oxidative damage (Chung et al., 2006). Taken together, our data for the first time showed that adult-onset CR could enhance the expression of kallikrein and reduce the expression of C3 and CCL-5, which might be involved in the protective effects of CR on age related oxidative damage and age related renal pathological change.

It can be inferred that 6 months of adult-onset CR could retard the age-related renal pathological changes and possibly extend the lifespan of rats through the reduction of chronic nephropathy, since chronic renal disease is the major cause of death in Fischer-344 rats. This inference needs to be further investigated. Thus, our data supported the idea that adult onset CR improved the health status by reducing age related diseases.

5.3 Conclusion

In conclusion, our study showed that GSE supplementation and CR initiated in middle age could inhibit age related oxidative damage. In addition, we investigated the gene expression pattern of the effects of GSE and adult onset CR on kidney tissue using the microarray method. To our knowledge, this is the first report that investigated the effect of GSE on the gene expression profiles in animal tissue. Our microarray and real time RT-PCR method analysis suggested that the decreased 15-LO and S100A8 gene expression by GSE might be involved in the protective role of GSE in the rat kidney. 6

months adult onset CR could retard age related oxidative damage and renal pathological changes through the increased catalase, Mn-SOD and kallikrein and the reduced expression of C3 and CCL-5 gene expression.

Chapter VI: Conclusion

6.1 Summary of significant conclusions

Firstly, a real time RT-PCR with valid housekeeping genes protocol was established. For the first time it was found that a wide variation in housekeeping gene expression existed in rat liver, kidney, auditory cortex and cochlea during the aging process, even though the aging process is regarded as a physiological process. Moreover, we found that HPRT was a valid HKG for liver and kidney; but EF and GAPDH were appropriate HKGs in rat auditory cortex and cochlea during aging studies, respectively, which suggested that the suitable HKG should be validated in different experiment conditions. Invalid housekeeping genes could cause the misinterpretation of gene expression levels. Especially, most of the age-related gene expression changes occurred in the 30% to 3 fold range (Pahlavani et al., 1994; Van Remmen et al., 1995). Taken together, validation of HKGs is absolutely vital for accurate gene expression quantification in aging research.

Furthermore, age related antioxidant gene changes were evaluated. We found age related decline of catalase expression in the rat liver and kidney and the decreased Cu/Zn-SOD expression in kidney aging, which suggested that the decrease of catalase mRNA expression might be involved in the decline of intrinsic antioxidant defense in liver, and the decrease of catalase mRNA and Cu/Zn-SOD mRNA expression might be involved in the decline of intrinsic antioxidant protection in kidney, supporting the free radical theory of aging. However, there was no significant antioxidative gene change in auditory cortex

and cochlea aging, which suggests that the role of antioxidant enzyme in auditory cortex and cochlea aging was complex as reported (Coling et al., 2003).

When the effect of GSE and CR in middle-aged rats was investigated, we found that urinary 8-isoprostane was significantly decreased by the low and high dose GSE and CR; and protein carbonyl in kidney was significantly decreased by the high dose GSE and CR. Furthermore, microarray and real time RT-PCR data for the first time showed that the high dose GSE significantly reduced the mRNA expression of 15-LO and S100A8 in kidney, which suggested that GSE could prevent age related oxidative damage by regulating 15-LO and S100A8 gene expression. In addition, age related renal pathological change could be retarded by CR initiated in middle-aged rats. In the CR group, the mRNA expression of catalase, Mn-SOD and kallikrein was significantly increased and the mRNA expression of C3 and CCL-5 was significantly decreased. These data indicated that 6 months CR could retard age related oxidative damage and renal pathological changes by increasing the expression of catalase, Mn-SOD and kallikrein and reducing the expression of C3 and CCL-5.

6.2 Suggestions for Future Work

There are some suggestions for future work. Our study showed that GSE could effectively reduce age related oxidative damage; however further investigation needs to be done to improve the effect of GSE in middle-aged rats. The main problem is how to improve the efficiency of GSE. Firstly, the effective components of GSE need to be

identified, since GSE is a mixture, which has proanthocyanidin dimer, trimer, tetramer and oligomer (Parakeet al., 2002). Our research showed that age related oxidative damage reduced by GSE was related with the decreased 15-LO and S100A8 genes expression by GSE supplement. Analysis of the expression of 15-LO and S100A8 genes expression and others oxidative marker might be helpful to identify the effective component(s) in GSE. However, the purification method of adequate proanthocyanidins is unavailable until now. Multidisciplinary cooperation will be needed to resolve these challenges. Secondly, oxidative damage is closely related with the development of age related diseases, such as atherosclerosis. Age related oxidative damage reduced by GSE suggests that it is worth investigating the effect of GSE on age related diseases. Thirdly, in future, after the most powerful component of GSE is identified and the technology to purify enough proanthocyanidin is available, the life span study could be performed.

6 months CR initiated in middle-aged rats effectively reduced age related oxidative damage and retarded age related renal pathological changes. These results suggest that adult onset CR is a possible intervention to slow the aging process and age related diseases. It remains to be evaluated whether adult onset CR can extend life span. More important, in order to investigate whether adult onset CR can promote healthier aging, more pathological and functional assessments will be needed during life span study, such as cognitive function and tumor incidence. The possible side effects of adult onset CR should also be noticed. Another suggestion is how to make CR more practical. The possible method is to evaluate the effects of different CR strategies, such as 10%CR and 20% CR because 40% CR, the classical CR protocol, is very difficult for most people. If

10% CR has the beneficial effects, it will increase the feasibility of CR. Finally, these findings need to be confirmed in other strains of rats and species. The functional effects of GSE and CR on different tissues are worth investigating.

References

Abou-Gazar H, Bedir E, Takamatsu S, Ferreira D, Khan IA. Antioxidant lignans from Larrea tridentata. Phytochemistry. 2004; 65(17):2499-2505.

Aerts JL, Gonzales MI, Topalian SL. Selection of appropriate control genes to assess expression of tumor antigens using real-time RT-PCR. *Biotechniques*. 2004; 36:84-91.

Andersen CL, Jensen, JL, Orntoft TF. Normalization of real-time quantitative reverse transcription-PCR data: a model-based variance estimation approach to identify genes suited for normalization, applied to bladder and colon cancer data sets. *Cancer Res.* 2004; 64:5245-5250.

Anderson RM, Weindruch R. Calorie restriction: progress during mid-2005-mid-2006. *Exp Gerontol.* 2006; 41(12):1247-1249.

Anjaneyulu M, Chopra K. Nordihydroguairetic acid, a lignin, prevents oxidative stress and the development of diabetic nephropathy in rats. *Pharmacology*. 2004; 72(1):42-50.

Archer JR & Harrison DE. L-Deprenyl treatment in aged mice slightly increases life spans, and greatly reduces fecundity by aged males. *J. Gerontol.* 1996; 31A:B448–B453.

Auger, C., Al Awwadi, N., Bornet, A., Rouanet, J. M., Gasc F., Cros G. Teissedre P. Catechins and procyanidins in Mediterranean diets. *Food Res. Int.* 2004, **37**, 233-245

Bagchi D, Bagchi M, Stohs SJ, Das DK, Ray SD, Kuszynski CA, Joshi SS, Pruess HG. Free radicals and grape seed proanthocyanidin extract: importance in human health and disease prevention. *Toxicology*. 2000; 148:187-197.

Bagchi D, Sen CK, Ray SD, Das DK, Bagchi M, Preuss HG, Vinson JA. Molecular mechanisms of cardioprotection by a novel grape seed proanthocyanidin extract. *Mutat Res.* 2003; 523-524:87-97.

Ball TB, Plummer FA, HayGlass KT. Improved mRNA quantitation in LightCycler RT-PCR. *Int Arch Allergy Immunol*. 2003; 130:82-86.

Balu M, Sangeetha P, Murali G, Panneerselvam C. Age-related oxidative protein damage in central nervous system of rats: modulatory role of grape seed extract. *Int J Dev Neurosci.* 2005; 23:501-507.

Bas A, Forsberg G, Hammarstrom S, Hammarstrom ML. Utility of the housekeeping genes 18S rRNA, beta-actin and glyceraldehyde-3-phosphate-dehydrogenase for normalization in real-time quantitative reverse transcriptase-polymerase chain reaction analysis of gene expression in human T lymphocytes. *Scand J Immunol.* 2004; 59:566-573.

Basu S. Isoprostanes: novel bioactive products of lipid peroxidation. *Free Radic. Res.* 2004; 38:105-122.

Baur JA, Pearson KJ, Price NL, Jamieson HA, Lerin C, Kalra A, Prabhu VV, Allard JS, Lopez-Lluch G, Lewis K, Pistell PJ, Poosala S, Becker KG, Boss O, Gwinn D, Wang M, Ramaswamy S, Fishbein KW, Spencer RG, Lakatta EG, Le Couteur D, Shaw RJ, Navas P, Puigserver P, Ingram DK, de Cabo R, Sinclair DA. Resveratrol improves health and survival of mice on a high-calorie diet. *Nature.* 2006; 444:337-342.

Bhoola KD, Figueroa CD, Worthy K. Bioregulation of kinins: kallikreins, kininogens, and kininases. *Pharmacol Rev.* 1992; 44:1–80.

Biederman J, Yee J, Cortes P. Validation of internal control genes for gene expression analysis in diabetic glomerulosclerosis. Kidney Int. 2004; 66:2308-2314.

Boorman G. A., Eustis S. L., Elwell M. R., Montgomery J. C. A., and MacKenzie W. F. (1990) Pathology of the Fischer rat. Academic Press, Inc, San Diego.

Bohr VA, Anson RM. DNA damage, mutation and fine structure DNA repair in aging. *Mutat. Res.* 1995; 338:25–34.

Bokov A, Chaudhuri A, Richardson A. The role of oxidative damage and stress in aging.

Mech Ageing Dev. 2004; 125(10-11):811-826.

Bredt DS. Endogenous nitric oxide synthesis: biological functions and pathophysiology. *Free Radic Res*. 1999 ; 31:577-96

Brown PO, Botstein DPO. Exploring the new world of the genome with DNA microarrays. *Nat. Genet.*1999; 21:33–37.

Burke A, Lawson JA, Meagher EA, Rokach J, FitzGerald GA. Specific analysis in plasma and urine of 2,3-dinor-5, 6-dihydro-isoprostane F(2alpha)-III, a metabolite of isoprostane F(2alpha)-III and an oxidation product of gamma-linolenic acid. *J Biol Chem.* 2000; 275:2499-2504.

Bustin SA. Quantification of mRNA using real-time reverse transcription PCR (RT-PCR): trends and problems. *J Mol Endocrinol.* 2002; 29:23-39.

Bustin SA and Nolan T. Pitfalls of quantitative real-time reverse-transcription polymerase chain reaction. *J Biomol Tech*. 2004; 15:155-166.

Cadenas E. & Sies H. The lag phase. *Free. Radic. Res.* 1998; 28:601–609.

Carr A, McCall MR, & Frei B. Oxidation of LDL by myeloperoxidase and reactive nitrogen species-reaction pathways and antioxidant protection. *Arterioscl. Thromb. Vasc. Biol.* 2000; 20:1716–1723.

Carrillo, M.C., Kitani, K., Kanai, S., Sato, Y., Ivy, G.O. The ability of (−)deprenyl to increase superoxide dismutase activities in the rat is tissue and brain region selective. *Life Sci.* 1992; 50: 1985–1992.

Carrillo MC, Minami C, Kitani K, Maruyama W, Ohashi K, Yamamoto T, Naoi M, Kanai S, Youdim MB. Enhancing effect of rasagiline on superoxide dismutase and catalase activities in the dopaminergic system in the rat. *Life Sci.* 2000; 67:577–585.

Chao J, Li HJ, Yao YY, Shen B, Gao L, Bledsoe G, Chao L. Kinin infusion prevents renal inflammation, apoptosis, and fibrosis via inhibition of oxidative stress and mitogen-activated protein kinase activity. *Hypertension.* 2007; 49(3):490-497.

Chanock SJ, El BJ, Smith RM, And Babior BM. The respiratory burst oxidase. *J. Biol. Chem.* 1994; 269:24519–24522.

Chen J, Rider DA, Ruan R. Identification of valid housekeeping genes and antioxidant enzyme gene expression change in the aging rat liver. *J Gerontol A Biol Sci Med Sci.* 2006; 61:20-27.

Chinnici CM, Yao Y, Ding T, Funk CD, Praticò D. Absence of 12/15 lipoxygenase reduces brain oxidative stress in apolipoprotein E-deficient mice. *Am J Pathol.* 2005; 167: 1371-1377.

Choi JK, Holtzer S, Chacko SA, Lin ZX, Hoffman RK, Holtzer H. Phorbol esters selectively and reversibly inhibit a subset of myofibrillar genes responsible for the ongoing differentiation program of chick skeletal myotubes. *Mol Cell Biol.* 1991; 11:4473-82.

Chung, H.Y., Sung, B., Jung, K. J., Zou, Y., and Yu, B.P. The molecular inflammatory process in aging. *Antioxid Redox Signal*. 2006; 8: 572-81

Clapp NK, Satterfield LC, Bowles ND. Effects of the antioxidant butylated hydroxytoluene (BHT) on mortality in BALB/c mice. *J. Gerontol.* 1979; 34:497–501.

Clerici WJ and Yang L. Direct effects of intraperilymphatic reactive oxygen species generation on cochlear function. *Hear Res.* 1996; 101:14-22.

Coling DE, Yu KC, Somand D, Satar B, Bai U, Huang TT, Seidman MD, Epstein CJ, Mhatre AN, Lalwani AK. Effect of SOD1 overexpression on age- and noise-related hearing loss. *Free Radic Biol Med*. 2003; 34:873-880.

Cook CI, Yu BP. Iron accumulation in aging: modulation by dietary restriction. *Mech Ageing Dev*. 1998;102(1):1-13.

Corder R, Mullen W, Khan NQ, Marks SC, Wood EG, Carrier MJ, Crozier A. Oenology: red wine procyanidins and vascular health. *Nature.* 2006; 444:566.

Cos P, De Bruyne T, Hermans N, Apers S, Berghe DV, Vlietinck AJ. Proanthocyanidins in health care: current and new trends. *Curr Med Chem.* 2004; 11:1345-1359.

Cracowski JL, Durand T, Bessard G. Isoprostanes as a biomarker of lipid peroxidation in humans: physiology, pharmacology and clinical implications. *Trends Pharmacol Sci.* 2002; 23(8):360-366.

Davi G, Ciabattoni G, Consoli A, Mezzetti A, Falco A, Santarone S, Pennese E, Vitacolonna E, Bucciarelli T, Costantini F, Capani F, Patrono C. In vivo formation of 8-iso-prostaglandin f2alpha and platelet activation in diabetes mellitus: effects of improved metabolic control and vitamin E supplementation. *Circulation.* 1999; 99(2):224-229.

Davies JE, Ellery PM, Hughes RE. Dietary ascorbic acid and life span of guinea-pigs. *Exp Gerontol.* 1977; 12(5-6):215-216.

De Kok JB, Roelofs RW, Giesendorf BA, Pennings JL, Waas ET, Feuth T, Swinkels DW, Span PN. Normalization of gene expression measurements in tumor tissues: comparison of 13 endogenous control genes. *Lab Invest.* 2005; 85:154-159.

Depreter M, Vandesompele J, Espeel M, Speleman F, Roels F. Modulation of the peroxisomal gene expression pattern by dehydroepiandrosterone and vitamin D: therapeutic implications. *J Endocrinol*. 2002; 175:779-792.

Dheda K, Huggett JF, Bustin SA, Johnson MA, Rook G, Zumla A. Validation of housekeeping genes for normalizing RNA expression in real-time PCR. *Biotechniques.* 2004; 37:112-119.

Dillin A, Crawford DK, Kenyon C. Timing requirements for insulin/IGF-1 signaling in C. elegans. *Science*. 2002; 298:830-834.

Dirks, A.J. & C. Leeuwenburgh. Caloric restriction in humans: potential pitfalls and health concerns. *Mech. Ageing Dev*. 2006; 127:1–7.

Donzelli M, Draetta GF. Regulating mammalian checkpoints through Cdc25 inactivation. *EMBO Rep*. 2003; 4: 671-677.

Duttaroy A, Paul A, Kundu M, Belton A. A Sod2 null mutation confers severely reduced adult life span in Drosophila, *Genetics*. 2003; 165:2295–2299.

Dvorák Z, Pascussi JM, Modrianský M. Approaches to messenger RNA detection - comparison of methods. *Biomed Pap Med Fac Univ Palacky Olomouc Czech Repub.* 2003;147: 131-5

Economos AC, Ballard RC, Miquel J, Binnard R, Philpott DE. Accelerated aging of fasted Drosophila. Preservation of physiological function and cellular fine structure by thiazolidine carboxylic acid (TCA). *Exp. Gerontol.* 1982; 17:105–114.

Elchuri S, Oberley TD, Qi W, Eisenstein RS, Jackson Roberts L, Van Remmen H, Epstein CJ, Huang TT. CuZnSOD deficiency leads to persistent and widespread oxidative damage and hepatocarcinogenesis later in life. *Oncogene.* 2005; 24:367–380.

Finkel T, Holbrook NJ. Oxidants,oxidative stress and the biology of ageing. *Nature*. 2000; 408:239-247.

Finlayson PG, Caspary DM. Response properties in young and old Fischer-344 rat lateral superior olive neurons: A quantitative approach. *Neurobiol. Aging*. 1993;14:127-139.

Foell D, Frosch M, Sorg C, Roth J. Phagocyte-specific calcium-binding S100 proteins as clinical laboratory markers of inflammation. *Clin Chim Acta*. 2004; 344:37-51.

Foss DL, Baarsch MJ, Murtaugh MP. Regulation of hypoxanthine phosphoribosyltransferase, glyceraldehyde-3-phosphate dehydrogenase and beta-actin mRNA expression in porcine immune cells and tissues. *Anim Biotechnol.* 1998; 9:67-78.

Frankel EN, Waterhouse AL. Inhibition of human LDL oxidation by resveratrol. *Lancet.* 1993; 341:1103–1104.

Ghafourifar P, and Cadenas, E. Mitochondrial nitric oxide synthase. *Trends Pharmacol. Sci.* 2005; 26:190–195.

Ginzinger DG. Gene quantification using real-time quantitative PCR: an emerging technology hits the mainstream. *Exp Hematol.* 2002; 30:503-512.

Glare EM, Divjak M, Bailey MJ, Walters EH. Beta-Actin and GAPDH housekeeping gene expression in asthmatic airways is variable and not suitable for normalising mRNA levels. *Thorax.* 2002; 57:765-770.

Glass WG, Hickey MJ, Hardison JL, Liu MT, Manning JE, Lane TE. Antibody targeting of the CC chemokine ligand 5 results in diminished leukocyte infiltration into the central nervous system and reduced neurologic disease in a viral model of multiple sclerosis. *J Immunol.* 2004; 172:4018-25.

Goeptar AR, Scheerens H, And Vermeulen NP. Oxygen and xenobiotic reductase activities of cytochrome P450. *Crit. Rev. Toxicol.* 1995; 25:25–65.

Goodrick CL, Ingram DK, Reynolds MA, Freeman JR, Cider N. Effects of intermittent feeding upon body weight and lifespan in inbred mice: interaction of genotype and age. *Mech Ageing Dev.* 1990; 55(1):69-87.

Goto S, Nakamura A, Radak Z, Nakamoto H, Takahashi R, Yasuda K, Sakurai Y, Ishii N. Carbonylated proteins in aging and exercise: immunoblot approaches. *Mech Ageing Dev*. 1999; 107:245-253.

Grune T, Davies KJ. Oxidative processes in aging. In: Masoro EJ, Austad SN eds. *Handbook of the biology of aging*. 5th ed. San Diego, CA: Academic Press; 2001:25-58.

Gu L, Kelm MA, Hammerstone JF, Beecher G, Holden J, Haytowitz D, Gebhardt S, Prior RL. Concentrations of proanthocyanidins in common foods and estimations of normal consumption. *J. Nutr.* 2004, 134, 613-617.

Guo ZM, Heydari AR, Richardson A. Nucleotide excision repair of actively transcribed versus nontranscribed DNA in rat hepatocytes: effect of age and dietary restriction. *Exp. Cell Res*. 1998; 245:228–238.

Gutteridge JM, And Halliwell B. The measurement and mechanism of lipid peroxidation in biological systems. *Trends Bio- chem. Sci.* 1990; 15:129–135.

Haller F, Kulle B, Schwager S, et al. Equivalence test in quantitative reverse transcription polymerase chain reaction: confirmation of reference genes suitable for normalization. *Anal Biochem*. 2004; 335:1-9.

Halliwell B & Gutteridge JMC. Free radicals in biology and medicine (3rd ed.). Oxford University Press. 1999.

Halliwell B, Whiteman M. Measuring reactive species and oxidative damage in vivo and in cell culture: how should you do it and what do the results mean? *Br J Pharmacol.* 2004; 142:231-255.

Hamalainen HK, Tubman JC, Vikman S, Kyrola T, Ylikoski E, Warrington JA, Lahesmaa R. Identification and validation of endogenous reference genes for expression profiling of T helper cell differentiation by quantitative real-time RT-PCR. *Anal Biochem.* 2001; 299:63-70.

Hamilton ML, Van Remmen H, Drake JA, Yang H, Guo ZM, Kewitt K,Walter CA, Richardson A. Does oxidative damage to DNA increase with age? *Proc. Natl. Acad. Sci. U.S.A.* 2001; 98:10469–10474.

Han E, Hilsenbeck SG. Array-based gene expression profiling to study aging. *Mech Ageing Dev*. 2001; 122:999-1018.

Han ES, Hickey M. Microarray evaluation of dietary restriction. *J Nutr*. 2005; 135:1343-1346.

Hard GC, Khan KN. A contemporary overview of chronic progressive nephropathy in the laboratory rat, and its significance for human risk assessment. *Toxicol Pathol.* 2004;32:171-80.

Harman D. The biologic clock: the mitochondria? J. Am. Geriatr Soc. 1972; 20:145–147.

Hauck SJ, Aaron JM, Wright C, Kopchick JJ, Bartke A. Antioxidant enzymes, free-radical damage, and response to paraquat in liver and kidney of long-living growth hormone receptor/binding protein gene-disrupted mice. Horm Metab Res. 2002; 34(9):481-486.

Hermans N, Cos P, Maes L, De Bruyne T, Vanden Berghe D, Vlietinck AJ, Pieters L. Challenges and Pitfalls in Antioxidant Research. Curr Med Chem. 2007;14(4):417-30

Indart A, Viana M, Grootveld MC, Silwood CJ, Sanchez-Vera I, Bonet B. Teratogenic actions of thermally-stressed culinary oils in rats. *Free Radic. Res.* 2002; 36:1051−1058.

Ishitani R, Sunaga K, Hirano A, Saunders P, Katsube N, Chuang DM. Evidence that glyceraldehyde-3-phosphate dehydrogenase is involved in age-induced apoptosis in mature cerebellar neurons in culture. *J Neurochem.* 1996; 66:928-935.

Iyer VR, Eisen MB, Ross DT, et al. The transcriptional program in the response of human fibroblasts to serum. *Science*. 1999; 283:83-87.

Janero D. R. Malondialdehyde and thiobarbituric acid-reactivity as diagnostic indices of lipid peroxidation and peroxidative tissue injury. *Free Radic Biol Med*. 1990; 9:515-540.

Jang I, Chae K, Cho J. Effects of age and strain on small intestinal and hepatic antioxidant defense enzymes in Wistar and Fisher 344 rats. *Mech Ageing Dev*. 2001; 122: 561-570.

Jennings CR, Jones NS. Presbyacusis. J Laryngol Otol. 2001;115(3):171-8

Jiang H, Talaska AE, Schacht J, Sha SH. Oxidative imbalance in the aging inner ear. *Neurobiol Aging.* 2007; 28:1605-1612.

Kadiiska MB, Gladen BC, Baird DD, Graham LB, Parker CE, Ames BN, Basu S, Fitzgerald GA, Lawson JA, Marnett LJ, Morrow JD, Murray DM, Plastaras J, Roberts LJ 2nd, Rokach J, Shigenaga MK, Sun J, Walter PB, Tomer KB, Barrett JC, Mason RP. Biomarkers of oxidative stress study III. Effects of the nonsteroidal anti-inflammatory agents indomethacin and meclofenamic acid on measurements of oxidative products of lipids in CCl4 poisoning. *Free Radic Biol Med.* 2005; 38(6):711-718.

Kannan S. Inflammation: a novel mechanism for the transport of extracellular nucleotide-induced arachidonic acid by S100A8/A9 for transcellular metabolism. *Cell Biol Int.* 2003; 27:593-595.

Keithley EM, Canto C, Zheng QY, Wang X, Fischel-Ghodsian N, Johnson KR. Cu/Zn

superoxide dismutase and age-related hearing loss. *Hear Res*. 2005; 209:76-85.

Kim S, Kim T. Selection of optimal internal controls for gene expression profiling of liver disease. *Biotechniques*. 2003; 35:456-460.

Kim YS, Reddy MA, Lanting L, Adler SG, Natarajan R. Differential behavior of mesangial cells derived from 12/15-lipoxygenase knockout mice relative to control mice. *Kidney Int*. 2003; 64:1702-1714.

Kitani, K., Miyasaka, K., Kanai, S., Carrillo, M.C., Ivy, G.O. Upregulation of antioxidant enzyme activities by deprenyl: implications for life span extension. Ann. N. Y. Acad. Sci. 1996; 786: 391–409.

Kitani K, Kanai S, Miyasaka K, Carrillo MC, Ivy GO. Dose-dependency of life span prolongation of F344/DuCrj rats injected with (-)deprenyl. *Biogerontology*. 2005; 6 :297-302.

Kitani K, Kanai S, Miyasaka K, Carrillo MC, Ivy GO. The necessity of having a proper dose of (-)deprenyl (D) to prolong the life spans of rats explains discrepancies among different studies in the past. *Ann N Y Acad Sci.* 2006; 1067:375-382.

Kowluru RA, Kowluru V, Xiong Y, Ho YS. Overexpression of mitochondrial superoxide dismutase in mice protects the retina from diabetes-induced oxidative stress. *Free Radic Biol Med.* 2006; 41(8):1191-1196.

Koya E, Spijker S, Homberg JR, Voorn P, Schoffelmeer AN, De Vries TJ, Smit AB. Molecular reactivity of mesocorticolimbic brain areas of high and low grooming rats after elevated plus maze exposure. *Brain Res Mol Brain Res*. 2005; 137:184-192.

Kristjansdottir K.and Rudolph J. Cdc25 phosphatases and cancer. *Chem. Biol*. 2004; 11:1043–1051.

Kurosu, H.; Yamamoto, M.; Clark, J. D.; Pastor, J. V.; Nandi, A.; Gurnani, P.; McGuinness, O. P.; Chikuda, H.; Yamaguchi, M.; Kawaguchi, H.; Shimomura, I.; Takayama, Y.; Herz, J.; Kahn, C. R.; Rosenblatt, K. P.; Kuro-o, M. Suppression of aging in mice by the hormone klotho**.** *Science* 2005; 309: 1829-1833.

Lambert AJ, Merry BJ. Effect of caloric restriction on mitochondrial reactive oxygen species production and bioenergetics: reversal by insulin. *Am. J. Physiol. Regul. Integr. Comp. Physiol.* 2004; 286:R71–R79.

Lee CK, Pugh TD, Klopp RG, Edwards J, Allison DB, Weindruch R, Prolla TA. The impact of alpha-lipoic acid, coenzyme Q10 and caloric restriction on life span and gene expression patterns in mice. *Free Radic Biol Med*. 2004; 36:1043-1057.

Lincoln AJ, Wickramasinghe D, Stein P, Schultz RM, Palko ME, De Miguel MP, Tessarollo L, Donovan PJ. Cdc25b phosphatase is required for resumption of meiosis during oocyte maturation. *Nat Gene*. 2002; 30:446–449.

Lipman RD, Smith DE, Blumberg JB, Bronson RT. Effects of caloric restriction or augmentation in adult rats: longevity and lesion biomarkers of aging. *Aging (Milano).* 1998;10(6):463-470.

Liu R, Liu IY, Bi X, Thompson RF, Doctrow SR, Malfroy B, Baudry M. Reversal of age-related learning deficits and brain oxidative stress in mice with superoxide dismutase/catalase mimetics. *Proc. Natl. Acad. Sci. U. S. A.* 2003; 100:8526-8531.

Lombard DB, Chua KF, Mostoslavsky R, Franco S, Gostissa M, Alt FW. DNA repair, genome stability, and aging. *Cell.* 2005; 120:497-512.

Maeda H, Gleiser CA, Masoro EJ, Murata I, McMahan CA, Yu BP. Nutritional influences on aging of Fischer 344 rats: II. Pathology. *J Gerontol.* 1985;40(6):671-688.

Martin R, Fitzl G, Mozet C, Martin H, Welt K, Wieland E. Effect of age and hypoxia/reoxygenation on mRNA expression of antioxidative enzymes in rat liver and kidneys. *Exp Gerontol*. 2002; 37:1481-1487.

Masoro EJ. Caloric restriction and aging: controversial issues. *J Gerontol A Biol Sci Med Sci.* 2006; 61(1):14-19.

Masoro EJ. Overview of caloric restriction and ageing. *Mech Ageing Dev.* 2005; 126:913-922.

Masternak MM, Al-Regaiey K, Bonkowski MS, et al. Divergent effects of caloric restriction on gene expression in normal and long-lived mice. *J Gerontol A Biol Sci Med Sci.* 2004; 59:784-788.

McCay CM, Crowell MF, Maynard LA. The effect of retarded growth upon the length of life and upon the ultimate body size. J. Nutr. 1935; 10:63–79.

McCord JM, Fridovich I. Superoxide dismutase. An enzymic function for erythrocuprein (hemocuprein). *J. Biol. Chem.* 1969; 244:6049–6055.

McFadden SL, Ding D, Burkard RF, Jiang H, Reaume AG, Flood DG, Salvi RJ. Cu/Zn SOD deficiency potentiates hearing loss and cochlear pathology in aged 129, CD-1 mice. *J Comp Neurol.* 1999; 413:101-112.

Meagher EA, Barry OP, Burke A, Lucey MR, Lawson JA, Rokach J, FitzGerald GA. Alcohol-induced generation of lipid peroxidation products in humans. *J Clin Invest.* 1999; 104: 805-813.

Melk, A., Mansfield, E.S., Hsieh, S.C., Hernandez-Boussard, T., Grimm, P., Rayner, D.C., Halloran, P.F., and Sarwal, M.M. Transcriptional analysis of the molecular basis of human kidney aging using cDNA microarray profiling. *Kidney Int.* 2005; 68: 2667-79.

Meisami E, Brown CM, Emerle HF. Sensory systems: normal aging, disorders, and treatments of vision and hearing in humans, In:Timiras, P.S.(Eds) Physiological basis of aging and geriatrics. *CRC Press LLC, Boca Raton.* 2002; 141-165.

Melov S, Ravenscroft J, Malik S, Gill MS, Walker DW, Clayton PE, Wallace DC, Malfroy B, Doctrow SR, Lithgow GJ. Extension of Life-Span with Superoxide Dismutase/Catalase Mimetics. *Science.* 2000; 289:1567-1569.

Migliaccio E, Giorgio M, Mele S, Pelicci G, Reboldi P, Pandolfi PP, Lanfrancone L, Pelicci PG. The p66shc adaptor protein controls oxidative stress response and life span in mammals. *Nature.* 1999; 402:309–313.

Miller RA, Harrison DE, Astle CM, Floyd RA, Flurkey K, Hensley KL, Javors MA, Leeuwenburgh C, Nelson JF, Ongini E, Nadon NL, Warner HR, Strong R. An Aging Interventions Testing Program: study design and interim report. *Aging Cell.* 2007; 6 :565-575.

Miquel J, Fleming J, Economos AC. Antioxidants, metabolic rate and aging in Drosophila. *Arch. Gerontol. Geriatr*. 1982; 1:159–165.

Mocco J, Mack WJ, Ducruet AF, Sosunov SA, Sughrue ME, Hassid BG, Nair MN, Laufer I, Komotar RJ, Claire M, Holland H, Pinsky DJ, Connolly ES Jr. Complement component C3 mediates inflammatory injury following focal cerebral ischemia. *Circ Res.* 2006 ; 99: 209-17.

Mohamed SA, Wesch D, Blumenthal A, et al. Detection of the 4977 bp deletion of mitochondrial DNA in different human blood cells. *Exp Gerontol*. 2004; 39:181-188.

Morrow JD, Awad JA, Boss HJ, Blair IA, Roberts LJ 2nd. Non-cyclooxygenase-derived prostanoids (F2-isoprostanes) are formed in situ on phospholipids. *Proc Natl Acad Sci U S A.* 1992; 89(22):10721-10725.

Morrow JD, Harris TM and Roberts LJ II. Non-cyclooxygenase oxidative formation of a series of novel prostaglandins: analytical ramification for measurement of eicosanoids. *Anal. Biochem.* 1990; 184:1–10.

Morrow JD, Hill KE, Burk RF, Nammour TM, Badr KF, Roberts LJ 2nd. A series of prostaglandin F2-like compounds are produced in vivo in humans by a non-cyclooxygenase, free radical-catalyzed mechanism. *Proc Natl Acad Sci U S A.* 1990; 87(23):9383-9387.

Moshier JA, Cornell T, Majumdar AP. Expression of protease genes in the gastric mucosa during aging. *Exp Gerontol.* 1993; 28:249-258.

Mote PL, Grizzle JM, Walford RL, Spindler SR. Influence of age and caloric restriction on expression of hepatic genes for xenobiotic and oxygen metabolizing enzymes in the mouse. *J Gerontol.* 1991; 46(3):B95-100.

Muller FL, Song W, Liu Y, Chaudhuri A, Pieke-Dahl S, Strong R, Huang TT, Epstein CJ, Roberts LJ 2nd, Csete M, Faulkner JA, Van Remmen H. Absence of CuZn superoxide dismutase leads to elevated oxidative stress and acceleration of age-dependent skeletal muscle atrophy, Free Radic. *Biol. Med.* 2006; 40:1993–2004.

Murai Y, Hishinuma T, Suzuki N, Satoh J, Toyota T, Mizugaki M. Determination of urinary 8-epi-prostaglandin F(2alpha) using liquid chromatography-tandem mass spectrometry: increased excretion in diabetics. *Prostaglandins Other Lipid Mediat.* 2000; 62(2):173-181.

Nicklas TA, Baranowski T, Cullen KW, Berenson G. Eating patterns, dietary quality and obesity. *J Am Coll Nutr.* 2001; 20(6):599-608.

Noda M, Kariura Y, Amano T, Manago Y, Nishikawa K, Aoki S, Wada K. Expression and function of bradykinin receptors in microglia. *Life Sci.* 2003; 72:1573-1581.

Pacifici RE, And Davies KJ. Protein, lipid and DNA repair systems in oxidative stress: the free-radical theory of aging revis- ited. *Gerontology.* 1991; 37:166–180.

Pang ST, Dillner K, Wu X, Pousette A, Norstedt G, Flores-Morales A. Gene expression profiling of androgen deficiency predicts a pathway of prostate apoptosis that involves genes related to oxidative stress. *Endocrinology*. 2002 ; 143:4897-906.

Pahlavani MA, Haley-Zitlin V, Richardson A. Influnce of dietary restriction on gene expression: changes in the transcription of specific genes. In Yu B.P, ed. *Modulation of the aging process by dietary restriction* . Boca Raton FL: CRC Press; 1994;143-156.

Pataki T, Bak I, Kovacs P, Bagchi D, Das DK, Tosaki A. Grape seed proanthocyanidins improved cardiac recovery during reperfusion after ischemia in isolated rat hearts. *Am J Clin Nutr*. 2002 ; 75:894-899.

Peinnequin A, Mouret C, Birot O, Alonso A, Mathieu J, Clarencon D, Agay D, Chancerelle Y, Multon E. Rat pro-inflammatory cytokine and cytokine related mRNA quantification by real-time polymerase chain reaction using SYBR green. *BMC Immunol[serial online]*. 2004; 5. Available at: http://www.biomedcentral.com/1471-2172/5/3. Accessed February 5, 2004.

Peters IR, Helps CR, Hall EJ, Day MJ. Real-time RT-PCR: considerations for efficient and sensitive assay design. *J Immunol Methods.* 2004; 286:203-217.

Phillips JP, Campbell SD, Michaud D, Charbonneau M, Hilliker AJ. Null mutation of copper/zinc superoxide dismutase in Drosophila confers hypersensitivity to paraquat and reduced longevity, *Proc. Natl. Acad. Sci. USA* 1989; 86:2761–2765.

Powers SK, Lawler J, Criswell D, Lieu FK, Dodd S. Alterations in diaphragmatic oxidative and antioxidant enzymes in the senescent Fischer 344 rat. *J Appl Physiol.* 1992 ;72: 2317-21.

Praticò D, Iuliano L, Mauriello A, Spagnoli L, Lawson JA, Rokach J, Maclouf J, Violi F, FitzGerald GA. Localization of distinct F2-isoprostanes in human atherosclerotic lesions. *J Clin Invest.* 1997; 100(8):2028-2034.

Proudfoot J, Barden A, Mori TA, Burke V, Croft KD, Beilin LJ, Puddey IB. Measurement of urinary F(2)-isoprostanes as markers of in vivo lipid peroxidation-A comparison of enzyme immunoassay with gas chromatography/mass spectrometry. *Anal Biochem.* 1999; 272(2):209-215.

Puiggros F, Llópiz N, Ardévol A, Bladé C, Arola L, Salvadó MJ. Grape seed procyanidins prevent oxidative injury by modulating the expression of antioxidant enzyme systems. *J Agric Food Chem.* 2005; 53:6080-6086.

Qi X, Lewin AS, Sun L, Hauswirth WW, Guy J.SOD2 gene transfer protects against optic neuropathy induced by deficiency of complex I. Ann Neurol. 2004 ;56:182-91.

Radák Z, Takahashi R, Kumiyama A, Nakamoto H, Ohno H, Ookawara T, Goto S. Effect of aging and late onset dietary restriction on antioxidant enzymes and proteasome activities, and protein carbonylation of rat skeletal muscle and tendon. *Exp Gerontol.* 2002; 37(12):1423-1430.

Rao G, Xia E, Nadakavukaren MJ, Richardson. A. Effect of dietary restriction on the age-dependent changes in the expression of antioxidant enzymes in rat liver. *J Nutr.* 1990; 120:602-609.

Rao G, Xia E, Richardson A. Effect of age on the expression of antioxidant enzymes in male Fisher F344 rats. *Mech Ageing Dev*. 1990; 53:49-60.

Rasmussen SE, Frederiksen H, Struntze Krogholm K, Poulsen L. Dietary proanthocyanidins: occurrence, dietary intake, bioavailability, and protection against cardiovascular disease. Mol Nutr Food Res. 2005 Feb; 49(2):159-74. Copyright Wiley-VCH Verlag GmbH & Co. KGaA. Reproduced with permission.

Ray SD, Parikh H, Bagchi D. Proanthocyanidin exposure to B6C3F1 mice significantly attenuates dimethylnitrosamine-induced liver tumor induction and mortality by

differentially modulating programmed and unprogrammed cell deaths. *Mutat Res*. 2005; 579:81-106.

Regoli D, Barabe J. Pharmacology of bradykinin and related kinins. *Pharmacol Rev*. 1980; 32(1):1-46.

Reveillaud I, Phillips J, Duyf B, Hilliker A, Kongpachith A, Fleming JE. Phenotypic rescue by a bovine transgene in a Cu/Zn superoxide dismutase-null mutant of Drosophila melanogaster. *Mol. Cell. Biol.* 1994; 14:1302–1307.

Richelle M, Turini ME, Guidoux R, Tavazzi I, Metairon S, Fay LB. Urinary isoprostane excretion is not confounded by the lipid content of the diet. *FEBS Lett.* 1999; 459(2):259-262.

Rikans LE, Moore DR, Snowden CD. Sex-dependent differences in the effects of aging on antioxidant defense mechanisms of rat liver. *Biochim Biophys Acta*. 1991; 1074:195-200.

Roberts LJ and Morrow JD. Measurement of F2-isoprostanes as an index of oxidative stress in vivo. Free Radic Biol Med, 2000; 28:505-513.

Rolfe DF, Brown GC. Cellular energy utilization and molecular origin of standard metabolic rate in mammals. Physiol Rev. 1997 ;77:731-58.

Reue K. mRNA quantitation techniques: considerations for experimental design and application.*J Nutr*. 1998 ;128:2038-44.

Ruehl WW, Entriken TL, Muggenburg BA, Bruyette DS, Griffith WC, Hahn FF. Treatment with L-deprenyl prolongs life in elderly dogs. *Life Sci.* 1997; 61:1037–1044.

Sadik CD, Sies H, Schewe T. Inhibition of 15-lipoxygenases by flavonoids: structure-activity relations and mode of action. *Biochem Pharmacol.* 2003; 65:773-781.

Segal AW. How neutrophils kill microbes. *Annu Rev Immunol* . 2005;23:197-223.

Salles N, Szanto I, Herrmann F,et al. Expression of mRNA for ROS-generating NADPH oxidases in the aging stomach. *Exp Gerontol*. 2005; 40:353-357.

Sanz N, Diez-Fernandez C, Alvarez A, Cascales M. Age-dependent modifications in rat hepatocyte antioxidant defense systems. *J Hepatol.* 1997; 27:525-534.

Sass B, Rabstein LS, Madison R, Nims RM, Peters RL, Kelloff GJ. Incidence of spontaneous neoplasms in F344 rats throughout the natural life-span. *J Natl Cancer Inst.* 1975; 54(6):1449-1456.

Schriner SE, Linford NJ, Martin GM, Treuting P, Ogburn CE, Emond M, Coskun PE, Ladiges W, Wolf N, Van Remmen H, Wallace DC, Rabinovitch PS. Extension of murine life span by overexpression of catalase targeted to mitochondria. *Science.* 2005; 308:1909-1911.

Seidman MD and Ahmad N. Molecular mechanisms of age-related hearing loss. *Ageing Res. Rev.* 2002; 1:331-334.

Seidman MD, Quirk WS, Shirwany NA. Mechanisms of alterations in the microcirculation of the cochlea. *Ann N Y Acad Sci.* 1999; 884:226-232.

Sentman ML, Granström M, Jakobson H, Reaume A, Basu S, Marklund SL. Phenotypes of mice lacking extracellular superoxide dismutase and copper- and zinc-containing superoxide dismutase. *J. Biol. Chem.* 2006; 281:6904–6909.

Silva JA , Araujo RC, Baltatu O, Oliveira SM, Tschope C, Fink E, Hoffmann S, Plehm R, Chai KX, Chao L, Chao J, Ganten D, Pesquero JB, Bader M. Reduced cardiac hypertrophy and altered blood pressure control in transgenic rats with the human tissue kallikrein gene. *FASEB J*. 2000; 14(13):1858-1860.

Singh R, Green MR. Sequence-specific binding of transfer RNA by glyceraldehyde-3-phosphate dehydrogenase. *Science*. 1993; 259:365-368.

Sohal RS, Ku HH, Agarwal S, Forster MJ, Lal H. Oxidative damage, mitochondrial oxidant generation and antioxidant defenses during aging and in response to food restriction in the mouse. *Mech. Ageing Dev.* 1994; 74:121–133.

Sohal RS, Weindruch R. Oxidative stress, caloric restriction, and aging. *Science.* 1996; 273:59–63.

Song G, Cechvala C, Resnick DK, Dempsey RJ, Rao VL. GeneChip analysis after acute spinal cord injury in rat. *J Neurochem.* 2001; 79:804-815.

Sorensen, T. L., M. Tani, J. Jensen, V. Pierce, C. Lucchinetti, V. A. Folcik, S. Qin, J. Rottman, F. Sellebjerg, R. M. Strieter. Expression of specific chemokines and chemokine receptors in the central nervous system of multiple sclerosis patients. *J. Clin. Invest.* 1999; 103:807.

Spanakis E. Problems related to the interpretation of autoradiographic data on gene expression using common constitutive transcripts as controls. *Nucleic Acids Res.* 1993; 21:3809-3819.

Spindler SR. Rapid and reversible induction of the longevity, anticancer and genomic effects of caloric restriction. *Mech Ageing Dev.* 2005;126(9):960-966.

Spiteller G. Enzymic lipid peroxidation: a consequence of cell injury? *Free Radic Biol Med.* 1996; 21:1003-1009.

Spongr VP, Flood DG, Frisina RD, Salvi RJ. Quantitative measures of hair cell loss in CBA and C57BL/6 mice throughout their life spans. *J Acoust Soc Am.* 1997;101(6):3546-3553.

Sreekumar R, Unnikrishnan J, Fu A, Nygren J, Short KR, Schimke J, Barazzoni R, Nair KS. Effects of caloric restriction on mitochondrial function and gene transcripts in rat muscle. *Am J Physiol Endocrinol Metab.* 2002; 283(1):E38-43.

Staecker H, Zheng QY, Van De Water TR. Oxidative stress in aging in the C57B16/J mouse cochlea. *Acta Otolaryngol.* 2001; 121:666-672.

Stankovic KM and Corfas G. Real-time quantitative RT-PCR for low-abundance transcripts in the inner ear: analysis of neurotrophic factor expression. *Hear Res.* 2003; 185:97-108.

Stoll S, Hafner U, Kraenzlin B, Müller We. Chronic Treatment of Syrian Hamsters with Low-Dose Selegiline Increases Life Span in Females, But Not Males. *Neurobiol. Aging.* 1997; 18:205–211.

Sun J, Folk D, Bradley TJ, Tower J. Induced overexpression of mitochondrial Mn-superoxide dismutase extends the life span of adult Drosophila melanogaster, *Genetics*. 2002; 161:661–672.

Suzuki T, Higgins PJ, Crawford DR. Control selection for RNA quantitation. *Biotechniques.* 2000; 29:332-337.

Swanson L W. Atlas of the rat brain, in**:** Swanson L. W. (Eds.), Brain Maps: structure of the rat brain. *Elsevier Science publishers B.V, The Netherlands.* 1992; 45-195.

Taber DF, Morrow JD, Roberts LJ 2nd. A nomenclature system for the isoprostanes. *Prostaglandins*. 1997; 53(2):63-67.

Tan PK, Downey TJ, Spitznagel EL Jr, et al. Evaluation of gene expression measurements from commercial microarray platforms. *Nucleic Acids Res.* 2003; 31:5676-5684.

Thellin O, Zorzi W, Lakaye B, et al. Housekeeping genes as internal standards: use and limits. *J Biotechnol.* 1999; 75:291-295.

Thomas RP, Guigneaux M, Wood T, Evers BM. Age-associated changes in gene expression patterns in the liver. *J Gastrointest Surg*. 2002; 6:445-453.

Tian L, Cai Q, Wei H. Alterations of antioxidant enzymes and oxidative damage to macromolecules in different organs of rats during aging. Free Radic Biol Med. 1998; 24: 1477-1484.

Tissenbaum, H.A., and Guarente, L. Increased dosage of a sir-2 gene extends lifespan in Caenorhabditis elegans. Nature 2001; 410: 227–230.

Tsay HJ, Wang P, Wang SL, Ku HH. Age-associated changes of superoxide dismutase and catalase activities in the rat brain. *J Biomed Sci.* 2000; 7:466-474.

Uno Y, Horii A, Uno A, Fuse Y, Fukushima M, Doi K, Kubo T. Quantitative changes in mRNA expression of glutamate receptors in the rat peripheral and central vestibular systems following hypergravity. *J. Neurochem.* 2002 ; 81 :1308–1317.

Valenzano DR, Terzibasi E, Genade T, Cattaneo A, Domenici L, Cellerino A . Resveratrol Prolongs Lifespan and Retards the Onset of Age-Related Markers in a Short-Lived Vertebrate." *Curr Biol*. 2006; 16:296-300.

Valko M, Izakovic M, Mazur M, Rhodes CJ, & Telser J. Role of oxygen radicals in DNA damage and cancer incidence. *Mol. Cell. Biochem.* 2004; 266:37–56.

Valls-Belles V, Torres MC, Muniz P, Beltran S, Martinez-Alvarez JR, Codoner-Franch P. Defatted milled grape seed protects adriamycin-treated hepatocytes against oxidative damage. *Eur J Nutr*. 2006; 45:251-258.

Van Laer L, Pfister M, Thys S, Vrijens K, Mueller M, Umans L, Serneels L, Van

Nassauw L, Kooy F, Smith RJ, Timmermans JP, Van Leuven F, Van Camp G. Mice lacking Dfna5 show a diverging number of cochlear fourth row outer hair cells. *Neurobiol Dis.* 2005; 19:386-399.

Van Remmen H, Ikeno Y, Hamilton M, Pahlavani M, Wolf N, Thorpe SR, Alderson NL, Baynes JW, Epstein CJ, Huang TT, Nelson J, Strong R, Richardson A. Life-long reduction in MnSOD activity results in increased DNA damage and higher incidence of cancer but does not accelerate aging, Physiol. *Genomics*. 2003; 16:29–37.

Van Remmen H, Ward W, Sabia RV, Richardson A. Effect of age on gene expression and protein degradation. In: Masoro E.J., ed. Handbook of physiology, volume on aging. New York, NY: Oxford University Press; 1995;171-234.

Vandesompele J, De Preter K, Pattyn F, Poppe B, Van Roy N, De Paepe A, Speleman F. Accurate normalization of real-time quantitative RT-PCR data by geometric averaging of multiple internal control genes. *Genome Biol [serial online]*. 2002; 3. Available at: http://genomebiology.com/2002/3/7/RESEARCH/0034 Accessed June 18, 2002.

Walker NJ. A technique whose time has come. *Science* 2002; 296:557-558.

Wall SJ and Edwards DR. Quantitative reverse transcription-polymerase chain reaction (RT-PCR): a comparison of primer-dropping, competitive, and real-time RT-PCRs. *Anal Biochem.* 2002; 300:269–273.

Ward WF, Qi W, Van Remmen H, Zackert WE, Roberts LJ 2nd, Richardson A. Effects of age and caloric restriction on lipid peroxidation: measurement of oxidative stress by F2-isoprostane levels. *J Gerontol A Biol Sci Med Sci.* 2005; 60:847-851.

Warner HR. Superoxide dismutase, aging, and degenerative disease. *Free Radic. Biol. Med*. 1994; 17:249–258.

Warner HR. Current status of efforts to measure and modulate the biological rate of aging. *J Gerontol A Biol Sci Med Sci.* 2004 ;59: 692-6.

Warner HR, Ingram D, Miller RA, Nadon NL, Richardson AG. Program for testing biological interventions to promote healthy aging. *Mech Ageing Dev*. 2000; 115:199-207.

Warrington JA, Nai,r A, Mahadevappa M, Tsyganskaya M. Comparison of human adult and fetal expression and identification of 535 housekeeping/maintenance genes. *Physiol Genomics*. 2000; 2:143-147.

Weindruch R. Caloric restriction and aging. *Sci Am.* 1996; 274:46-52.

Weindruch R, Masoro EJ. Concerns about rodent models for aging research. *J Gerontol.* 1991; 46: B87-8.

Weindruch R, Walford RL. Dietary restriction in mice beginning at 1 year of age: effect on life-span and spontaneous cancer incidence. *Science.* 1982; 215(4538):1415-1418.

Williams MD, Van Remmen H, Conrad CC, Huang TT, Epstein CJ, Richardson A. Increased oxidative damage is correlated to altered mitochondrial function in heterozygous manganese superoxide dismutase knockout mice. *J Biol Chem.* 1998; 273(43):28510-28515.

Wittwer CT, Herrmann MG, Moss AA, Rasmussen RP. Continuous fluorescence monitoring of rapid cycle DNA amplification. *Biotechniques*. 1997; 22:130–138.

Wood JG, Rogina B, Lavu1 S, Howitz K, Helfand SL, Tatar M, Sinclair D. Sirtuin activators mimic caloric restriction and delay ageing in metazoans. *Nature*. 2004; 430: 686-689.

Wren AF, Cleary M, Frantz C, Melton S, Norris L. 90-day oral toxicity study of a grape seed extract (IH636) in rats. *J Agric Food Chem.* 2002; 50:2180-2192.

Yao YY, Yin H, Shen B, Chao L, Chao J. Tissue kallikrein infusion prevents cardiomyocyte apoptosis, inflammation and ventricular remodeling after myocardial infarction. *Regul Pept.* 2007; 140(1-2):12-20.

Yamada H, Chen D, Monstein HJ and Hakanson R. Effects of fasting on the expression of gastrin, cholecystokinin, and somatostatin genes and of various housekeeping genes in the pancreas and upper digestive tract of rats. *Biochem. Biophys. Res. Commun.* 1997; 231:835–838.

Yin H, Morrow JD, Porter NA. Identification of a novel class of endoperoxides from arachidonate autoxidation. *J Biol Chem.* 2004; 279(5):3766-3776.

Youngman LD, Park JY, Ames BN. Protein oxidation associated with aging is reduced by dietary restriction of protein or calories. *Proc Natl Acad Sci U S A.* 1992; 89(19):9112-9116.

Zhao L, Funk CD. Lipoxygenase pathways in atherogenesis. *Trends Cardiovasc Med.* 2004; 14:191-195.

Zhang AS, Xiong S, Tsukamoto H, Enns CA. Localization of iron metabolism-related mRNAs in rat liver indicate that HFE is expressed predominantly in hepatocytes. *Blood*. 2004; 103:1509-1514.

Zini R, Morin C, Bertelli A, Bertelli AA, Tillement JP. Effects of resveratrol on the rat brain respiratory chain. *Drug. Exp. Clin. Res*. 1999; 25:87-97.

Appendices

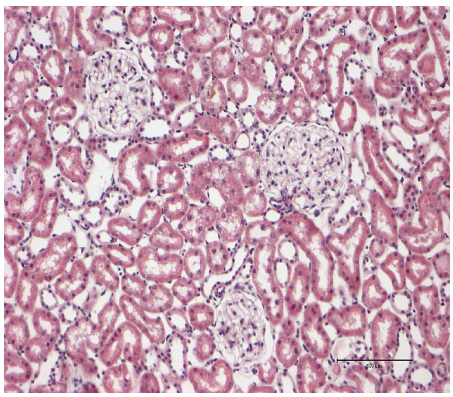

Grade 1 of renal pathology

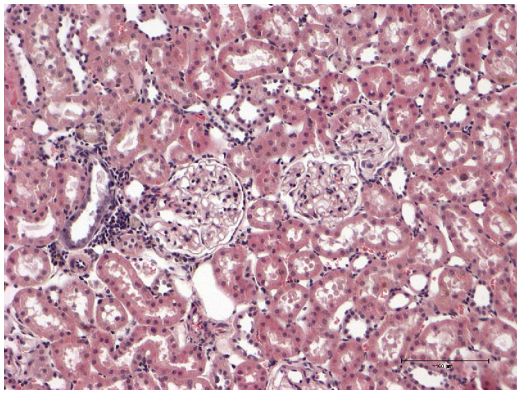

Grade 2 of renal pathology

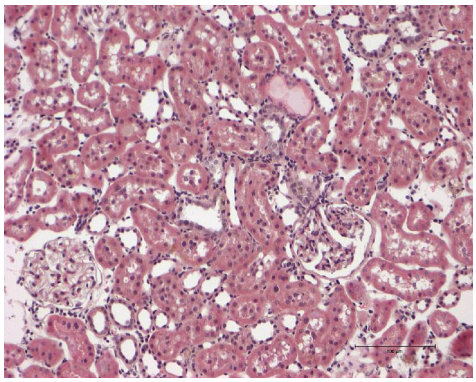

Grade 3 of renal pathology

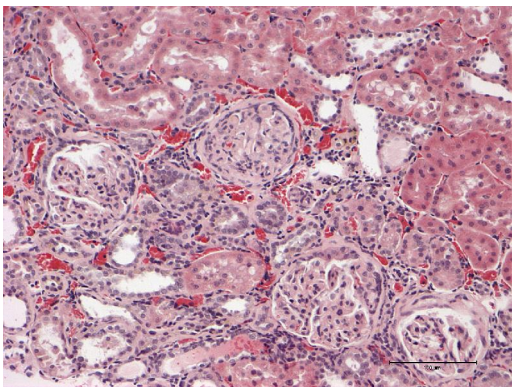

Grade 4 of renal pathology

Figure 6.1 Grades of renal pathology
Photomicrographs made with 200x magnification; bar = 100 micrometers

Table 5.3 Gene expression significantly changed by CR

Probe	Fold Change	Gene name
1398390_at	6.993	Transcribed sequence with weak similarity to protein ref:NP_006410.1 (H.sapiens) small inducible cytokine B subfamily
1379340_at	5.373	Similar to laminin gamma 2 chain precursor (LOC289096), mRNA
1367998_at	4.423	secretory leukocyte peptidase inhibitor
1368540_at	3.721	trophoblast glycoprotein
1387306_a_at	3.606	early growth response 2
1371412_a_at	3.464	Transcribed sequence with moderate similarity to protein pdb:1LBG (E. coli) B Chain B, Lactose Operon Repressor Bound To 21-Base Pair Symmetric Operator Dna, Alpha Carbons Only
1394051_at	3.377	Transcribed sequences
1395126_at	3.353	Similar to MMAN-g (LOC310694), mRNA
1367581_a_at	3.333	secreted phosphoprotein 1
1389413_at	3.207	Transcribed sequence with weak similarity to protein pir:A35329 (H.sapiens) A35329 EVI2 protein precursor - human
1384787_at	3.05	Similar to T-cell surface glycoprotein CD3 gamma chain precursor (T-cell receptor T3 gamma chain) (LOC300678), mRNA
1383747_at	3.003	Transcribed sequences
1389675_at	2.997	Transcribed sequence with strong similarity to protein ref:NP_084520.1 (M.musculus) RIKEN cDNA 2610524G09 [Mus musculus]
1379345_at	2.988	Similar to type XV collagen (LOC298069), mRNA
1376390_at	2.973	Similar to MS4A6D protein (LOC361735), mRNA
1372006_at	2.894	Transcribed sequences
1373628_at	2.877	Transcribed sequences
1388116_at	2.859	collagen, type 1, alpha 1
1370959_at	2.833	collagen, type III, alpha 1
1393252_at	2.826	Transcribed sequence with strong similarity to protein pir:S34968 (M.musculus) S34968 fibulin, splice form D precursor - mouse
1393187_at	2.795	Transcribed sequences
1373368_at	2.792	UI-R-DE0-caf-d-09-0-UI.s1 UI-R-DE0 Rattus norvegicus cDNA clone UI-R-DE0-caf-d-09-0-UI 3', mRNA sequence.
1382531_at	2.785	Similar to toll-like receptor 7 (LOC317468), mRNA
1371079_at	2.763	Fc receptor, IgG, low affinity IIb
1368519_at	2.758	serine (or cysteine) peptidase inhibitor, clade E, member 1
1368482_at	2.72	B-cell leukemia/lymphoma 2 related protein A1
1373309_at	2.703	UI-R-DD0-bzr-f-03-0-UI.s1 UI-R-DD0 Rattus norvegicus cDNA clone UI-R-DD0-bzr-f-03-0-UI 3', mRNA sequence.
1372685_at	2.648	Similar to cyclin-dependent kinase inhibitor 3; CDK2-associated dual specificity phosphatase; cyclin-dependent

		kinase interactor 1; cyclin-dependent kinase interacting protein 2; kinase-associated phosphatase (LOC289993), mRNA
1370155_at	2.636	procollagen, type I, alpha 2
1392296_at	2.633	UI-R-C1-lc-g-03-0-UI.s1 UI-R-C1 Rattus norvegicus cDNA clone UI-R-C1-lc-g-03-0-UI 3', mRNA sequence.
1373401_at	2.607	EST219610 Normalized rat ovary, Bento Soares Rattus sp. cDNA clone ROVBJ66 3' end, mRNA sequence.
1387854_at	2.581	procollagen, type I, alpha 2
1368000_at	2.574	complement component 3
1383320_at	2.563	lymphocyte-specific protein tyrosine kinase
1390420_at	2.542	Similar to Carboxypeptidase X 1 (M14 family) (LOC296156), mRNA
1382622_at	2.532	UI-R-C1-lb-g-10-0-UI.s1 UI-R-C1 Rattus norvegicus cDNA clone UI-R-C1-lb-g-10-0-UI 3', mRNA sequence.
1376693_at	2.528	Transcribed sequence with weak similarity to protein ref:NP_060124.1 (H.sapiens) hypothetical protein FLJ20073 [Homo sapiens]
1392264_s_at	2.507	serine (or cysteine) proteinase inhibitor, member 1
1368464_at	2.482	macrophage galactose N-acetyl-galactosamine specific lectin 1
1390659_at	2.481	Transcribed sequence
1377023_at	2.474	Similar to dual specificity phosphatase 2 (LOC311406), mRNA
1382566_at	2.472	Transcribed sequences
1379791_at	2.46	Similar to T3-epsilon protein (LOC315609), mRNA
1385832_s_at	2.455	Similar to RIKEN cDNA 1200013B08 (LOC317578), mRNA
1368171_at	2.45	lysyl oxidase
1368914_at	2.445	runt related transcription factor 1
1369964_at	2.443	coronin, actin binding protein 1A
1376845_at	2.427	putative ISG12(b) protein
1389006_at	2.422	macrophage expressed gene 1
1388275_at	2.421	T-cell receptor beta chain
1382311_at	2.419	Similar to Ab2-389 (LOC310877), mRNA
1391450_at	2.4	Similar to Lysyl oxidase homolog 2 precursor (Lysyl oxidase-like protein 2) (Lysyl oxidase related protein 2) (Lysyl oxidase-related protein WS9-14) (LOC290350), mRNA
1392322_at	2.386	Transcribed sequence with weak similarity to protein ref:NP_060796.1 (H.sapiens) hypothetical protein FLJ11110 [Homo sapiens]
1397167_at	2.364	UI-R-C4-alm-d-12-0-UI.s1 UI-R-C4 Rattus norvegicus cDNA clone UI-R-C4-alm-d-12-0-UI 3', mRNA sequence.
1387351_at	2.363	fibrillin 1
1376197_at	2.347	Transcribed sequence with moderate similarity to protein sp:P00722 (E. coli) BGAL_ECOLI Beta-galactosidase
1389553_at	2.342	Similar to RIKEN cDNA 3110037K17 (LOC362431), mRNA
1381357_at	2.319	Similar to Protein-tyrosine phosphatase, non-receptor type 8 (Hematopoietic cell protein-tyrosine phosphatase 70Z-PEP) (LOC295338), mRNA
1370585_a_at	2.308	protein kinase C, beta 1
1368683_at	2.305	oxidized low density lipoprotein (lectin-like) receptor 1
1368518_at	2.298	CD53 antigen
1391026_at	2.295	Transcribed sequence with moderate similarity to protein

		sp:P00722 (E. coli) BGAL_ECOLI Beta-galactosidase
1370895_at	2.293	collagen, type V, alpha 2
1368167_at	2.264	cathepsin E
1385702_at	2.255	Similar to Ifi204 protein (LOC304988), mRNA
1390798_at	2.253	protein tyrosine phosphatase, receptor type, C
1373463_at	2.25	collagen, type V, alpha 2
1370603_a_at	2.235	Protein tyrosine phosphatase, receptor type, C
1387276_at	2.223	Transcribed sequences
1379598_at	2.22	Transcribed sequences
		UI-R-CV1-bsu-c-11-0-UI.s1 UI-R-CV1 Rattus norvegicus
1383322_at	2.218	cDNA clone UI-R-CV1-bsu-c-11-0-UI 3', mRNA sequence.
1379766_at	2.198	src-like adaptor
1368762_at	2.19	ubiquitin D
1370892_at	2.184	palmitoyl-protein thioesterase 2
		UI-R-CN1-cjf-k-17-0-UI.s1 UI-R-CN1 Rattus norvegicus
1377239_at	2.166	cDNA clone UI-R-CN1-cjf-k-17-0-UI 3', mRNA sequence.
1387134_at	2.164	schlafen 3
1368829_at	2.158	fibrillin-1
1368420_at	2.152	ceruloplasmin
1375010_at	2.149	Similar to macrosialin (LOC287435), mRNA
		Transcribed sequence with weak similarity to protein
1392515_at	2.147	pir:I49049 (M.musculus) I49049 Ly-49D-GE antigen - mouse
1388939_at	2.139	Similar to type XV collagen (LOC298069), mRNA
1372404_at	2.136	Similar to EN-7 protein (LOC366957), mRNA
1382680_at	2.119	adipose differentiation-related protein
		R.norvegicus (F344/Crj) rearranged mRNA for T-cell receptor
1387945_at	2.113	gamma chain (1474bp)
		Similar to dendritic cell immunoreceptor (LOC297584),
1382153_at	2.101	mRNA
		UI-R-C1-kh-a-12-0-UI.s1 UI-R-C1 Rattus norvegicus cDNA
1398616_at	2.095	clone UI-R-C1-kh-a-12-0-UI 3', mRNA sequence.
1389651_at	2.082	Transcribed sequences
1381311_at	2.082	Similar to cell surface glycoprotein (LOC316137), mRNA
		Similar to interferon consensus sequence-binding protein -
1372097_at	2.081	mouse (LOC292060), mRNA
1392407_at	2.069	Transcribed sequences
1369943_at	2.061	transglutaminase 2, C polypeptide
		UI-R-C1-kg-h-02-0-UI.s1 UI-R-C1 Rattus norvegicus cDNA
1393227_at	2.059	clone UI-R-C1-kg-h-02-0-UI 3', mRNA sequence.
		UI-R-C1-kk-e-12-0-UI.r1 UI-R-C1 Rattus norvegicus cDNA
1384187_at	2.058	clone UI-R-C1-kk-e-12-0-UI 5', mRNA sequence.
1391979_at	2.05	Transcribed sequences
1368418_a_at	2.044	ceruloplasmin
		Similar to transcription factor NRF; ITBA4 gene
1382442_at	2.042	(LOC298316), mRNA
1369944_at	2.042	MARCKS-like 1
1368558_s_at	2.036	allograft inflammatory factor 1
1380250_at	2.035	Transcribed sequences
1379344_at	2.035	endothelial type gp91-phox gene
1379499_at	2.032	Similar to lymphotoxin-beta (LOC361795), mRNA

		UI-R-E1-fh-g-01-0-UI.s1 UI-R-E1 Rattus norvegicus cDNA clone UI-R-E1-fh-g-01-0-UI 3' similar to gi|2064126|gb|AA406145|AA406145 zu20c07.s1 Soares NhHMPu S1 Homo sapiens cDNA clone 738540 3', mRNA
1383137_at	2.025	sequence.
1379482_at	2.016	hepatoma-derived growth factor, related protein 3
1379688_at	2.009	Transcribed sequences
1373860_at	2.008	Similar to sox-4 protein - mouse (LOC364712), mRNA
1368419_at	2.007	ceruloplasmin
1370924_at	2.006	Rat T-cell receptor active beta-chain C-region mRNA, partial cds, clone TRB4
1373286_at	1.996	Transcribed sequences
1384939_at	1.995	UI-R-C2p-rw-e-09-0-UI.r1 UI-R-C2p Rattus norvegicus cDNA clone UI-R-C2p-rw-e-09-0-UI 5', mRNA sequence.
1368294_at	1.994	deoxyribonuclease I-like 3
1385143_at	1.993	Transcribed sequence with moderate similarity to protein pir:I60486 (R.norvegicus) I60486 gene trg protein - rat
1369983_at	1.992	chemokine (C-C motif) ligand 5
1388673_at	1.984	Similar to Lsp1 protein (LOC361680), mRNA
1373932_at	1.984	endothelial type gp91-phox gene
1380682_at	1.976	Similar to KIAA2009 protein (LOC308790), mRNA
1373575_at	1.972	Transcribed sequence with moderate similarity to protein pir:A35241 (H.sapiens) A35241 IgE Fc receptor gamma chain precursor - human
1383658_at	1.972	lysosomal-associated protein transmembrane 5
1384298_at	1.962	Similar to myosin-1F-like protein (LOC314654), mRNA
1368455_at	1.961	natural killer cell group 7 sequence
1383614_at	1.948	Similar to 1200013B22Rik protein (LOC289419), mRNA
1389210_at	1.943	Similar to lymphocyte cytosolic protein 1 (LOC306071), mRNA
1381819_at	1.938	UI-R-C2p-oj-d-05-0-UI.s1 UI-R-C2p Rattus norvegicus cDNA clone UI-R-C2p-oj-d-05-0-UI 3', mRNA sequence.
1368896_at	1.937	MAD homolog 7 (Drosophila)
1371518_at	1.935	nidogen (entactin)
1368006_at	1.917	lysosomal-associated protein transmembrane 5
1387776_at	1.915	tissue-type transglutaminase
1367846_at	1.914	S100 calcium-binding protein A4
1385571_at	1.908	Transcribed sequence with weak similarity to protein pir:A37244 (H.sapiens) A37244 nuclear autoantigen Sp-100 - human
1387946_at	1.9	lectin, galactoside-binding, soluble, 3 binding protein
1374493_at	1.898	Transcribed sequences
1376282_at	1.894	Transcribed sequences
1368565_at	1.892	solute carrier family 1 (glial high affinity glutamate transporter), member 3
1371441_at	1.882	Similar to phosphoprotein enriched in astrocytes 15 (LOC364052), mRNA
1377955_at	1.881	LOC367996 (LOC367996), mRNA
1370987_at	1.881	sialophorin
1372439_at	1.875	Similar to collagen alpha 1(IV) chain precursor - mouse (LOC290905), mRNA

1379284_at	1.874	Similar to RIKEN cDNA 2810457I06 (LOC315579), mRNA
1390707_at	1.87	regulator of G-protein signaling 10
1371016_at	1.864	Rat T-cell receptor active alpha-chain C-region mRNA, partial cds, clone TRA29
1368940_at	1.862	purinergic receptor P2Y, G-protein coupled 2
1369958_at	1.858	ras homolog gene family, member B
1369955_at	1.857	procollagen, type V, alpha 1
1388339_at	1.854	Similar to phosphoprotein enriched in astrocytes 15 (LOC364052), mRNA
1380909_at	1.841	Transcribed sequences
1367776_at	1.838	cell division cycle 2 homolog A (S. pombe)
1392547_at	1.835	Hypothetical LOC302884 (LOC302884), mRNA
1389873_at	1.833	apoptosis-associated speck-like protein containing a CARD
1368555_at	1.829	CD37 antigen
1393149_at	1.822	protocadherin alpha 13
1376030_at	1.82	Similar to centaurin, beta 1 (LOC287443), mRNA
1370621_at	1.819	CD3 antigen, zeta polypeptide
1370516_at	1.815	solute carrier family 15, member 3
1370864_at	1.812	collagen, type 1, alpha 1
1389189_at	1.81	actinin, alpha 1
1373818_at	1.809	Transcribed sequences
1369204_at	1.779	hemopoietic cell kinase
1389885_at	1.778	Similar to RIKEN cDNA 0610025L06 (LOC360646), mRNA
1393672_at	1.775	Similar to hemicentin; fibulin 6 (LOC289094), mRNA
1392655_at	1.772	Similar to Nuclear autoantigen Sp-100 (Speckled 100 kDa) (Nuclear dot-associated Sp100 protein) (LOC363269), mRNA
1383702_at	1.761	UI-R-BS0-anu-f-09-0-UI.s1 UI-R-BS0 Rattus norvegicus cDNA clone UI-R-BS0-anu-f-09-0-UI 3', mRNA sequence.
1373785_at	1.755	Transcribed sequence with weak similarity to protein ref:NP_036400.1 (H.sapiens) similar to vaccinia virus HindIII K4L ORF [Homo sapiens]
1372852_at	1.753	Similar to S6 kinase 2 (LOC361696), mRNA
1380621_at	1.749	Similar to tyrosine kinase Fps/Fes (LOC293041), mRNA
1371537_at	1.742	Transcribed sequence with strong similarity to protein sp:O43286 (H.sapiens) B4G5_HUMAN Beta-1,4-galactosyltransferase 5
1376652_at	1.738	Similar to Complement component 1, q subcomponent, alpha polypeptide (LOC298566), mRNA
1378150_at	1.737	Similar to caspase recruitment domain family member 11 (LOC304314), mRNA
1372200_at	1.736	Transcribed sequence with moderate similarity to protein ref:NP_071390.1 (H.sapiens) chromosome 6 open reading frame 9; G18.2 protein [Homo sapiens]
1390821_at	1.732	protocadherin alpha 13
1368822_at	1.732	follistatin-like
1388784_at	1.727	Similar to Macrophage colony stimulating factor I receptor precursor (CSF-1-R) (Fms proto-oncogene) (c-fms) (LOC307403), mRNA
1390738_at	1.724	DAMP-1 protein
1388698_at	1.716	extracellular matrix protein 1
1373245_at	1.714	Similar to collagen alpha 1(IV) chain precursor - mouse

		(LOC290905), mRNA
1388740_at	1.714	Similar to cDNA sequence BC032204 (LOC309186), mRNA
1377916_at	1.709	Similar to schlafen2 (LOC303380), mRNA
1378131_at	1.698	Similar to hypothetical protein FLJ35613 (LOC363115), mRNA
1389039_at	1.695	Transcribed sequence with strong similarity to protein prf:2018199A (E. coli) 2018199A beta lactamase IRT-4 [Escherichia coli]
1391206_at	1.692	Similar to hypothetical protein FLJ10901 (LOC289399), mRNA
1379698_at	1.687	Transcribed sequence with strong similarity to protein sp:P00722 (E. coli) BGAL_ECOLI Beta-galactosidase
1388131_at	1.685	Rat mRNA for beta-tubulin T beta15
1377390_at	1.685	UI-R-CT0-bud-a-09-0-UI.s1 UI-R-CT0 Rattus norvegicus cDNA clone UI-R-CT0-bud-a-09-0-UI 3', mRNA sequence.
1384292_at	1.682	downstream of tyrosine kinase-1
1367784_a_at	1.682	clusterin
1380930_at	1.68	Similar to KIAA1607 protein (LOC290569), mRNA
1368754_at	1.677	pyrimidinergic receptor P2Y, G-protein coupled, 6
1377325_a_at	1.675	Transcribed sequences
1380410_at	1.672	Transcribed sequences
1392922_at	1.668	UI-R-BS1-ayd-d-02-0-UI.s1 UI-R-BS1 Rattus norvegicus cDNA clone UI-R-BS1-ayd-d-02-0-UI 3', mRNA sequence.
1380537_at	1.666	Similar to RIKEN cDNA 4930568P13 (LOC315348), mRNA
1374730_at	1.658	Similar to DAP12 (LOC361537), mRNA
1373262_at	1.653	Transcribed sequences
1367986_at	1.652	prostaglandin F2 receptor negative regulator
1395781_at	1.652	Transcribed sequences
1389208_at	1.648	Similar to hypothetical protein MGC40053 (LOC363495), mRNA
1385213_at	1.648	Similar to Epithelial stromal interaction 1, isoform a (LOC364433), mRNA
1376218_a_at	1.641	Similar to Potential phospholipid-transporting ATPase ID (ATPase class I type 8B member 2) (LOC361984), mRNA
1372055_at	1.634	Transcribed sequences
1398294_at	1.63	actinin, alpha 1
1391537_at	1.629	Similar to hypothetical protein DJ667H12.2 (LOC360899), mRNA
1371331_at	1.627	DRABXE03 Rat DRG Library Rattus norvegicus cDNA clone DRABXE03 5', mRNA sequence.
1389477_at	1.624	Transcribed sequences
1368723_at	1.615	linker for activation of T cells
1374337_at	1.615	Transcribed sequence with moderate similarity to protein pdb:1LBG (E. coli) B Chain B, Lactose Operon Repressor Bound To 21-Base Pair Symmetric Operator Dna, Alpha Carbons Only
1376153_at	1.614	Transcribed sequences
1375908_at	1.613	Transcribed sequences
1373656_at	1.607	Transcribed sequences
1372604_at	1.605	Similar to Apolipoprotein L3 (Apolipoprotein L-III) (ApoL-III) (TNF-inducible protein CG12-1) (CG12_1) (LOC315106),

		mRNA
1367655_at	1.603	thymosin, beta 10
1370265_at	1.591	arrestin, beta 2
1391737_at	1.591	Similar to p40-phox (LOC366956), mRNA
1373151_at	1.59	Similar to lipoma HMGIC fusion partner (LOC365795), mRNA
1368207_at	1.579	FXYD domain-containing ion transport regulator 5
1378633_at	1.578	Similar to 4933402K05Rik protein (LOC293783), mRNA
1373106_at	1.576	R.norvegicus mRNA for parathyroid hormone regulated sequence (215bp)
1389809_at	1.574	Transcribed sequences
1382283_at	1.574	Wiskott-Aldrich syndrome protein interacting protein
1393957_at	1.57	UI-R-C3-td-e-06-0-UI.s1 UI-R-C3 Rattus norvegicus cDNA clone UI-R-C3-td-e-06-0-UI 3', mRNA sequence.
1375224_at	1.565	Transcribed sequence with strong similarity to protein ref:NP_036528.1 (H.sapiens) pleckstrin homology-like domain, family A, member 3; pleckstrin homology-like domain, family A, member 2 [Homo sapiens]
1388493_at	1.557	Similar to Expressed sequence AW146242 (LOC362374), mRNA
1372294_at	1.553	Similar to mKIAA0230 protein (LOC314016), mRNA
1391741_a_at	1.55	Transcribed sequences
1393638_at	1.54	UI-R-C3-ts-g-07-0-UI.s1 UI-R-C3 Rattus norvegicus cDNA clone UI-R-C3-ts-g-07-0-UI 3', mRNA sequence.
1392737_at	1.539	Transcribed sequences
1379295_at	1.538	Transcribed sequence with moderate similarity to protein ref:NP_113686.1 (H.sapiens) guanine nucleotide binding protein-gamma transducing activity polypeptide 2; gamma-T2 subunit; G protein cone gamma 8 subunit [Homo sapiens]
1367791_at	1.538	receptor (calcitonin) activity modifying protein 1
1375862_at	1.534	Similar to mKIAA0230 protein (LOC314016), mRNA
1371923_at	1.534	Similar to hypothetical protein FLJ20481 (LOC361467), mRNA
1390925_a_at	1.527	Transcribed sequences
1388427_at	1.521	Similar to adipocyte-specific protein 3 (LOC313770), mRNA
1382043_at	1.52	Similar to unc93 homolog B (LOC361689), mRNA
1376005_at	1.52	Transcribed sequences
1372726_at	1.519	Similar to germinal histone H4 gene (LOC306963), mRNA
1397866_at	1.51	Similar to NK13 (LOC364705), mRNA
1372034_at	1.507	Transcribed sequence with moderate similarity to protein pdb:1LBG (E. coli) B Chain B, Lactose Operon Repressor Bound To 21-Base Pair Symmetric Operator Dna, Alpha Carbons Only
1392037_at	1.501	Transcribed sequences
1394228_at	0.667	Transcribed sequence with weak similarity to protein ref:NP_060531.1 (H.sapiens) hypothetical protein FLJ10330 [Homo sapiens]
1385624_at	0.665	Similar to Transcription initiation protein SPT3 homolog (SPT3-like protein) (LOC301257), mRNA
1368272_at	0.664	glutamate oxaloacetate transaminase 1
1380828_at	0.663	Transcribed sequences

1379350_at	0.663	Similar to transcription factor CP2; Transcription factor CP2, alpha globin (LOC315309), mRNA
1393123_at	0.662	UI-R-DO1-ckp-e-14-0-UI.s1 UI-R-DO1 Rattus norvegicus cDNA clone UI-R-DO1-ckp-e-14-0-UI 3', mRNA sequence.
1372889_at	0.655	matrin F/G 1
1370747_at	0.654	fibroblast growth factor 9
1369081_at	0.653	neuraminidase 1
1369705_at	0.647	X transporter protein 3
1381006_at	0.645	hepatocyte growth factor activator
1379726_at	0.641	Similar to pre-B-cell leukemia transcription factor 4 (LOC361131), mRNA
1368084_at	0.632	deoxyribonuclease I
1388426_at	0.625	sterol regulatory element binding factor 1
1383722_at	0.621	Similar to Proline synthetase associated (LOC306544), mRNA
1382496_at	0.616	hepatocyte nuclear factor 4, alpha
1387672_at	0.616	glycine N-methyltransferase
1369289_at	0.615	hepatocyte nuclear factor 4, alpha
1378295_at	0.61	Similar to six transmembrane epithelial antigen of prostate 2; six transmembrane prostate protein; prostate cancer associated gene 1; prostate cancer associated protein 1 (LOC312052), mRNA
1368661_at	0.606	solute carrier family 13 (sodium-dependent dicarboxylate transporter), member 2
1381574_at	0.603	Transcribed sequences
1387492_at	0.6	solute carrier organic anion transporter family, member 2a1
1370329_at	0.597	cytochrome P450, family 2, subfamily d, polypeptide 22
1371104_at	0.583	sterol regulatory element binding factor 1
1387065_at	0.569	phospholipase C, delta 4
1387913_at	0.561	cytochrome P450, family 2, subfamily d, polypeptide 22
1371012_at	0.524	phytanoyl-CoA 2-hydroxylase 2
1368442_at	0.519	coagulation factor II
1381251_at	0.505	Transcribed sequences
1380562_at	0.49	Similar to hypothetical protein MGC29784 (LOC362416), mRNA
1386969_at	0.477	neuritin
1379376_at	0.457	Transcribed sequences
1372920_at	0.432	Similar to proline dehydrogenase; PRODH (LOC287950), mRNA
1371080_at	0.355	kallikrein
1393139_at	0.345	Similar to Apolipoprotein C2 (LOC292697), mRNA

Fold change >1 indicated that the gene was down regulated by CR, compared to control group, and vice-versa.